

2013

## Thermal Characterization Of As4/3501-6 Carbon-Epoxy Composite

Bradley R. Doleman  
*North Carolina Agricultural and Technical State University*

Follow this and additional works at: <https://digital.library.ncat.edu/theses>

---

### Recommended Citation

Doleman, Bradley R., "Thermal Characterization Of As4/3501-6 Carbon-Epoxy Composite" (2013). *Theses*. 185.

<https://digital.library.ncat.edu/theses/185>

This Thesis is brought to you for free and open access by the Electronic Theses and Dissertations at Aggie Digital Collections and Scholarship. It has been accepted for inclusion in Theses by an authorized administrator of Aggie Digital Collections and Scholarship. For more information, please contact [iyanna@ncat.edu](mailto:iyanna@ncat.edu).

Thermal Characterization of AS4/3501-6 Carbon-Epoxy Composite

Bradley R. Doleman

North Carolina A&T State University

A thesis submitted to the graduate faculty  
in partial fulfillment of the requirements for the degree of

MASTER OF SCIENCE

Department: Mechanical Engineering

Major: Mechanical Engineering

Major Professor: Dr. Messiha Saad

Greensboro, North Carolina

2013

The Graduate School  
North Carolina Agricultural and Technical State University  
This is to certify that the Master's Thesis of

Bradley R. Doleman

has met the thesis requirements of  
North Carolina Agricultural and Technical State University

Greensboro, North Carolina  
2013

Approved by:

---

Dr. Messiha Saad  
Major Professor

---

Dr. Dhananjay Kumar  
Committee Member

---

Dr. Samuel Owusu-Ofori  
Department Chair

---

Dr. Paul Akangah  
Committee Member

---

Dr. Sanjiv Sarin  
Dean, The Graduate School

© Copyright by  
Bradley R. Doleman  
2013

### Biographical Sketch

On the third day of March in the year 1988, Bradley R. Doleman was born to Mr. and Mrs. Robert and Linda Doleman in St. Paul, Minnesota. He spent his elementary and high school days in Reston, Virginia where he attended Herndon High School. After being accepted to both North Carolina A&T State University and Howard University, Mr. Doleman decided upon his father's alma mater and also the option that would not only get him out of the city but farther away from home. Wanting to become an engineer, NC A&T was a best fit as it is one of the top engineering universities in the country. He attended the greatest homecoming on Earth almost every year growing up, so putting two and two together, Mr. Doleman was certainly destined to become an alumnus of the illustrious historically black university. Because he enjoys math and has a variety of talents, mechanical engineering was the best major suited for him, and it gave him the most options and career paths upon graduating being the broadest discipline of engineering.

Mr. Doleman earned his Bachelor of Science degree in May of 2011 and went on to pursue his Master of Science degree also in mechanical engineering. He plans on working with NASA in the future and is interested in multiple other degrees including an MBA to follow in the footsteps of his father, mother, and sister. He is also interested in pursuing a Ph.D. in one of his other interests whether it is in music, engineering, theology, or related disciplines.

## Dedication

I dedicate this thesis work to Jesus Christ and every individual in whom my life made a positive impact in some way shape or form. Thank you to my parents who raised me and have always supported me by showing me grace, love, wisdom, and encouraging words. Thank you to all who played a part in this journey and time in my life. You all are very much appreciated.

## Acknowledgements

Firstly, I want to thank God for allowing me to have and experience life. I want to recognize my advisor, Dr. Messiha Saad. Thank you for continually pushing me to be my best and to do my best. I would not be here without you. I also would like to thank Dr. Mannur Sundaresan for working with me as the graduate coordinator to allow me to even be in this position. A special thanks to Dr. Paul Akangah and Dr. Dhananjay Kumar for not only serving on my committee but for the relationship that was built over the years. It means a lot to me.

Additionally, I would like to acknowledge NASA-URC-Center for Aviation Safety (CAS) (Grant# NNX09AV08A), the Center for Composite Materials Research (CCMR) at North Carolina A&T State University, and the Oak Ridge National Laboratory's High Temperature Materials Laboratory (HTML) sponsored by the U.S. Department of Energy, Office of Energy Efficiency and Renewable Energy, and the Vehicle Technologies Program.

## Table of Contents

List of Figures .....	viii
List of Tables .....	x
Nomenclature .....	xi
Abstract .....	2
CHAPTER 1 Introduction.....	3
1.1 Objective.....	3
1.2 About the Composite .....	4
1.2.3 SEM Images .....	5
CHAPTER 2 Literature Review .....	8
2.1 Heat Transfer .....	8
2.2 Thermal Conductivity .....	9
2.3 Thermal Diffusivity .....	10
2.4 Theoretical Methods .....	11
2.5 Experimental Methods.....	12
2.6 Thermal Contact Resistance .....	14
CHAPTER 3 Methodology Measurements .....	15
3.1 Thermal Diffusivity .....	15
3.1.1 The Flash Method.....	15
3.1.2 Experimental Apparatus. ....	19
3.2 Specific Heat.....	21
3.2.1 Differential Scanning Calorimetry (DSC).....	21
3.2.2 Experimental Apparatus. ....	24



CHAPTER 4 Experimental Procedure.....	27
4.1 Thermal Diffusivity .....	27
4.1.1 Test Specimen Preparation.....	27
4.1.2 Experimental Procedure.....	28
4.1.3 Computational Procedure.....	28
4.2 Specific Heat.....	34
4.2.1 Test Specimen Preparation.....	34
4.2.2 Experimental Procedure.....	34
4.2.3 Computational Procedure.....	36
CHAPTER 5 Results.....	41
5.1 Thermal Diffusivity .....	41
5.2 Specific Heat.....	45
5.3 Thermal Conductivity .....	46
CHAPTER 6 Discussion and Future Research.....	52
6.1 Discussion.....	52
6.2 Future Research .....	52
References.....	54
Appendix A Flash Method Derivation of Thermal Diffusivity .....	58
Appendix B Complete Computational Procedure: Thermal Diffusivity .....	62
Appendix C Complete Computational Procedure: Specific Heat.....	74
Appendix D Future Research: Computational Procedure for Thermal Expansion.....	85

## List of Figures

Figure 1.1 AS4/3501-6 Carbon-Epoxy Composite Sample.....	5
Figure 1.2. 100x Magnification SEM Image of the AS4/3501-6 Composite .....	6
Figure 1.3. 1000x Magnification SEM Image of the AS4/3501-6 Composite .....	6
Figure 2.1. Block Diagram of a Flash System .....	13
Figure 3.1. Schematic of the Flash Method .....	16
Figure 3.2. Experimental Setup for the Thermal Diffusivity .....	20
Figure 3.3. The Flash Method Thermogram.....	21
Figure 3.4. Experimental Setup of the DSC 200 F3 Maia® and Intracooler.....	24
Figure 3.5. Cross-Section Diagram of the Differential Scanning Calorimeter .....	25
Figure 4.1. Thermal Diffusivity Sample Specimens of AS4/3501-6.....	27
Figure 4.2. Initial FlashLine™ 2000 Software Window .....	29
Figure 4.3. Hardware Interlock Enable on the FlashLine™ Apparatus.....	29
Figure 4.4. Test Information Window .....	30
Figure 4.5. Oil, Vacuum, Gas, and Detector Check Window.....	30
Figure 4.6. Purge Gas Inlet Adjuster and the Purge Gas Outlet Oiler .....	31
Figure 4.7. Testing Window with the Last Shot .....	32
Figure 4.8. Test Completion and Displayed Results.....	32
Figure 4.9. Specific Heat Sample Specimen of AS4/3501-6.....	34
Figure 4.10. Crucibles Placed on the Heat Flux Sensor .....	35
Figure 4.11. Initial DSC Measurement Application Window .....	36
Figure 4.12. First Measurement Application Window .....	37
Figure 4.13. Temperature Program Tab in the Measurement Definition Window.....	38

Figure 4.14. Graph of the Specific Heat Runs .....	38
Figure 4.15. Segments Window .....	39
Figure 4.16. Export Data and Export Format Window.....	40
Figure 5.1. Thermal Diffusivity Shots of the AS4/3501-6 Composite .....	41
Figure 5.2. Magnified View of the Thermal Diffusivity with Error Bars.....	43
Figure 5.3. Half-Times of the AS4/3501-6 Composite.....	44
Figure 5.4. Thermal Diffusivity of the AS4/3501-6 Composite.....	45
Figure 5.5. Specific Heat of the AS4/3501-6 Composite .....	46
Figure 5.6. Thermal Conductivity of the AS4/3501-6 Composite .....	47
Figure 5.7. Rear Face Radiation Heat Loss .....	47
Figure 5.8. Rear Face Finite Pulse Time Effect.....	48
Figure 5.9. Thermogram of the AS4/3501-6 Composite .....	49

## List of Tables

Table 1.1 Typical Fiber Properties of AS4 Carbon Fiber .....	7
Table 3.1 Technical Specifications of the FlashLine™ 2000 Thermal Properties Analyzer .....	19
Table 3.2 Technical Specifications of the DSC 200 F3 Maia®.....	25
Table 5.1 Percent Error of the Thermal Diffusivity.....	43
Table 5.2 Specifications of AS4/3501-6 Testing Specimens.....	50
Table 5.3 Thermal Properties of AS4/3501-6.....	50
Table 5.4 Range of Thermal Properties for AS4/3501-6.....	51

## Nomenclature

$A$	cross-sectional area
$\bar{a}$	measurement mean
$a_i$	$i^{\text{th}}$ measurement of the sample
$c_p$	specific heat (J/kg·K)
$e$	margin of error
$E$	calibration constant
$\dot{g}$	constant rate of heat generation per unit volume
$g$	depth (m)
$h$	specific enthalpy (J/kg)
$h_c$	convection heat transfer coefficient
$H$	enthalpy (J)
$k$	thermal conductivity (W/m·K)
$K_1$	constant
$K_2$	constant
$K_r$	correction factor
$L$	sample thickness (cm)
$m$	mass (kg)
$n$	number of iterations
$N$	number of measurements
$q$	rate of heat conducted per unit volume (W/m <sup>3</sup> )
$\dot{Q}$	rate of heat flow (W)
$Q$	pulse of radiant energy, heat (J/cm <sup>2</sup> )

$R_C$	thermal contact resistance ( $\text{m}^2 \cdot ^\circ\text{C}/\text{W}$ )
$SE$	standard deviation of the mean
$t$	time (s)
$T$	temperature (K)
$V$	dimensionless quantity
$x$	distance (m)

### **Greek Symbols**

$\alpha$	thermal diffusivity ( $\text{cm}^2/\text{s}$ )
$\Delta$	differential quantity
$\rho$	density ( $\text{kg}/\text{m}^3$ )
$\sigma$	standard deviation
$\tau$	triangle of duration
$\omega$	dimensionless quantity

### **Subscripts**

$ref$	reference
$\frac{1}{2}$	half
1C	in-plane composite property
1f	in-plane fiber property
2f	through-the-thickness fiber property
$f$	fiber
$m$	matrix
$x$	in-plane direction
$y$	transverse direction

## Abstract

Thermal diffusivity, specific heat, and thermal conductivity are important thermophysical properties of composite materials and foams. Thermal characterization provides these material properties which play a significant role in the engineering design process of space systems, aerospace vehicles, transportation, energy storage devices, and power generation including fuel cells. Thermal conductivity is the parameter that is important in problems involving heat transfer and thermal structures. Because it determines the working temperature levels of a material, the thermal conductivity is critical when considering the performance of materials in high temperature applications as well as safety, process control, and quality assurance.

As a result of the scarce thermal property data for the AS4/3501-6 carbon-epoxy composite, this research has developed the thermophysical property database. Using the xenon flash method in accordance with the ASTM E1461 standard, the thermal diffusivity was measured through the thickness. Differential scanning calorimetry (DSC) was used to measure the specific heat in accordance with the ASTM E1269 standard. Both of these properties were measured from room temperature up to the service temperature range of the material.

The AS4 composite is recommended for general purpose structural applications. The epoxy matrix is amine cured up to the service temperature of 175 °C, and the composite was made using the high pressure autoclave process. After measuring the specific heat and thermal diffusivity, the thermal conductivity was calculated using a directly proportional relationship between the density, specific heat, and thermal diffusivity, thus adding to the currently insufficient thermal properties database for composite materials and foams.

## **CHAPTER 1**

### **Introduction**

Technology in today's world is rapidly developing at a rate that was once unimaginable. Because of this exponential growth, the demand for new materials that will outperform traditional materials also increases dramatically. To meet these challenges, monolithic materials are being combined to develop new unique materials called composites. The formation of composites provides properties unobtainable separately with either constituent (Daniel & Ishai, 2006). Besides improvements in the mechanical properties such as tensile strength, stiffness, and fatigue endurance, materials must retain functionality at much higher operating temperatures than before. Due to extreme temperatures, material properties may alter in operation resulting in severely reduced properties which may lead to disastrous failures during usage. Thermal properties play a significant role in design applications, determining safe operating temperatures, process control characteristics, and quality assurance of these materials.

#### **1.1 Objective**

The objective of this research is to develop a thermal properties database for the carbon-epoxy AS4/3501-6 composite. The AS4 carbon fiber used is a unidirectional continuous PAN based fiber. The 3501-6 epoxy resin is amine cured and provides low shrinkage during the curing process while maintaining excellent resistance to chemicals and solvents. The 3501-6 was developed to operate in a temperature environment of up to 350°F (177°C). The AS4/3501-6 carbon-epoxy composite used in the investigation is an 8-ply laminate compiled of laminas alternating between 0° and 90° orientations. The composite material has a high gloss and smooth black finish that was surface treated to improve the fiber-to-resin interfacial bond strength which met the Hexcel aerospace specification, HS-CP-5000.



The thermophysical properties of AS4/3501-6 carbon-epoxy have been investigated using experimental methods. The flash method was used to measure the thermal diffusivity of the composite (Doleman & Saad, 2013). This method is based on the American Society for Testing and Materials standard, ASTM E1461. In addition, the Differential Scanning Calorimeter was used in accordance with the ASTM E1269 standard to measure the specific heat. The measured thermal diffusivity, specific heat, and density data were used to compute the thermal conductivity of the AS4/3501-6 carbon-epoxy composite. Thermal conductivity is the property that determines the working temperature levels of the material; it plays a critical role in the performance of materials in high temperature applications, and it is an important parameter in problems involving heat transfer and thermal structures (Vital *et al.*, 2013).

## **1.2 About the Composite**

The materials used in the investigation were developed and fabricated at the Center for Composite Materials Research (CCMR) at North Carolina A&T State University. The mechanical properties of the AS4 composite have been measured (Akangah & Shivakumar, 2013). The AS4/3501-6 autoclave processed carbon/epoxy composite was made from a unidirectional [non-woven] carbon fiber/epoxy tape pre-preg molded in its particular [8-ply 0/90°] stacking sequence of the following specification: fiber area weight of 150 gram per square meter with a resin content of 33% [that is 33% weight portion of the uncured pre-preg tape, which is the area weight of the fiber plus the area weight of the resin =  $150 \text{ g/m}^2$  (fiber) +  $74 \text{ g/m}^2$  (resin) =  $224 \text{ g/m}^2$  (total area weight of the uncured pre-preg)] (Baker *et al.*, 2011). AS4/3501-6 is a carbon composite commonly used and recommended for general purpose structural applications (U.S. Department of Defense, 1999). Manufactured by Hexcel Corporation, the AS4's epoxy resin has properties that allows for the composite to withstand

temperatures up to 200°C as well as provide a high strength to weight ratio. In short, it can withstand some high temperature applications and also provide the light weight desired in these industries to reduce fuel consumption for wind power turbine blades (Hexcel, 1998; Hexcel, 2010).



*Figure 1.1 AS4/3501-6 Carbon-Epoxy Composite Sample*

**1.2.3 SEM Images** The following images were created using the scanning electron microscope (SEM) located in the Interdisciplinary Research Center (IRC) on the campus of North Carolina A&T State University (A&T). Both images, Figures 1.2 and 1.3, were captured at a distance of roughly 17 mm from the sample and at a voltage of 5.0 kV. The SEM is capable of magnifications from about 10 to 500,000 times. Figure 1.2 shows a magnification of 100 times and Figure 1.3 shows a magnification of 100 times. Because the SEM uses secondary and back scattered electrons to capture images and produces a single value per pixel, the image will only display black and white. To focus the image, one can only make changes to the contrast, brightness, focus, and astigmatism. The SEM provides a closer look at the makeup of the AS4/3501-6 carbon-epoxy composite to further analyze the structure and nature of the material.

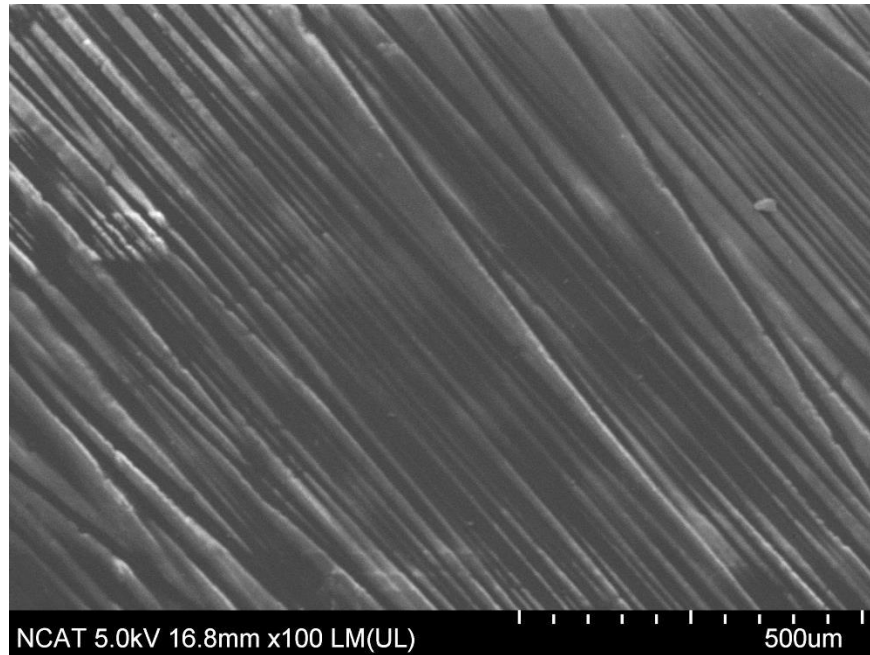


*Figure 1.2.* 100x Magnification SEM Image of the AS4/3501-6 Composite

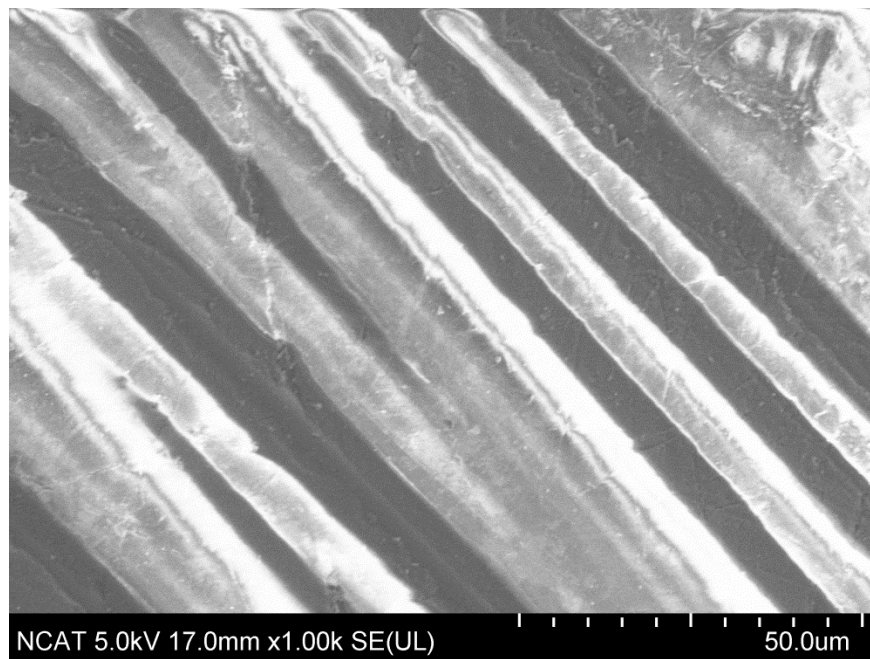


*Figure 1.3.* 1000x Magnification SEM Image of the AS4/3501-6 Composite

From the SEM image in Figure 1.3, the carbon fibers are represented by the brighter parts of the image, and the 3501-6 epoxy resin has a much duller color. This is because the electrons will bounce off of the carbon fiber much more than the resin, and therefore, the carbon fiber

produces a brighter and lighter image. The carbon atoms of the AS4 are bonded together in crystals aligned parallel to the unidirectional axis which gives the fiber a high strength-to-volume ratio. Properties of carbon fibers are high stiffness and tensile strength, low weight, high chemical resistance and temperature tolerance, and low thermal expansion. The thickness of the carbon fibers of the AS4 composite range from about five microns to about 10 microns. With a one-hundred times magnification as shown in Figure 1.2, one can take a closer look at the unidirectional PAN based fibers of the AS4/3501-6 carbon-epoxy composite. The combination of the AS4 carbon fiber and the 3501-6 epoxy matrix produces this unique composite material.

The AS4 carbon fiber is available in 3,000 (3K), 6,000 (6K), and 12,000 (12K) filament count tows. The filament count tow is not significant for this research because the AS4 used is pre-impregnated. This fiber has been surface treated and can be sized to improve its interlaminar shear properties, handling characteristics, and structural properties, and is suggested for use in weaving, prepregging, filament winding, braiding, and pultrusion (Hexcel, 2013). Table 1.1 shows the fiber properties provided by Hexcel.

Table 1.1

*Typical Fiber Properties of AS4 Carbon Fiber*

<i>Typical Fiber Properties</i>			
<i>Tensile Strength</i>	4,620 MPa	<i>Carbon Content</i>	94.0%
<i>Tensile Modulus</i>	231 GPa	<i>Specific Heat</i>	0.27 cal/g-°C
<i>Ultimate Elongation at Failure</i>	1.8%	<i>Electrical Resistivity</i>	1.7 x 10 <sup>-3</sup> ohm-cm
<i>Density</i>	1.79 g/cm <sup>3</sup>	<i>Coefficient of Thermal Expansion</i>	-0.63 ppm/°C
<i>Filament Diameter</i>	7.1 microns	<i>Thermal Conductivity</i>	6.83 W/m-°K
<i>Cross-Sectional Area</i>	0.12 mm <sup>2</sup>	<i>Twist</i>	Never Twisted

## CHAPTER 2

### Literature Review

#### 2.1 Heat Transfer

Thermodynamics examines the amount of heat transfer as a system goes through a process from one equilibrium state to another; however, it makes no reference to how long this process might actually take. In engineering, the interest is more along the lines of the rate of heat transfer. The three basic mechanisms of heat transfer are conduction, convection, and radiation. All of these three are related to the thermal conductivity. Conduction is the transfer of energy from the more energetic particles of a substance to the adjacent, less energetic ones as a result of interactions between the particles (Çengel, 1998).

Energy exists in various forms; however, the focus of this research is on heat and the characterization of materials undergoing thermal applications. Heat is the form of energy that can be transferred from one system to another as a result of temperature difference (Çengel, 1998). The second law of thermodynamics requires that heat be transferred in the direction of decreasing temperature. Thermal transfer, or heat transfer, is the science of determining the rates of such energy transfers. The many modes of heat transfer, although many occur simultaneously, can be independently analyzed.

Conduction can take place in solids as well as liquids and gases. In solids, conduction is due to the combination of energy transport by free electrons and vibrations of molecules. The rate of heat conduction through a material is contingent upon the thickness, the material itself, and the temperature difference across the material. The temperature difference and the area are proportional to the rate of heat conduction while the thickness is inversely proportional. The relationship is displayed in Equation (2.1).

$$\text{Rate of Heat Conduction} \propto \frac{(\text{Area})(\text{Temperature Difference})}{\text{Thickness}} \quad (2.1)$$

Including the thermal conductivity,  $k$ , which is a measure of the ability of a material to conduct heat, the relationship above can be rewritten to form the Fourier's law of heat conduction equation after Joseph Fourier who first voiced the equation in 1822.

$$\dot{Q}_{cond} = -kA \frac{dT}{dx} \quad (2.2)$$

where  $k$  is the thermal conductivity or constant of proportionality of the material in W/m·K,  $A$  is the heat transfer area which is always normal to the direction of heat transfer,  $dT/dx$  is the temperature gradient. Heat transfers in the direction of decreasing temperature; therefore, the temperature gradient becomes negative when temperature decreases with increasing thickness,  $dx$ . In Equation (2.2), the negative sign is added to make the transfer of heat in the positive  $x$  direction a positive value.

## 2.2 Thermal Conductivity

The thermal conductivity,  $k$ , of a material, in general, depends on the temperature,  $T$  (and therefore  $x$ ), and thus it cannot be taken out of the derivative in Equation (2.2). In most practical applications, the thermal conductivity can be assumed to remain constant at some average value. At constant conductivity and using one-dimensional analysis, the Fourier-Biot equation is formed.

$$\frac{1}{\alpha} \frac{\partial T}{\partial t} = \frac{\partial^2 T}{\partial x^2} + \frac{\dot{g}}{k} \quad (2.3)$$

where  $\dot{g}$  is the constant rate of heat generation per unit volume and  $\alpha$  is the thermal diffusivity in m<sup>2</sup>/s. Hahn & Özişik (2012) also executed an energy balance with constant thermal conductivity in a differential form:

$$\frac{1}{\alpha} \frac{\partial T}{\partial t} = \frac{\partial^2 T}{\partial x^2} + \frac{q}{k} \quad (2.4)$$

where  $q$  is the rate of heat conducted per unit volume in  $\text{W/m}^3$ .

Fourier's law of heat conduction is viewed by many scientists as the defining thermal conductivity equation. Thermal conductivity has a major role in thermal characterization because it is directly proportional to the flow of heat for a given temperature gradient. Thermal conductivity is defined as the rate of heat transfer through a unit thickness of the material per unit area per unit temperature difference (Çengel, 1998). In other words, the material property describing the ability to conduct energy is called thermal conductivity, and a conductor is generally a material with a high thermal conductivity because it can transfer heat energy relatively well (e.g., metals). An insulator has relatively poor conduction of heat energy and lower thermal conductivity values (e.g., wood).

### 2.3 Thermal Diffusivity

Thermal diffusivity is the ratio of the time derivative of temperature to its curvature. This quantity, more specifically, is the measure of the rate at which heat propagates through a material. Like all other units of measurement in this research, the International System of Units (SI) for thermal diffusivity is  $\text{m}^2/\text{s}$ . The thermal diffusivity,  $\alpha$ , and thermal conductivity,  $k$ , are related through a proportional relationship.

$$k = \rho c_p \alpha \quad (2.5)$$

Rearranging to solve for the thermal diffusivity yields:

$$\alpha = \frac{k}{\rho c_p} \quad (2.6)$$

where  $\rho$  is the density and  $c_p$  is the specific heat. The product of the density and specific heat is known as the volumetric heat capacity which represents the material storage capacity of energy per unit volume.

## 2.4 Theoretical Methods

Predicting the thermal properties of composite materials can be possible if there are first assumptions made about the flow of heat through the fibers, matrix, and other elements to make up the composite. Isotropic materials are especially predictable because they have the same properties in all directions including the axial direction. Using Hull & Clyne (1996) rule of mixtures, the thermal conductivity can be found because the thermal gradient is the same throughout the composite.

$$k_{1C} = V_f k_{1f} + V_m k_m \quad (2.7)$$

where  $k_{1C}$  is the in-plane thermal conductivity of the composite,  $V_f$  is the fiber volume fraction,  $k_{1f}$  is the in-plane thermal conductivity of the fiber,  $V_m$  is the matrix volume fraction, and  $k_m$  is the thermal conductivity of the matrix. When looking at the AS4/3501-6 carbon-epoxy composite, the AS4 carbon fiber is the reinforcement, and the 3501-6 epoxy resin is the composite's matrix.

Salazar (2003) also found that using the rule of mixtures in a similar equation was more suitable for composite materials than the Fourier's law of heat conduction and the general heat conduction equation. Because materials are more heterogeneous in nature, the properties of these materials are discontinuous functions depending on locality. The rule of mixtures equation can be compared to electrical circuits when adding resistors that are in parallel. Taking the inverse of the in-plane thermal conductivity,  $k_{1C}$ , in Equation (2.7), the following equation is produced:



$$\frac{1}{k_1} = \frac{V_f}{k_{1f}} + \frac{V_m}{K_m} \quad (2.8)$$

where  $k_1$  is now the minimum thermal conductivity. Using these equations, a relationship can now be developed to calculate the thermal diffusivity in both the in-plane and transverse direction.

$$\alpha_x = \frac{k_{1c}}{\rho c_p} = \frac{v_1 k_{1f} + v_2 k_2}{v_1 \frac{k_{1f}}{\alpha_1} + v_2 \frac{k_2}{\alpha_2}} \quad (2.9)$$

where  $\alpha_x$  is the thermal diffusivity in the in-plane direction, and:

$$\frac{1}{\alpha_y} = \frac{\rho c_p}{k_1} = \frac{v_1^2}{\alpha_1} + \frac{v_2^2}{\alpha_2} + v_1 v_2 \left( \frac{k_2}{k_{1f} \alpha_2} + \frac{k_{1f}}{k_2 \alpha_1} \right) \quad (2.10)$$

where  $\alpha_y$  is the transverse direction.

If the fiber and matrix thermal conductivities are similar, the many models that predict the transverse thermal conductivity of composite would be applicable. If the fiber conductivity substantially exceeds the matrix conductivity, certain problems can arise (Wetherhold & Wang, 1994). Because the thermal conductivity of the AS4 carbon fiber does not coincide with the assumptions made for this technique, they cannot be utilized in this research.

## 2.5 Experimental Methods

Thermal Wave Interferometry (TWI) is one way of the available techniques to measure the thermal diffusivity of a material. There are also Thermographic and flash methods available including the xenon flash method which is used in this research and the laser flash method. TWI is used to measure the thermal diffusivity of coatings and thin slabs (Cernuschi *et al.*, 2002). This method uses thermal waves with specific angular frequencies to propagate through the material

layers. The waves reflect and then transmit, like conventional waves, at the separation surface of the materials. The measurement comes from the interference between propagating and reflected waves which alter the amplitude and phase of the AC component of the surface temperature. This method, however, is not commonly used.

The method where a Gaussian shaped source instantaneously heats an infinite slab is called the Thermographic method. This method focuses on the temperature at the rear of the slab surface. The distribution of the temperature only assumes an infinite testing specimen. Use the Thermographic method in order to determine the in-plane thermal diffusivity. Note that the material used here must be much larger in diameter when compared with the flash method.

The flash method is the most common method to determine the thermal diffusivity. Below is a block diagram of a flash system. For the flash source, a lamp or a laser can be used to create the instantaneous pulse, and for the detector, thermocouples, an infrared detector, or any other temperature recording device can be used. In this research, an infrared detector was used to measure the temperature difference across the material.

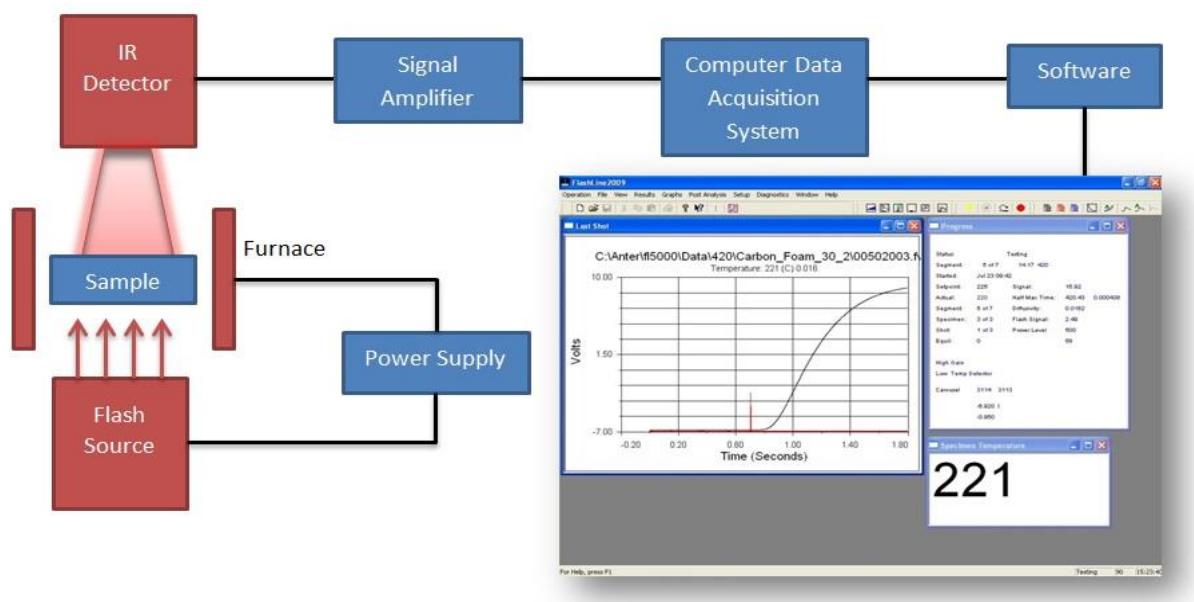


Figure 2.1. Block Diagram of a Flash System

## 2.6 Thermal Contact Resistance

When analyzing heat conduction through multiple layers of solids, perfect contact is assumed at the interface of the layers. The contact point between two materials, in actuality, is never perfectly smooth and is, in fact, very rough. To the naked eye, two surfaces may appear to have good thermal contact, but under a microscope, there is a different story. Taking a closer look, one will see peaks and valleys where the peaks cause good contact, but the valleys will form voids filled with air. Thus, an interface offers some resistance to heat transfer, and this resistance per unit interface area is called the thermal contact resistance,  $R_c$  (Çengel, 1998).

$$\dot{Q} = \dot{Q}_{contact} + \dot{Q}_{gap} \quad (2.11)$$

The solid contact spots and the gaps in the noncontact areas equation can also be expressed in an analogous manner to Newton's law of cooling as:

$$\dot{Q} = h_c A \Delta T_{interface} \quad (2.12)$$

where  $A$  is the apparent interface area,  $\Delta T_{interface}$  is the effective temperature difference at the interface, and  $h_c$  is the thermal contact conductance or convection heat transfer coefficient.  $h_c$  is represented by:

$$h_c = \frac{\dot{Q}/A}{\Delta T_{interface}} \quad (2.13)$$

The thermal contact resistance,  $R_c$ , in  $m^2 \cdot ^\circ C/W$ , can now be given by:

$$R_c = \frac{1}{h_c} = \frac{\Delta T_{interface}}{\dot{Q}/A} \quad (2.14)$$

## CHAPTER 3

### Methodology Measurements

#### 3.1 Thermal Diffusivity

In order to determine the working temperature levels of a material, it is expedient to measure how rapidly heat will pass through that material. This measurement, or property, is called thermal diffusivity. Thermal diffusivity plays a critical role in the performance of materials in high temperature applications, and this material property can be measured in several different ways. There are steady-state methods as well as transient techniques. Available procedures include Thermal Wave Interferometry (TWI), Thermographic methods, the Flash Method, the Hot-wire method, and others. Transient techniques have been preferred in measuring thermal properties of materials more recently; however, the Flash Method is the most common of these methods (Nunes dos Santos, 2007; Patrick & Saad, 2012).

**3.1.1 The Flash Method.** In 1961, W.J. Parker founded the Flash method, and it is the most frequently used transient photothermal technique and it has the versatility of using a laser or lamp as the energy source. In many countries, it is considered a standard for thermal diffusivity measurement of solid materials (Cernuschi *et al.*, 2004). It can also be used to measure the thermal conductivity as well (Wei, 1989). Being embraced by the United States, the laser flash method is a standard test method and is defined by the American Society for Testing and Materials E1461 standard. It involves a small cylindrical, thin disk specimen being heated to a desired temperature, usually between 20 and 500°C. Once the disk has reached the specified temperature the front face is subjected to an instantaneous radiant energy pulse as shown in Figure 3.1. The energy source can be a laser or a lamp. A detector measures the resulting temperature change with respect to time on the rear face of the sample. The data acquisition

system then records the temperature change of the rear face of the specimen versus time. A graphical representation of this data is called the thermogram of the flash. Figure 3.2 displays the theoretical model thermogram. The time in which it takes the rear face of the specimen to reach half the maximum temperature rise is called the half-time,  $t_{1/2}$ .

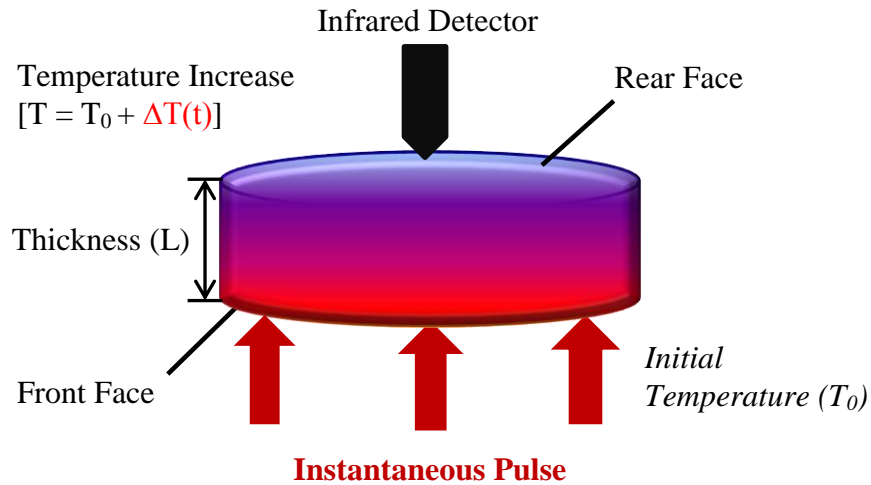


Figure 3.1. Schematic of the Flash Method

Employing Carslaw and Jaeger's equation of the temperature distribution within a thermally insulated solid of uniform thickness  $L$ , Parker *et al.* (1961) was able to derive a mathematical expression to calculate thermal diffusivity (Carslaw *et al.*, (1959). An abbreviated version of this derivation is given as:

$$T(x, t) = \frac{1}{L} \int_0^L T(x, 0) dx + \frac{2}{L} \sum_{n=1}^{\infty} \exp\left(\frac{-n^2 \pi^2 \alpha t}{L^2}\right) \cos \frac{n\pi x}{L} \int_0^L T(x, 0) \cos \frac{n\pi x}{L} dx \quad (3.1)$$

where  $\alpha$  is the thermal diffusivity of the solid material. If a pulse of radiant energy,  $Q$ , is instantaneously and uniformly absorbed into a small depth referred as  $g$ , at the front face ( $x=0$ ) of the thermally insulated solid material, the temperature distribution at that initial point is given by:

$$T(x, 0) = \frac{Q}{\rho \cdot c_p \cdot g} \quad \text{for } 0 < x < g \quad (3.2)$$

$$T(x, 0) = 0 \quad \text{for } g < x < L \quad (3.3)$$

These initial conditions are substituted into the temperature distribution equation above. It is considered that the very small depth  $g$  of an opaque solid will yield a small angle. It is also known that for a very small angle,  $\theta$ ,  $\sin(\theta) \approx \theta$  and  $\cos(n\pi x/L) = (-1)^n$ . Applying these two expressions, the temperature distribution at the rear face ( $x=L$ ) is:

$$T(L, t) = \frac{Q}{\rho \cdot C \cdot L} \left[ 1 + 2 \sum_{n=1}^{\infty} (-1)^n \exp\left(\frac{-n^2 \pi^2}{L^2} \alpha t\right) \right] \quad (3.4)$$

Parker *et al.* (1961) then defined two dimensionless parameters,  $V$  and  $\omega$  as:

$$V(L, t) = \frac{T(L, t)}{T_m} \quad (3.5)$$

$$\omega = \frac{\pi^2 \alpha t}{L^2} \quad (3.6)$$

where  $T_m$  is the maximum temperature at the rear face. Combining Equations (3.4), (3.5), and (3.6) results in (Parker *et al.*, 1961):

$$V = 1 + 2 \sum_{n=1}^{\infty} (-1)^n \exp(-n^2 \cdot \omega) \quad (3.7)$$

Setting  $V = 0.5$  allows for the determination of  $\omega$ , and then substitution into Equation (3.7) allows for a mathematical equation for thermal diffusivity to be stated as:

$$\alpha = 0.1388 \frac{L^2}{t_{1/2}} \quad (3.8)$$

This derivation by W.J. Parker is a theoretical model of the flash method and is the ideal case. It assumes that the specimen is mostly homogeneous and isotropic, that there is one dimensional heat flow, and that there are no heat losses from the specimen (Cernuschi *et al.*, 2002). It also assumes that energy pulse is uniformly subjected across the front face of the specimen and that the pulse is instantaneous. Because of this assumption, many researchers have developed correction factors since the time of Parker's original derivation. These include, but are not limited to, Cowan, Clark and Taylor, Koski, and Heckman (Beck & Dinwiddie, 1995). Each of these correction factors use different methods or a combination of methods to reanalyze the theoretical model and impose additional parameters to improve accuracy of the result. The Clark and Taylor correction factor accounts for radiation heat losses and is used in the research conducted in this experiment. Clark and Taylor (1975) examined the thermogram at different points immediately before the maximum temperature rise was reached and developed a correction factor. The correction factor is calculated using the following equation:

$$K_r = -0.3461467 + 0.361578 \left( \frac{t_{3/4}}{t_{1/4}} \right) - 0.06520543 \left( \frac{t_{3/4}}{t_{1/4}} \right)^2 \quad (3.9)$$

Instead of taking the half-time, the ratio between the time to reach 25% and 75% of the maximum temperature change was used. The corrected thermal diffusivity equation is now defined by Clark and Taylor as:

$$\alpha_{corrected} = \frac{\alpha K_r}{0.13885} \quad (3.10)$$

**3.1.2 Experimental Apparatus.** In general, the ASTM E1461 standard (2007) provides the minimum requirements for the apparatus. The key components are the flash source, specimen holder, temperature response detector, recording device, and an environmental enclosure is needed when testing above and below room temperature (ASTM, 2007). The flash source can be any device able to emit a quick energy pulse, usually a lamp or laser. The apparatus used in this facility was commercialized and purchased from Anter Corporation. The name of the apparatus is the FlashLine™ 2000, and it utilizes a high intensity xenon lamp as the pulse source. The pulse duration time should be less than 2% halftime of the specimen to be measured in order to keep the error due to finite pulse less than 0.5%. The apparatus is automated and capable of testing up to four specimens in each run. The technical specifications are displayed in Table 3.1 below.

Table 3.1

*Technical Specifications of the FlashLine™ 2000 Thermal Properties Analyzer*

<i>Technical Specifications</i>	
<i>Pulse Source:</i>	High Speed Xenon Discharge
<i>Thermal Diffusivity Range:</i>	0.001 – 10 cm <sup>2</sup> /s
<i>Operating Temperature Range:</i>	Room Temperature to 330°C
<i>Furnace:</i>	Nichrome Heaters
<i>Atmosphere:</i>	Air or Inert Gas Purge
<i>Interlock:</i>	Four Sample (Indexed) System
<i>Testing Samples</i>	Cylindrical shape, 1 – 6 mm thick, 6 – 30 mm diameter, wide range of materials and compositions
<i>Cooling Options:</i>	LN <sub>2</sub>



Figure 3.2, from left to right, shows the experimental setup which includes the FlashLine™ 2000 Thermal Properties Analyzer, the i401 My Weigh® scale with a weighing capacity of up to 400g, and the computer data acquisition system utilizing Windows XP.



*Figure 3.2.* Experimental Setup for the Thermal Diffusivity

The thermal property analyzer also contains a vacuum capable environmental enclosure in which nitrogen gas is used to evacuate the chamber. The detector should be any sensor that can measure a linear electrical output proportional to a small temperature rise, and it, along with its amplifier, must have a response time of no more than 2% of the half-time. The Indium Antimonide (InSb) Infrared Detector outputs a linear electrical signal proportional to a small temperature change experienced by the rear face of the specimen after the energy pulse has been initiated. The data acquisition system can be pre-programmed within one time period for the acceptable resolution of at least 1% for the quickest thermogram the system can deliver (ASTM, 2007). Figure 3.3 shows the normalized temperature versus the normalized time.

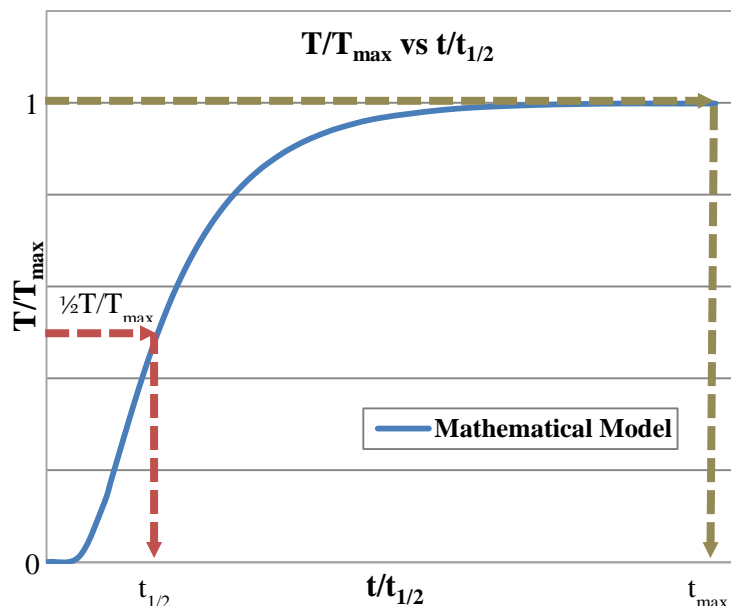


Figure 3.3. The Flash Method Thermogram

### 3.2 Specific Heat

Specific heat is a measurement of the amount of heat per unit mass that is required to raise the temperature of a material on degree Celsius. The differential scanning calorimetry (DSC) technique was used to measure the specific heat of the materials. This technique is based on the measurement of the change of the difference in the heat flow rate to the sample and to a reference sample while they are subjected to a controlled temperature program (Höhne *et al.*, 2003). Using the measured heat flow rate of the sample, differential scanning calorimetry can determine how a material's heat capacity varies with respect to temperature.

**3.2.1 Differential Scanning Calorimetry (DSC).** Widely used for the measurement of specific heat, differential scanning calorimetry (DSC) is a thermoanalytical technique. Its methodology is defined by the ASTM E1269 standard. When performing a differential scanning calorimetry measurement a test specimen and reference are enclosed in the same furnace together on a metallic block with high thermal conductivity within the calorimeter. The metallic

block ensures a good heat-flow path between the specimen and reference. The sample and the reference are subjected to an identical temperature program. The heat capacity change in the specimen differs from that of the reference. The calorimeter measures the temperature difference and calculates heat flow from calibration data. As a result, the specific heat of the sample can be calculated using the heat flow results. Differential scanning calorimetry is an ASTM test method standard for determining specific heat capacity (ASTM, 2005).

To calculate the specific heat of an unknown material, the heat flux of the unknown and a reference must be measured using the differential scanning calorimeter. Using the measured heat flux and the known specific heat of the reference, the specific heat of the unknown material can be calculated by using the ratio method technique. Since the differential scanning calorimeter is at constant pressure, the change in enthalpy of the reference is equal to the heat absorbed or released by the reference (ASTM, 2005). The mathematical depiction is:

$$dQ = (m)dh \quad (3.11)$$

Equation (3.11) leads to the following relationship:

$$\dot{Q} = m \frac{dh}{dt} = m \frac{dq}{dt} \quad (3.12)$$

where  $dq/dt$  is the heat flux, and  $dh/dt$  is the change of enthalpy with respect to time. At constant pressure, the relationship for specific heat can be written as:

$$c_p = \frac{1}{m} \frac{dH}{dT} \quad (3.13)$$

Using chain rule the relation for specific heat can be written as:

$$c_p = \frac{1}{m} \frac{dt}{dT} \frac{dH}{dt} = \frac{1}{m} \frac{dQ}{dt} \frac{dt}{dT} \quad (3.14)$$

From Equations (3.12) and (3.14) the specific heat can be written as:

$$c_p = \frac{\left(\frac{dQ}{dt}\right) \left(\frac{dt}{dT}\right)}{m} \quad (3.15)$$

where the  $dt/dT$  is the inverse temperature distribution over time. Using Equation (3.15) and the ratio method, the calibration constant is multiplied through the specific heat equation for the reference.

$$c_{p_{ref}} = E \frac{\left(\frac{dQ}{dt}\right)_{ref} \left(\frac{dt}{dT}\right)}{m_{ref}} \quad (3.16)$$

Solving for the calibration constant:

$$E = \frac{c_{p_{ref}} m_{ref}}{\left(\frac{dQ}{dt}\right)_{ref} \left(\frac{dt}{dT}\right)} \quad (3.17)$$

To determine the specific heat for the unknown material, Equation (3.16) is used again but in terms of the sample.

$$c_p = \frac{E}{m} \left(\frac{dQ}{dt}\right) \left(\frac{dt}{dT}\right) \quad (3.18)$$

Substituting Equation (3.17) into equation (3.18):

$$c_p = \left[ \frac{c_{p_{ref}} m_{ref}}{\left(\frac{dQ}{dt}\right)_{ref} \left(\frac{dt}{dT}\right)} \right] \frac{1}{m} \left(\frac{dQ}{dt}\right) \left(\frac{dt}{dT}\right) \quad (3.19)$$

The above equation can be written as:

$$c_p = c_{p_{ref}} \frac{m_{ref}}{m} \frac{\left(\frac{dQ}{dt}\right)}{\left(\frac{dQ}{dt}\right)_{ref}} \quad (3.20)$$

**3.2.2 Experimental Apparatus.** The calorimeter used in this research is the DSC 200 F3 Maia®, Differential Scanning Calorimeter manufactured by NETZSCH. It is a heat flux system that combines high stability, high resolution, and fast response time throughout a substantial temperature range. With the addition of the Intracooler 40, the temperature range extends from ambient temperature to cryostatic temperatures covering a larger temperature spectrum (-40°C to 600°C). The heating rate is adjustable from as low as 0.001K/min to as high as 100K/min while keeping a temperature accuracy of 0.1 K. Figure 3.4 shows the apparatus, Figure 3.5 shows a profile view of the interior workings of the calorimeter, and Table 3.2 shows the apparatus specifications provided by the company (NETZSCH, 2008).



*Figure 3.4.* Experimental Setup of the DSC 200 F3 Maia® and Intracooler

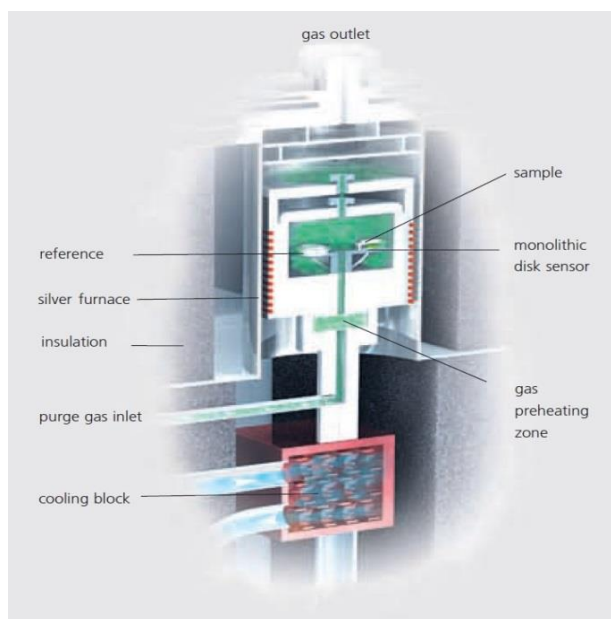


Figure 3.5. Cross-Section Diagram of the Differential Scanning Calorimeter

Table 3.2

*Technical Specifications of the DSC 200 F3 Maia®*

<i>Technical Specifications</i>	
<i>Temperature Range:</i>	-170 °C to 600 °C
<i>Heating Rates:</i>	0.001 K/min to 100 K/min
<i>Cooling Rates:</i>	0.001 K/min to 100 K/min (depending on temp.)
<i>Sensor:</i>	Heat flux system
<i>Measurement Range:</i>	0 mW to $\pm 600$ mW
<i>Temperature Accuracy:</i>	0.1 K
<i>Enthalpy Accuracy:</i>	< 1%
<i>Cooling Options:</i>	Forced air, LN <sub>2</sub> , Intracooler
<i>Atmospheres:</i>	oxid., inert (static, dynamic)
<i>Automatic Sample Changer:</i>	for up to 20 samples and references (optional)

The DSC 200 F3 Maia® Differential Scanning Calorimeter consists of a furnace block, sample chamber, cooling system, heat flux sensor, and purge gas. The furnace block contains a miniature jacketed heater that provides the source of heat during the experiment. The furnace temperature is measured by a thermocouple integrated into the furnace walls. The sample chamber is sealed within the instrument's lid, and has two additional lids to prevent a contamination from outside sources. The system's temperature can be reduced by using an Intracooler device. The calorimeter uses a high sensitivity type E heat flux sensor for its measurements (NETZSCH, 2008).

## CHAPTER 4

### Experimental Procedure

#### 4.1 Thermal Diffusivity

**4.1.1 Test Specimen Preparation.** The test specimens were prepared to be thin circular disks of 10 to 30 mm in diameter, whose front face surface area is less than that of the energy pulse beam. According to ASTM E1461 standard (2007) each specimen should be thick enough to be representative of the test material but remain within 1 to 6 mm range. Overall, the optimum thickness depends upon the magnitude of the estimated thermal diffusivity, and should be chosen so that the time to reach half of the maximum temperature falls within the 10 to 1000 ms range. In order to accomplish these specified dimensions, a drill press equipped with a diamond plated drill bit was used to cut the material to the appropriate diameter. When necessary, the specimens were milled to achieve the preferred thickness. The thermal diffusivity samples of the composite are shown in Figure 4.1.

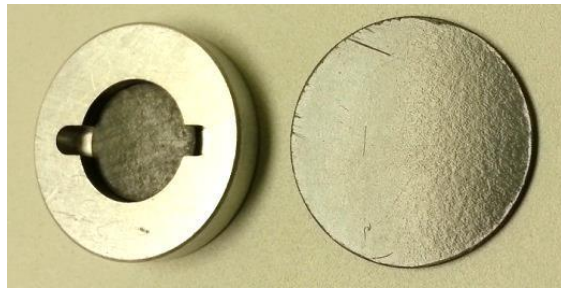


*Figure 4.1.* Thermal Diffusivity Sample Specimens of AS4/3501-6

The 12.69 mm (0.50 inch) diameter sample requires an adapter to be used in the testing apparatus. There is no difference in the results between the two. Both the rear and front faces were flat and parallel within 0.5% of their thickness to maintain pulse uniformity. The standard suggests that a thin, uniform layer of graphite be applied to both faces of the specimens to improve the capability of absorbing the applied energy flash by reducing the reflection from the



specimen. This was not necessary for the experiments performed in this work due to the material nature of the AS4 composite. Because the composite is a black body and will absorb the pulse energy, it does not need surface treatment.

**4.1.2 Experimental Procedure.** The experiments were conducted following the testing standard, ASTM E1461. 12.7 mm (0.5 inch) and 25.4 mm (1 inch) diameter samples were used depending on the availability or size limitations of the material. This will not account for any changes in the thermal diffusivity. The diameter, thickness, mass, and density were documented. Each sample was placed in the specimen holder housed inside a vacuum sealed environmental enclosure. The environmental enclosure was purged using nitrogen gas to form an inert environment for the samples.

Approximately 1 L of liquid nitrogen was manually poured in the receptacle of the IR detector. The thickness, diameter, and mass were input into the FlashLine™ 2000 System, and the test was initiated at ambient temperature. Each sample was tested to a maximum temperature of 170°C. At each designated temperature, a minimum of three flashes were performed at a time. The results were compiled, analyzed, and necessary corrections were made. The time required for each experimental run varies depending on the range of temperatures tested and the temperature increment.

**4.1.3 Computational Procedure.** The following is a step by step procedure for running thermal diffusivity measurements using the xenon flash method and the Anter Corporation FlashLine™ 2000 software. Step one is to open the software. The platform is displayed in Figure 4.2.

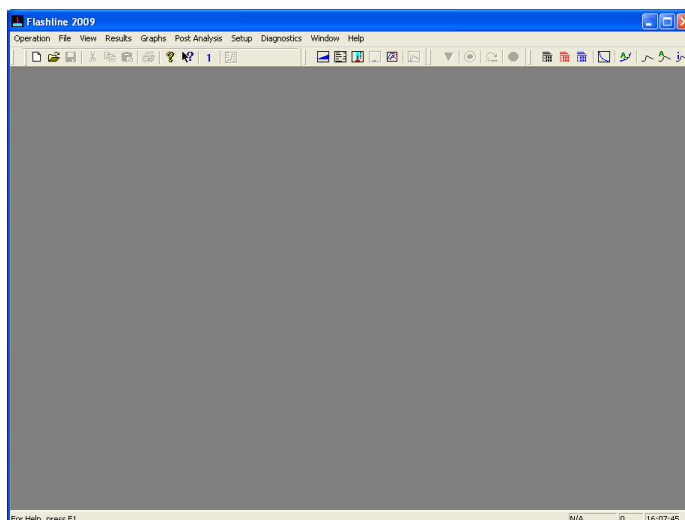


*Figure 4.2.* Initial FlashLine™ 2000 Software Window

From here, click on “Operation” and then “Startup Information.” The next window to appear will be the furnace type selection. There should only be one furnace type which is the “2000” furnace. Select “OK.” Turn the FlashLine™ 2000 Thermal Properties Analyzer apparatus on in order to use the “Controller Parameter File.” Select “Yes.”



*Figure 4.3.* Hardware Interlock Enable on the FlashLine™ Apparatus

Press the “Hardware Enable” button on the apparatus to enable carousel movement. Press firmly until the green light comes on as displayed in Figure 4.3.

Load the specimens desired for testing and note the position (one to four) in which each specimen is placed. Enter the test and specimen information as shown in Figure 4.4, and select “Start Test.” Make sure the environment has been purged and the Indium detector is full of liquid nitrogen as shown in Figure 4.5.

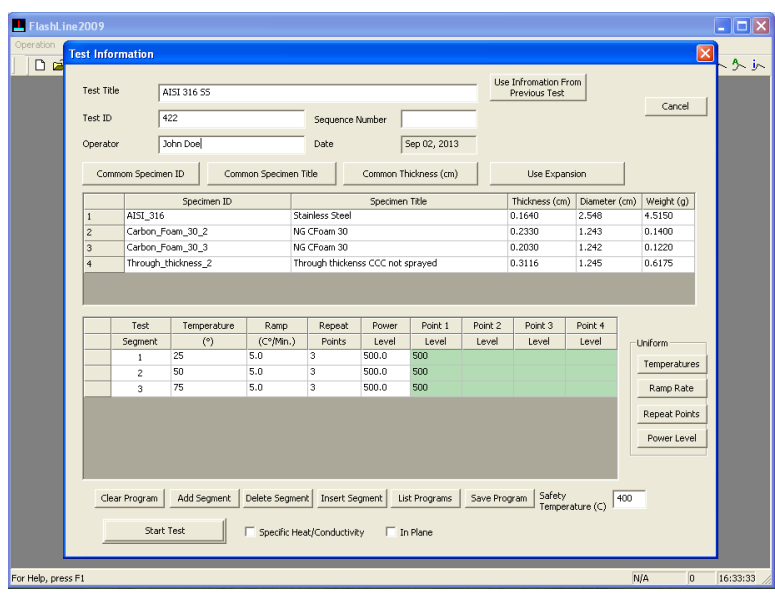


Figure 4.4. Test Information Window

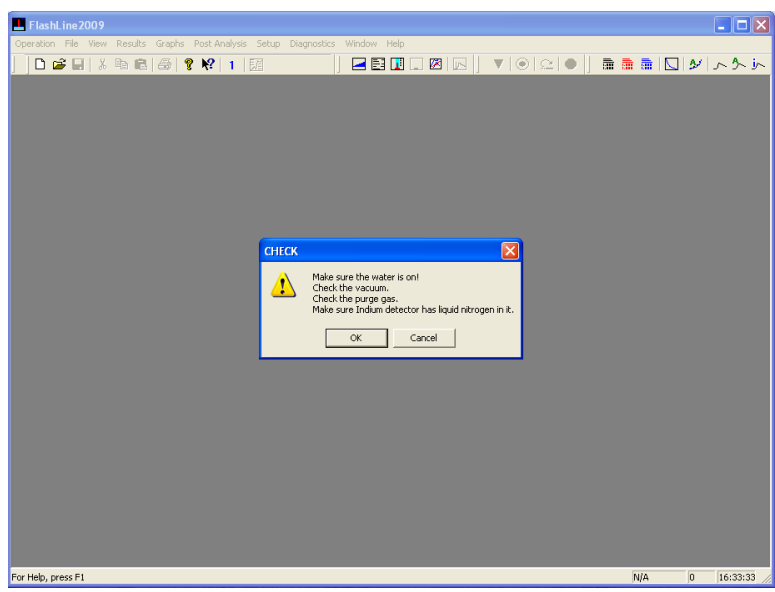
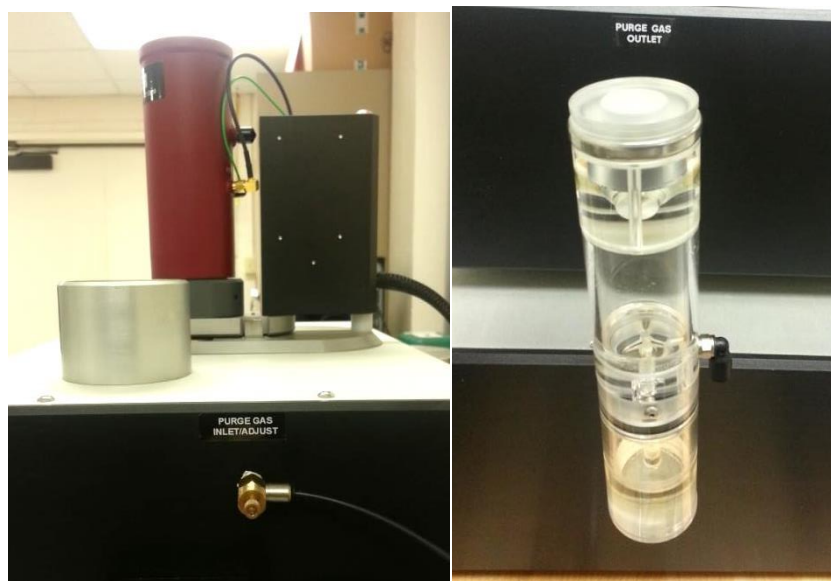


Figure 4.5. Oil, Vacuum, Gas, and Detector Check Window

(Note: Allow for half an hour of periodic pouring of liquid nitrogen in order to fill the Indium detector. If the liquid nitrogen is continuously poured, it will continue to boil and cause condensation to freeze inside the detector. The Indium detector needs to cool down dramatically for it to fill up with liquid nitrogen.)



*Figure 4.6.* Purge Gas Inlet Adjuster and the Purge Gas Outlet Oiler

After the compressed nitrogen gas is set to about 5 psi, adjust the gas inlet knob, as shown in Figure 4.6, so that the bubbles in the purge gas outlet oiler appear approximately 3 times per second. The inlet is located on the right of the apparatus and the oiler on the left side of the apparatus. Press the “ON” button to turn on the manual interlock, and then select “OK” in the “Manual Interlock” window. The test will commence.

Figure 4.7 shows the testing output screen after a flash has been fired. The window shows important information regarding the status of the test. Always check the half-time to make sure that it is within the acceptable range. In addition, if the volts vs. time graph has noise in it, this could be an indication that there is little to no liquid nitrogen in the Indium detector.

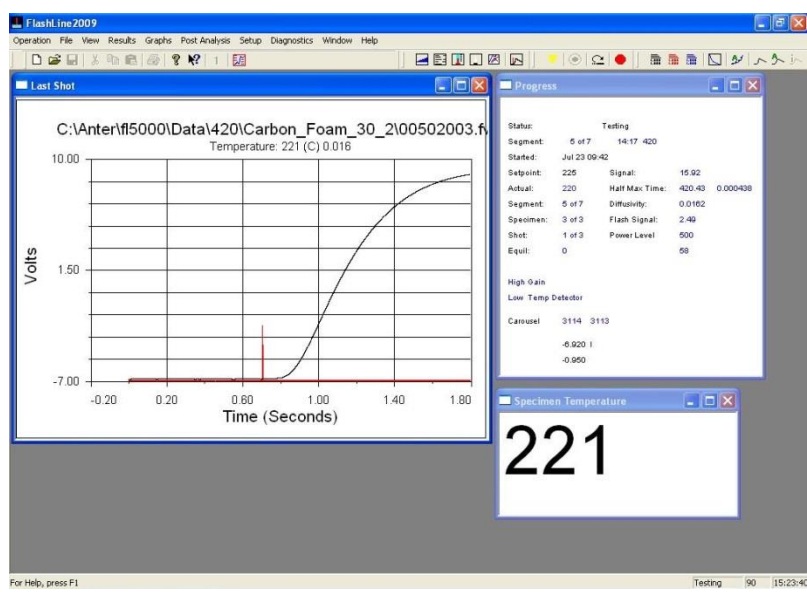


Figure 4.7. Testing Window with the Last Shot

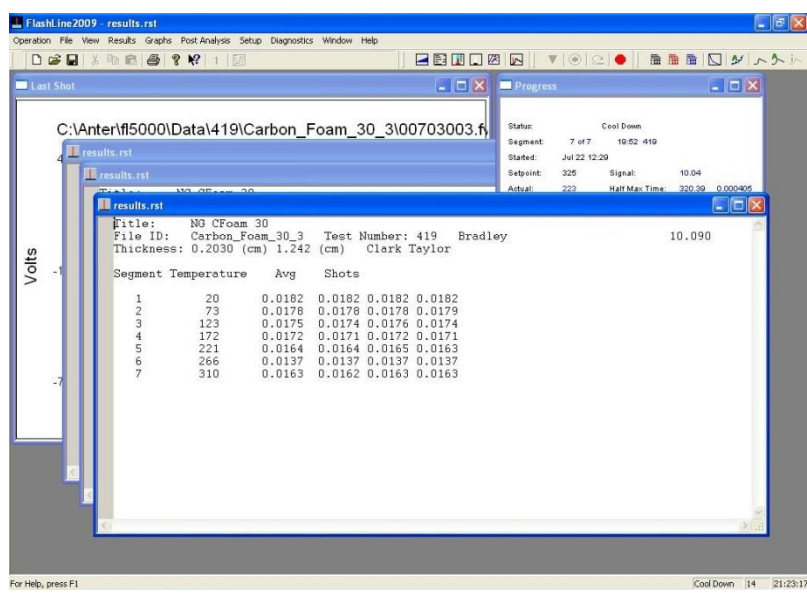


Figure 4.8. Test Completion and Displayed Results

Figure 4.8 shows the results of the completed test. The test duration can range from a few hours up to as much as 24 hours depending on the number of shots, temperature range, and the time increment that is chosen. If running a longer test, it is important to refill the liquid nitrogen indium detector about halfway through the test in order to ensure that there is no noise in the graph and also that the results will be accurate. (Note: During testing, only fill the Indium

detector with liquid nitrogen while the apparatus is heating and not while it is shooting. The data can be altered if the apparatus is not stable during the shots.) If there is anything else wrong with the test run (e.g., the gas is not thoroughly purged or the half-times are too high or too low), this will be indicated by noise in the “Last Shot” graph.

Once the test is completed, the data is now ready to be analyzed further in Excel. Note the folder in which the data was saved. After opening this folder, each sample folder will be displayed. Open a sample folder, and find the files named “results.all,” “results.clt,” and the files with the extension “.fw0.” The results files will provide the thermal diffusivity results, and the “.fw0” extension files will provide the thermogram data. The results files are easily imported into Excel for analyzing.

In order to convert the “.fw0” extension files into Excel compatibility, open the FlashLine™ 2000 software. Select the tab “Post Analysis” and click “Shot to Text File.” Select the file and sample folder that contains the “.fw0” extension. Change the “Files of Type” to “.fw0” to display the corresponding extension files, select a file, and click “OK.” (Note: Only one file can be converted to a text file at a time.) A “Copy Successful” should be displayed. Note the folder in which the text file was saved. Repeat these steps as necessary, and import the text files into excel for analyzing. See Appendix B for the complete computational procedure for thermal diffusivity.

## 4.2 Specific Heat

**4.2.1 Test Specimen Preparation.** Good thermal contact between the heat flux sensor and sample is vital for optimum results. To achieve this, the sample should lay as flat as possible with the bottom of the aluminum crucible. The samples were cut using a hole saw and drill press to less than 4 mm or 6 mm in diameter in order to fit within the 4 mm and 6 mm diameter crucibles. A 1-mm thick sample can be used with this equipment using the corresponding crucible size. Each sample was then weighed three times, and the average mass was documented. The samples were placed into the crucible, and it is important to note that the samples must be in the same position inside the crucible for each test run. The lid was positioned on top of the crucible to fully enclose the sample.

Using tweezers, the aluminum crucibles are carefully placed on the heat flux sensor making sure that the crucibles are centered on the sensor and also in the same position for each test run. This will decrease the thermal contact resistance and other erroneous variables. The faces of the samples must be flat and parallel. A picture of the AS4 composite in an aluminum crucible is shown in Figure 4.9.



*Figure 4.9.* Specific Heat Sample Specimen of AS4/3501-6

**4.2.2 Experimental Procedure.** The differential scanning calorimetry experiment was performed following the ASTM E1269 testing standard for determining specific heat. The differential scanning calorimeter and data acquisition system were initialized and were allowed

to reach thermal equilibrium. During this period the apparatus was purged with argon gas at a rate of 50 mL/min to produce an inert testing atmosphere. To measure the specific heat of a sample a minimum of three runs must be performed.

Before the specific heat of the AS4 composite was determined, baseline and reference tests were performed. Since the samples were placed inside an aluminum crucible for testing, the crucible will add a contact resistance to the samples. The baseline corrects for this contact resistance increasing the accuracy of the results. The initial baseline run was performed by placing two empty crucibles in the designated location on heat flux sensors as seen in Figure 4.10. The furnace was heated to the designated initial temperature of the program, and held there isothermally at least four minutes while the calorimeter recorded the thermal curve. The crucibles were heated to the final temperature at rate of 20°C/min and held isothermally again while the calorimeter recorded the thermal curve.



*Figure 4.10.* Crucibles Placed on the Heat Flux Sensor

Following the baseline run, the calorimeter testing chamber was cooled to ambient temperature. The crucible on reference location in the testing chamber was replaced with a sapphire reference. After applying the previous baseline to correct for the aluminum crucible, the same temperature program used for the baseline was executed for the sapphire reference. The



measured specific heat of the sapphire was compared to the known specific heat value for sapphire to determine the error. The test was repeated for the AS4/3501-6 samples. To verify that the baseline did not alter, a baseline was established after every fourth test. Using the measured sapphire as a reference, the ratio method was used to determine the specific heat of the AS4 carbon-epoxy.

**4.2.3 Computational Procedure.** The following is a step by step procedure for running specific heat measurements using differential scanning calorimetry and the NETSZCH DSC Measurement software. Step one is to open the software. Figure 4.11 will be displayed.

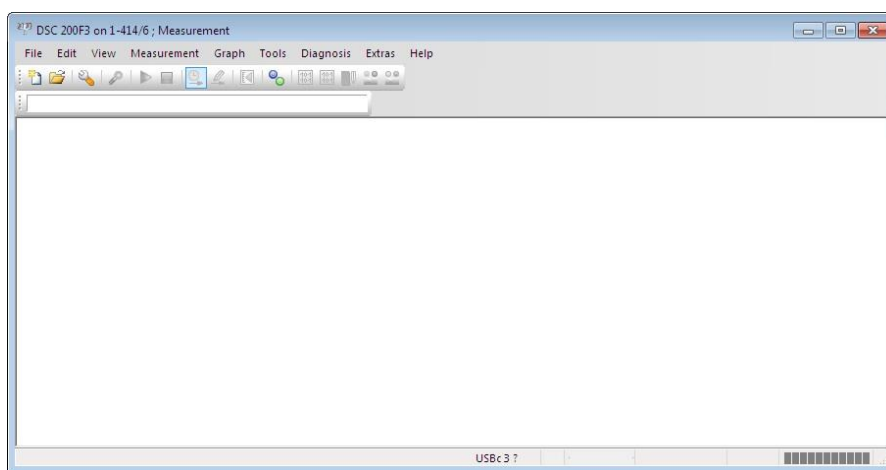


*Figure 4.11.* Initial DSC Measurement Application Window

From here, click on “File” and “New” to open up the “Measurement Definition” screen and to begin a new specific heat experimental run as shown in Figure 4.12. On this screen, the green circles indicate that the inputs are “OK.” If the inputs are not “OK;” however, the circles will light up red instead. The first tab is the “Fast Definition” tab. Select the desired measurement type, identity, sample name, sample mass, and crucible mass. Run a correction measurement type for a baseline run, a sample for just a sample run only, or a correction and sample run for both. Once all of the data is typed in, select “Forward.” It is important to note that throughout the measurement definition window, some of the circles will still be red after

“Forward” is selected. Some circles might not change green until the “Last Items” tab and folder is selected in which to save the data.

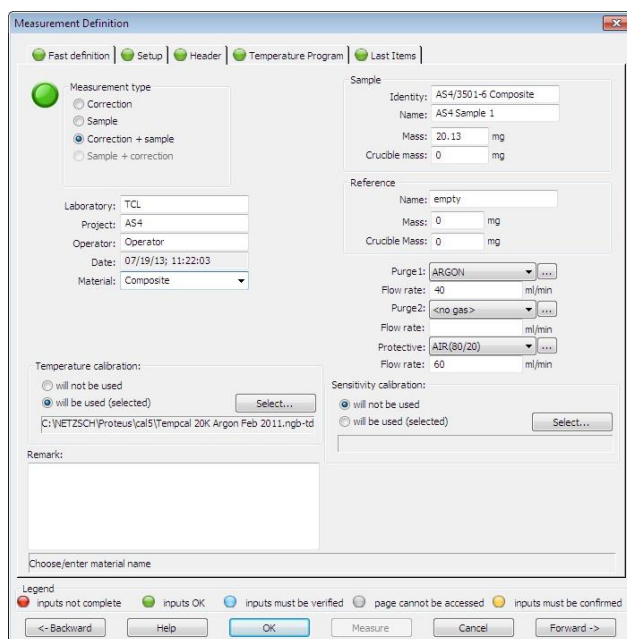


Figure 4.12. First Measurement Application Window

The “Temperature Program” tab, as shown in Figure 4.13, is an important window to pay close attention to because it determines the working temperatures during the experiment. Here, the temperatures for initial standby, dynamic, isothermal, and final categories are chosen in accordance with the limitations of the material being tested. The first temperature that is set is the initial temperature. This temperature is generally room temperature, and it will be the starting temperature of the material. During the test displayed, the specimen is cooled down to 5 degrees Celsius and is then held at an isotherm. Next, the apparatus dynamically heats until the desired temperature and holds at another isotherm. From there, set the emergency cut-off temperature at roughly 10 degrees higher than the isothermal temperature for safety. Finally, the chiller will cool the apparatus. Remember to select the rate in Kelvin per minute at which to cool and heat. Select a destination for the results, and save.

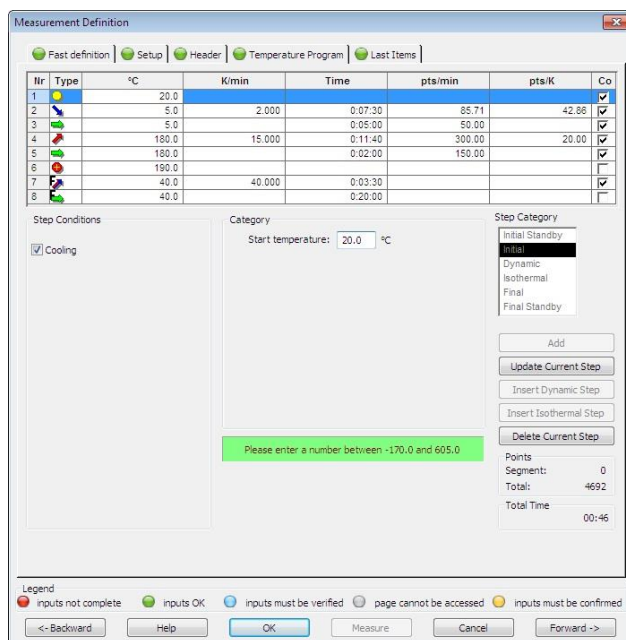


Figure 4.13. Temperature Program Tab in the Measurement Definition Window

Set the compressed Argon gas tank to about 4-5 psi to purge the environment within the apparatus, and start the test. After the test is completed, the data is now ready for analysis. Open the NETZSCH Proteus Thermal Analysis software. Go to “File” and “Open” and select the test runs that were saved along with the concurrent baseline. A graph of the data will open as shown in Figure 4.14.

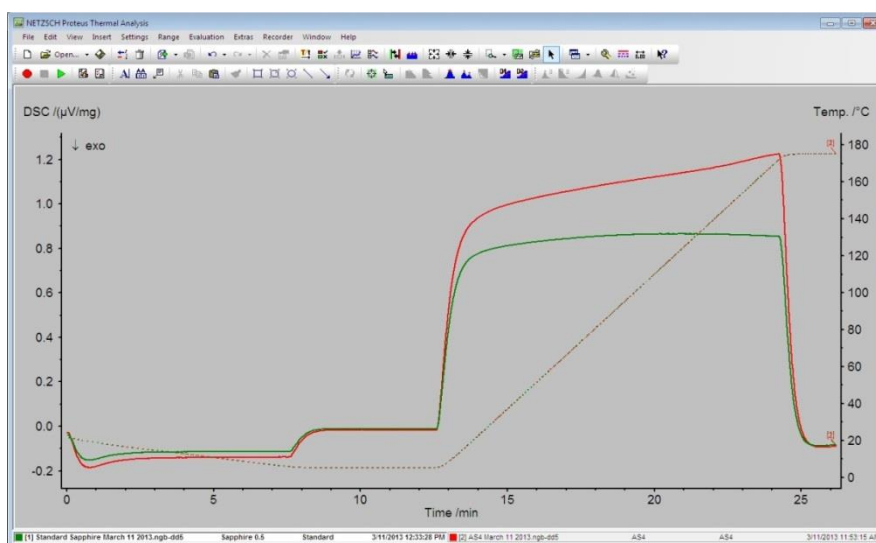


Figure 4.14. Graph of the Specific Heat Runs

Right-click anywhere on the graph, and select “Segments...” (Note: The “Segments...” option will not appear if a curve is right-clicked. The curve that is highlighted is also highlighted at the bottom of the screen for differentiation). The “Segments” window will pop up as shown in Figure 4.15. Segments allow for the change of visibility and connection of segments.

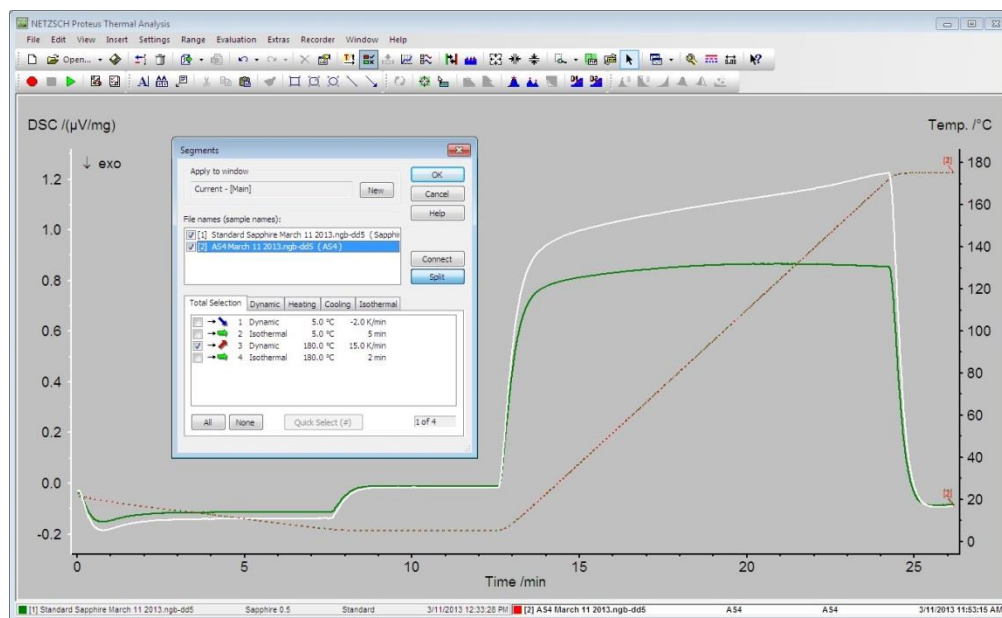


Figure 4.15. Segments Window

Under the “File names (sample names):” box, click on the standard sample and tested sample one at a time, and only check the **dynamic** heating and/or cooling boxes to display the dynamic heating and/or cooling segments of the graph for both the standard and the sample. The result will be shown. For the AS4 sample, dynamic cooling was not applicable. In order to compute the specific heat, click on “Evaluation,” and select “Cp: Ratio Method...” This option will calculate the specific heat of the curve of the graph. The “Open Cp Standard File” window will appear. Select the corresponding standard, and click “Open.”

The “Select DSC Curves for Cp Calculation” window should appear next. It is important to check the standard as the standard and the sample as the sample. The “Baseline” column does not necessarily matter. Select “OK.” The specific heat curve will now be shown on the graph.

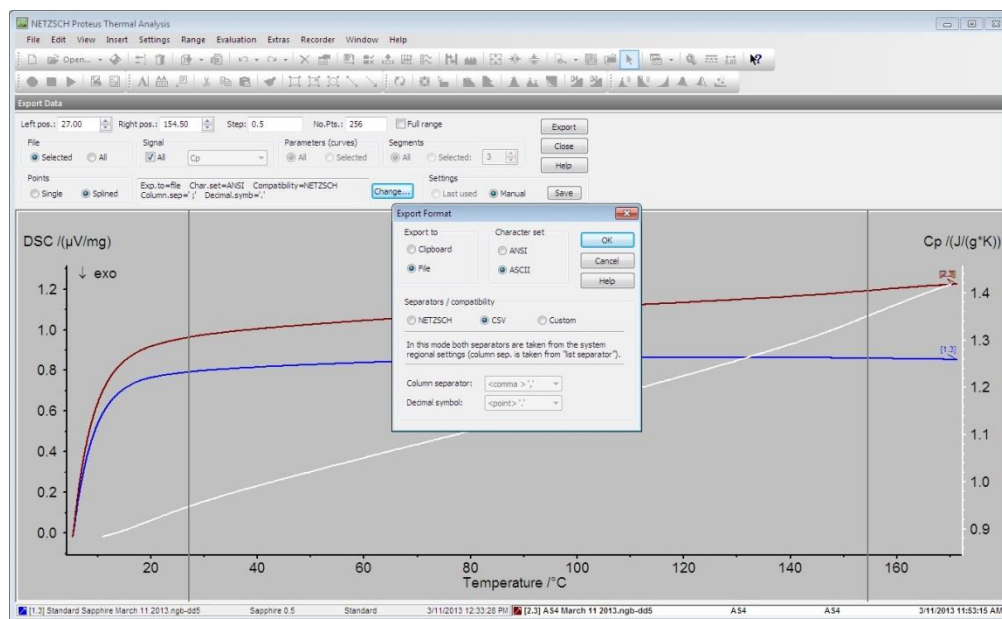


Figure 4.16. Export Data and Export Format Window

Finally, the data is now ready to be exported and analyzed further in Excel. In order to do this, click on the “Extras” tab, and select “Export Data...” This will export all measurement data ranges as data tables in ASCII or ANSI format. The first window displayed is the “Export Data” option set as displayed in Figure 4.16. After the range for the specific heat values has been selected, click “Change...” to modify the format of the exported specific heat data. The ASCII character set and the CSV separator are the most practical for general purpose use in an Excel file. Select “OK,” and transfer the data using a flash drive to further analyze the specific heat data in Excel. Close the software. See Appendix C for the complete computational procedure for specific heat.

## CHAPTER 5

### Results

#### 5.1 Thermal Diffusivity

The flash method was used to measure the thermal diffusivity of the AS4/3501-6 composite. The thermal diffusivity was measured between room temperature and 175°C which is the temperature limitation for this material. Thermal diffusivity decreases over the temperature range by approximately 15% as shown in Figure 5.1. This is apparent because the energy pulse will travel through the material faster at room temperature. In other words, the specific heat will be higher because it will take more heat to raise the temperature of the material by one degree Celsius thus signifying that the material has a lower threshold for heat at higher temperatures.

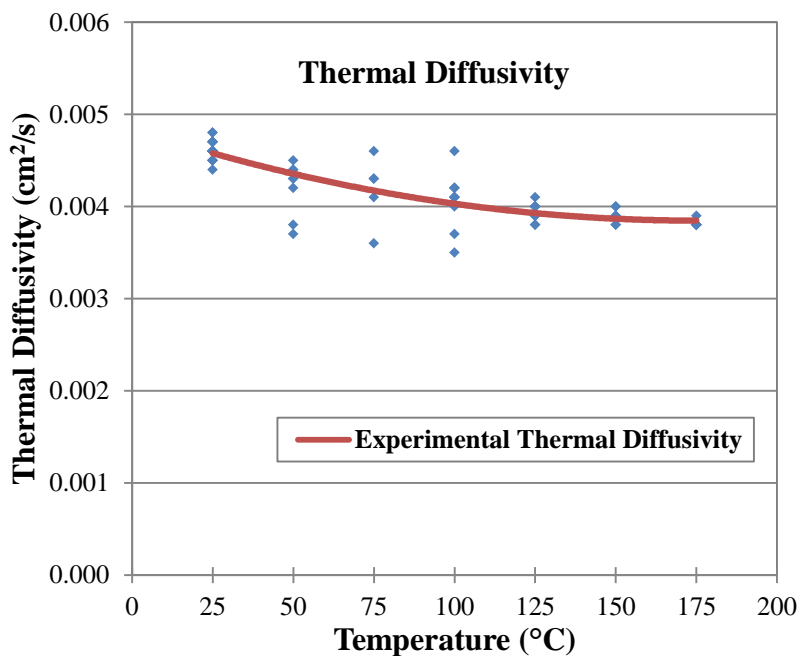


Figure 5.1. Thermal Diffusivity Shots of the AS4/3501-6 Composite

Three shots were recorded at each temperature during the experiment for each test. The data points represent the shots, or flashes, and the error at two standard deviations is displayed in

Figure 5.2. While there is more variation at the temperature range of 50° to 100°C, which is depicted by larger error bars, all of the data still falls within two standard deviations. This indicates that the error is minimal.

The error was calculated at each temperature and the error bars shows the interval where 95% of the data collected at each shot should lie. Population data sets provide the statistical estimates known as the population mean value and the population standard deviation defined by (Figliola & Beasley, 2011):

$$\sigma = \sqrt{\frac{1}{N} \sum_{i=1}^N (a_i - \bar{a})^2} \quad (5.1)$$

The results from each temperature tested are considered as a population where N is the total number of measurements,  $a_i$  represents a single  $i^{\text{th}}$  measurement, and  $\bar{a}$  is the mean value of the data at each temperature. Additionally, the margins of error were calculated for each temperature using standard error of the mean, as shown in Equation (5.2) below:

$$SE = \frac{\sigma}{\sqrt{N}} \quad (5.2)$$

The critical value from the normal distribution chart based on 95% confidence is 1.96, and the margin of error,  $e$ , is determined by the following:

$$e = \pm 1.96 \cdot SE \quad (5.3)$$

The percent error can now be found using:

$$\text{error \%} = \frac{e}{\text{mean}} \times 100 \% \quad (5.4)$$

The results for the thermal diffusivity and the percent error for the corresponding temperature values have been calculated and are displayed in Table 5.1.

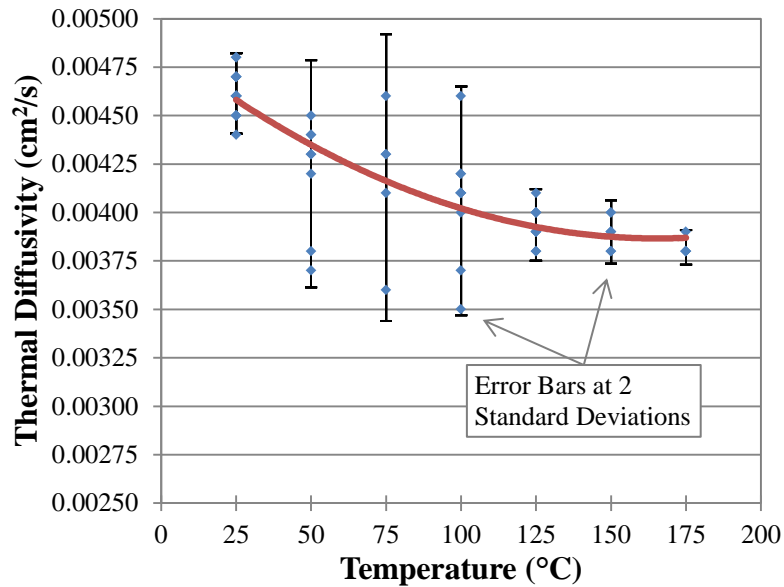


Figure 5.2. Magnified View of the Thermal Diffusivity with Error Bars

Table 5.1

*Percent Error of the Thermal Diffusivity*

<i>Temperature</i> (°C)	<i>Mean</i> (cm <sup>2</sup> /s)	<i>Standard Deviation</i> (cm <sup>2</sup> /s)	<i>Margin of Error</i> (± cm <sup>2</sup> /s)	<i>Percent Error</i> (%)
25	4.615E-03	1.01366E-04	4.44255E-05	0.96
50	4.200E-03	2.73861E-04	1.20025E-04	2.86
75	4.180E-03	3.31059E-04	1.45093E-04	3.47
100	4.073E-03	2.69986E-04	1.18327E-04	2.91
125	3.936E-03	8.81396E-05	3.86289E-05	0.98
150	3.900E-03	7.55929E-05	3.31300E-05	0.85
175	3.813E-03	3.30719E-05	1.44944E-05	0.38



According to the testing standard, the optimum thickness of the tested samples should be chosen so that the time to reach half of the maximum temperatures (half-time),  $t_{1/2}$  falls within the 10 to 1000 ms (0.01 to 1 s) range (ASTM, 2007). To verify that the samples were the proper thickness, an initial test was performed to check the half-times of the tested material. The half-times attained at each temperature were recorded. The corresponding half-times at different temperatures are shown in Figure 5.3. The half-time for each sample fell within the acceptable range according to the testing standard verifying that the proper thickness was chosen. According to the ASTM standard, the thickness may vary (1 to 6 mm) based on the thermal conductivity of the material (i.e., the more conductive a material is, the larger the thickness can be). The optimum thickness of the AS4 composite used in this research was 1.140 mm.

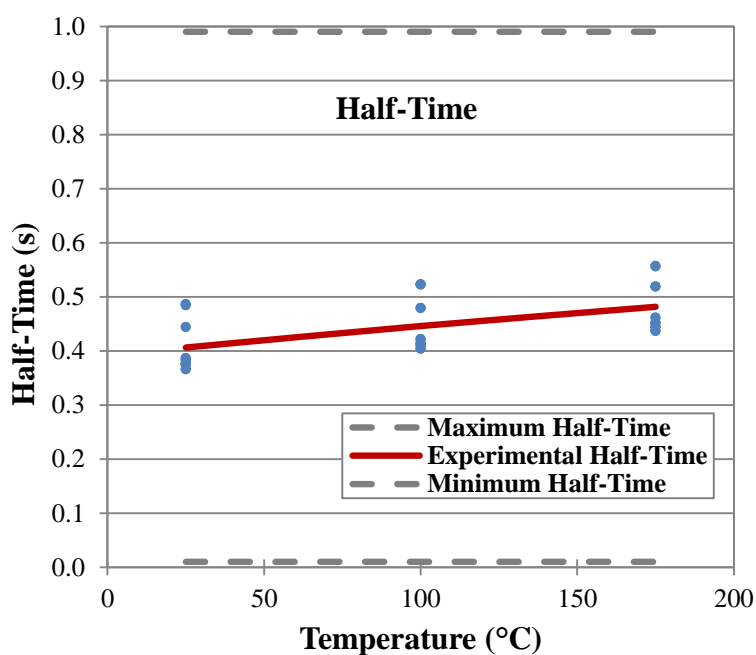


Figure 5.3. Half-Times of the AS4/3501-6 Composite

The material has also been tested at the Oak Ridge National Laboratory (ORNL) in Oak Ridge, Tennessee. The apparatus at ORNL is capable of attaining cryogenic thermal diffusivity measurements. The subzero results for the AS4 composite are displayed and compared with the

results from North Carolina A&T's Thermal Characterization Research Laboratory (TCL) as shown in Figure 5.4. The TCL apparatus uses an infrared detector to measure the temperature changes; on the other hand, ORNL uses thermocouples instead. The results of the thermal diffusivity at both labs were consistent and within a 5% margin of error.

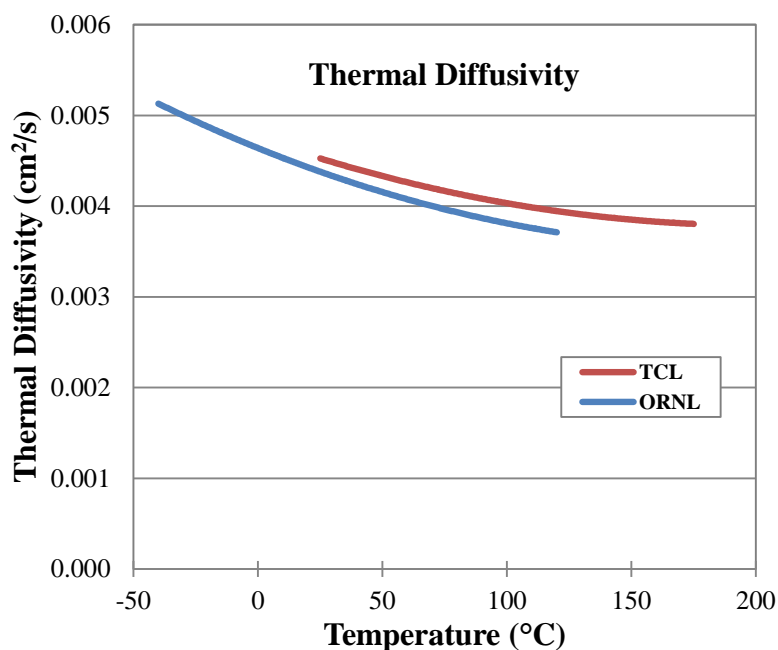


Figure 5.4. Thermal Diffusivity of the AS4/3501-6 Composite

## 5.2 Specific Heat

The specific heat of the AS4/3501-6 composite consistently increases from approximately 0.9 J/g °C at room temperature to 1.4 J/g °C at 170°C as shown in Figure 5.5. The material has been tested at the TCL and also at ORNL. An agreement has been achieved at both labs. Figure 8 displays the specific heat measurements of TCL versus ORNL. The material has been tested at NETZSCH, and the data is also displayed in Figure 5.5. All three specific heat results overlap indicating accurate and precise measurements. The heating curve was used in the analysis.

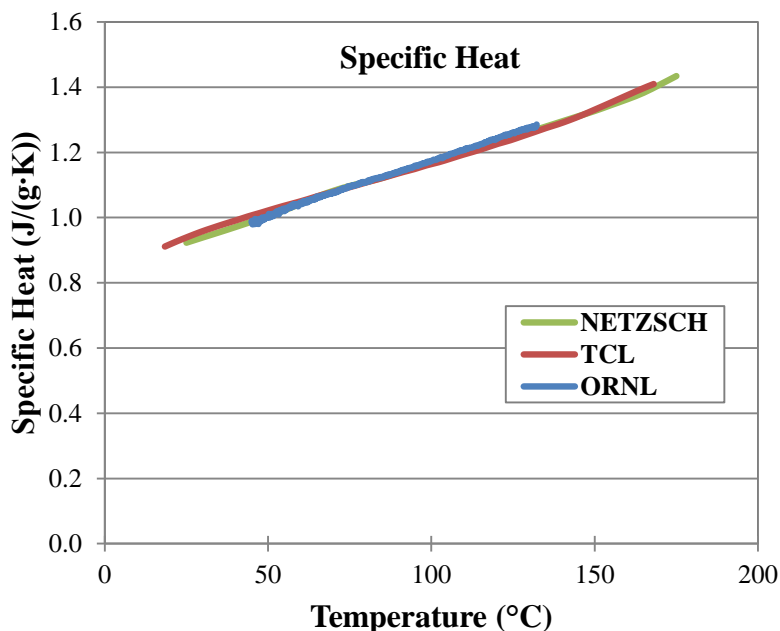


Figure 5.5. Specific Heat of the AS4/3501-6 Composite

### 5.3 Thermal Conductivity

Using the density (the density for the tested AS4/3501-6 composite was  $1.46 \text{ g/cm}^3$ ), specific heat, and thermal diffusivity, the thermal conductivity of the AS4/3501-6 composite was determined using the following relationship:

$$k = \rho \cdot c_p \cdot \alpha \quad (5.5)$$

The results for the thermal conductivity of the AS4/3501-6 composite are shown in Figure 5.6. There is a 20% increase in the thermal conductivity of the composite over the service temperature range. The results of the thermal conductivity at both labs were consistent and within a 5% margin of error. Because the apparatus at Oak Ridge is cryogenic, the results for the measurements are only up to about  $125^\circ\text{C}$ .

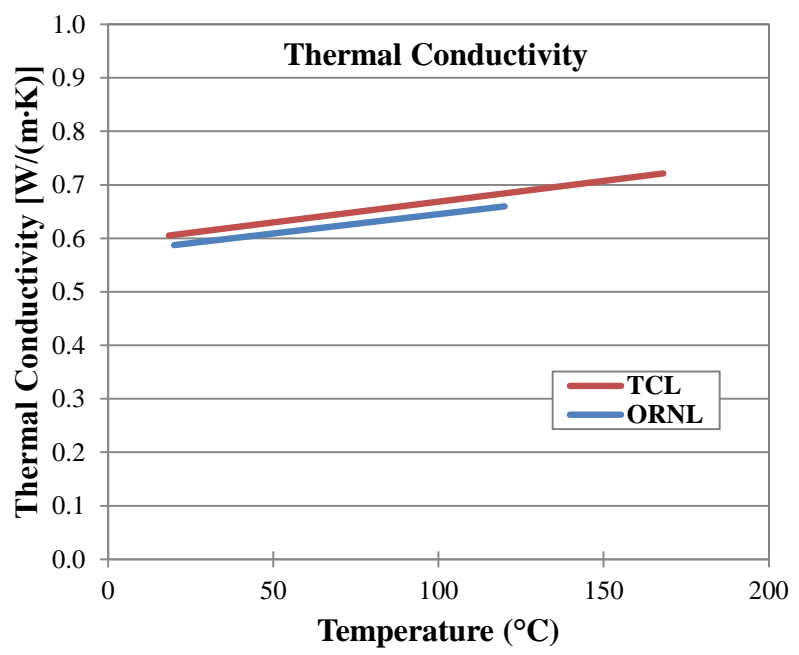


Figure 5.6. Thermal Conductivity of the AS4/3501-6 Composite

Figure 5.7 shows the normalized rear face temperature rise. It is a comparison of the mathematical model with no heat losses versus the experimental values with radiation heat losses as shown by a dashed line.

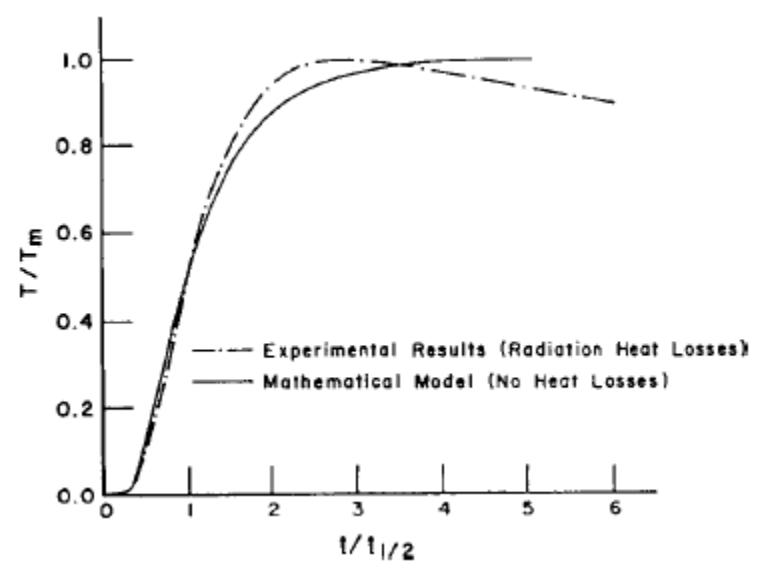


Figure 5.7. Rear Face Radiation Heat Loss

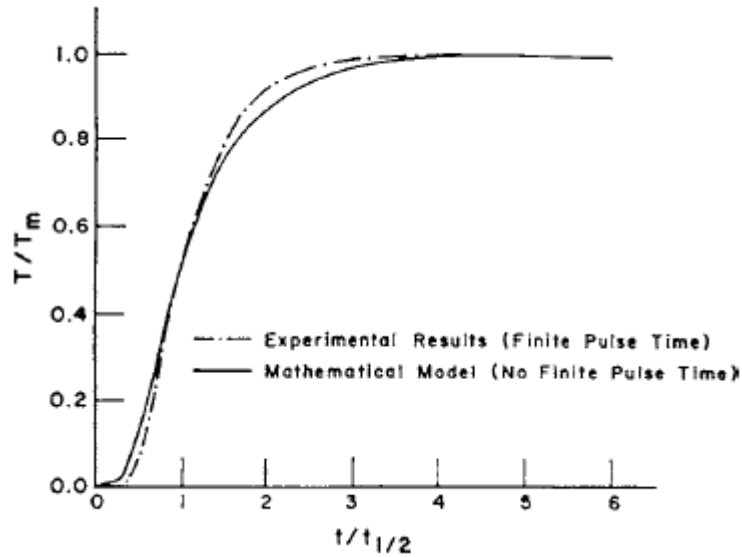


Figure 5.8. Rear Face Finite Pulse Time Effect

Like Figure 5.7, Figure 5.8 shows the normalized rear face temperature rise as well. The difference is that Figure 5.8 shows the comparison of the mathematical model with no finite pulse time effect versus the experimental values which do have the finite pulse effect. It is seen in Figure 5.9 that the AS4/3501-6 carbon-epoxy composite shows very little finite pulse time effect as well as radiation heat loss throughout the entire temperature range.

Finite pulse time effects usually can be corrected for using the equation (ASTM, 2007):

$$\alpha = K_1 L^2 / (K_2 t_x - \tau) \quad (5.6)$$

where  $K_1$  and  $K_2$  are constants and  $\tau$  is the triangle of duration. Heat loss corrections can be performed by using the Clark and Taylor procedure aforementioned. Both corrections are affected by non-uniform heating effects.

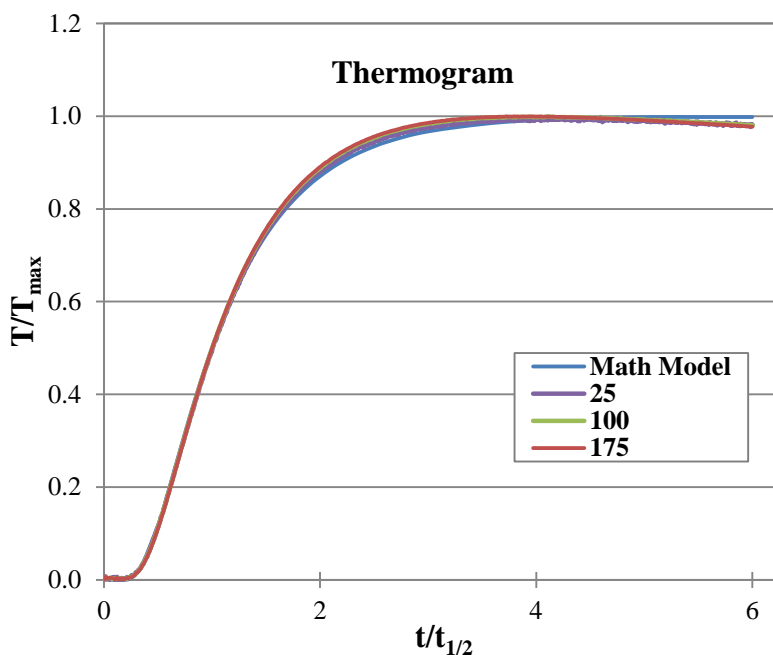


Figure 5.9. Thermogram of the AS4/3501-6 Composite

Figure 5.9 shows the thermogram graph of the AS4/3501-6 carbon-epoxy composite as it compares with the mathematical model. The thermogram displays the relationship between the temperature divided by the maximum temperature versus the time divided by the half-time. The data acquisition system can be pre-programmed within one time period for the acceptable resolution of at least 1% for the quickest thermogram the system can deliver which is represented by the mathematical model.

As shown in Figure 10, immediately before the temperature reaches its maximum, it is noticed that there is slightly more radiation heat loss at room temperature than the 100°C and 175°C measurements. After the flash occurs, the heat will radiate more from the sample in a lower temperature environment than in a higher temperature environment. The AS4/3501-6 composite shows relatively no heat loss with respect to temperature and is nearly consistent with the theoretical model. Table 5.2 shows the sample specifications of the AS4 composite while Table 5.3 shows the measured thermal properties.

Table 5.2

*Specifications of AS4/3501-6 Testing Specimens*

<i>Test</i>	<i>Diameter</i> mm (inch)	<i>Thickness</i> mm (inch)	<i>Mass</i> (g)
<i>Specific Heat</i>	4.00 (0.157)	0.960 (0.038)	0.02013
<i>Thermal Diffusivity</i>	12.69 (0.50)	1.135 (0.447)	0.21000

Table 5.3

*Thermal Properties of AS4/3501-6*

<i>Temperature</i> (°C)	<i>Density</i> (g/cm <sup>3</sup> )	<i>Thermal Diffusivity</i> (cm <sup>2</sup> /s)	<i>Specific Heat</i> (J/g*K)	<i>Thermal Conductivity</i> (W/m*K)
25	1.4629	0.004615	0.94171	0.6127445
50	1.4629	0.004200	1.02508	0.6347415
75	1.4629	0.004180	1.09773	0.6492697
100	1.4629	0.004073	1.16040	0.6622167
125	1.4629	0.003936	1.23705	0.6803271
150	1.4629	0.003900	1.32987	0.7088875
175	1.4629	0.003813	1.40960	0.7376534

Table 5.4 shows the range of thermal properties for the AS4/3501-6 carbon-epoxy composite over the working temperatures for the material. The thermal diffusivity decreases over the temperature range from about 0.0046 cm<sup>2</sup>/s to 0.0038 cm<sup>2</sup>/s. The specific heat increases from about 0.9417 to 1.4096 J/g\*K, and the thermal conductivity also increases from approximately 0.6127 to 0.7377 W/m\*K.

Table 5.4

*Range of Thermal Properties for AS4/3501-6*

<i>Thermal Property</i>	<i>Low Temperature Applications (25°C)</i>	<i>High Temperature Applications (175°C)</i>
<i>Density (g/cm<sup>3</sup>)</i>	1.4629	1.4629
<i>Thermal Diffusivity (cm<sup>2</sup>/s)</i>	0.0046	0.0038
<i>Specific Heat (J/g*K)</i>	0.9417	1.4096
<i>Thermal Conductivity (W/m*K)</i>	0.6127	0.7377



## CHAPTER 6

### Discussion and Future Research

#### 6.1 Discussion

The thermophysical properties database of the AS4/3501-6 composite has been developed over the service temperature range of the material. Using the flash method, the thermal diffusivity was measured through the thickness. Specific heat was measured using the differential scanning calorimeter. The thermal conductivity was determined using the density, specific heat, and thermal diffusivity of the composite. The thermophysical properties have been validated using different apparatuses at ORNL and TCL from 25°C to 175°C. This composite material is suitable for general purpose structural applications.

#### 6.2 Future Research

Upon the completion of this research, there are several recommendations for work in the future.

1. Continue the thermal expansion work (Appendix D) that was commenced by analyzing the calibration tested standard material. Measure the thermal expansion of various materials and note the role it plays in thermal characterization. Add to the thermal properties database.
2. Compare composite materials of similar constituents, fiber volume, resins, and fibers, and examine the differences in the thermal properties. Examine the potential effects the differences will make in high temperature applications. Note which combination produces the most desirable composite.
3. Continue to develop the thermal properties database by characterizing other various composite materials and foams.

4. Continue to build relationship with NASA University Research Centers (URC), NASA Glenn Research Center, and the Ohio Aerospace Institute.

## References

- Akangah, P., & Shivakumar, K. (2013). Assessment of Impact Damage Resistance and Tolerance of Polymer Nanofiber Interleaved Composite Laminates. *Journal of Chemical Science and Technology*, 2(2), 39-52.
- Anter Corporation. FlashLine™ Thermal Diffusivity Measuring System Operation and Maintenance Manual Part 1 Flashline 2000.
- ASTM Standard E-1269. (2005). Standard Test Method for Determining Specific Heat Capacity by Differential Scanning Calorimetry. West Conshohocken, PA: ASTM International.
- ASTM Standard E-1461. (2007). Standard Test Method for Thermal Diffusivity by the Flash Method. West Conshohocken, PA: ASTM International.
- Baker, D., Reaves, R., & Saad, M. (2011). *Thermal Characterization of Carbon-Carbon Composites*. Paper presented at the ASME Conference Proceedings, Denver, CO. IMECE2011-64061 doi: <http://dx.doi.org/10.1115/IMECE2011-64061>
- Beck, J. V., & Dinwiddie, R. B. (1995). Parameter Estimation Method for Flash Thermal Diffusivity with Two Different Heat Transfer Coefficients. *23rd International Thermal Conductivity Conference*, 123-136.
- Carslaw, H. S., & Jaeger, J. C. (1959). *Conduction of Heat in Solids*. New York: Oxford University Press.
- Çengel, Y. A., (1998). *Heat Transfer, A Practical Approach*. The McGraw-Hill Companies, Inc., Boston, MA., 4, 20-25, 70, 140-141.
- Cernuschi, F., Bison, P. G., Figari, A., Marinetti, S., & Grinzato, E. (2004). Thermal Diffusivity Measurements by Photothermal and Thermographic Techniques. *International Journal of*

*Thermophysics*, 25(2), 439-457. doi:

<http://dx.doi.org/10.1023/B:IJOT.0000028480.27206.cb>

Cernuschi, F., Bison, P. G., Figari, A., Marinetti, S., Grinzato, E., & Lorenzoni, L. (2002).

Comparison of Thermal Diffusivity Measurement Techniques. *Quantitative InfraRed Thermography Journal*, 28, 211-221.

Clark, L. M., & Taylor, R. E. (1975). Radiation Loss in the Flash Method for Thermal

Diffusivity. *Journal of Applied Physics*, 46(2), 714-719. doi:

<http://dx.doi.org/10.1063/1.321635>

Daniel, I. M., & Ishai, O. (2006). *Engineering Mechanics of Composite Materials* (2nd ed.). New York: Oxford University Press.

Doleman, B., & Saad, M. (2013). Thermal Characterization of AS4/3501-6 Carbon-Epoxy

Composite. *Frontiers in Heat and Mass Transfer*, 4(2). doi:

<http://dx.doi.org/10.5098/hmt.v4.2.3006>

Figliola, R. S., & Beasley, D. E. (2011). *Theory and Design for Mechanical Measurements* (5th ed.): John Wiley & Sons.

Hahn, D. W., & Özışik, M. N. (2012). *Heat Conduction* (3rd ed.). New Jersey: John Wiley & Sons, Inc.

Hexcel Corporation. (1998). *3501-6 Epoxy Matrix*. Product Data. Retrieved from

[http://www.hexcel.com/Resources/DataSheets/Prepreg-Data-Sheets/3501-6\\_eu.pdf](http://www.hexcel.com/Resources/DataSheets/Prepreg-Data-Sheets/3501-6_eu.pdf)

Hexcel Corporation. (2013). *HexTow® AS4 Carbon Fiber*. Product Data. Retrieved from

<http://www.hexcel.com/resources/datasheets/carbon-fiber-data-sheets/as4.pdf>

Höhne, G., Hemminger, W. F., & Flammersheim, H. J. (2003). *Differential Scanning*

*Calorimetry*. Germany: Springer - Verlag Berlin Heidelberg.

- Hull, D., & Clyne, T. W. (1996). *An Introduction to Composite Materials*. New York: Cambridge University Press.
- NETZSCH. (2008). Operating Instructions DSC 200 F3 Maia. Selb, Germany.
- Nunes dos Santos, W. (2007). Thermal Properties of Polymers by Non-Steady-State Techniques. *Polymer Testing*, 26(4), 556-566. doi: <http://dx.doi.org/10.1016/j.polymertesting.2007.02.005>
- Parker, W. J., Jenkins, R. J., Butler, C. P., & Abbott, G. L. (1961). Flash Method of Determining Thermal Diffusivity, Heat Capacity, and Thermal Conductivity. *Journal of Applied Physics*, 32(9), 1679-1684. doi: <http://dx.doi.org/10.1063/1.1728417>
- Patrick, M., & Saad, M. (2012). Examination of Carbon-Carbon and Graphitized Carbon-Carbon Composites. *Frontiers in Heat and Mass Transfer*, 3(4). doi: <http://dx.doi.org/10.5098/hmt.v3.4.3007>
- Salazar A., (2003). On Thermal Diffusivity. *European Journal of Physics*, 24(4), 351–358. doi: <http://dx.doi.org/10.1088/0143-0807/24/4/353>
- U.S. Department of Defense. (2002). *Composite Materials Handbook: Volume 2. Polymer Matrix Composites Materials Properties*. Department of Defense Handbook. Retrieved from <http://www.lib.ucdavis.edu/dept/pse/resources/fulltext/HDBK17-2F.pdf>
- Vital, A., Doleman, B., & Saad, M. (2013). *Thermophysical Properties of AS4/3501-6 Carbon-Epoxy Composite*. Paper presented at the ASME Conference Proceedings, San Diego, CA. IMECE2013-65186
- Wei, J. (1989). Carbon Fiber Thermal Conductivity Measurement and Analysis (Defense Technology Information Center Technical Report Database, Trans.): Beijing Institute of Materials Science.

Wetherhold, R. C., & Wang, J. (1994). Difficulties in the Theories for Predicting Transverse Thermal Conductivity of Continuous Fiber Composites. *Journal of Composite Materials*, 28(15), 1491-1498. doi: <http://dx.doi.org/10.1177/002199839402801507>

## Appendix A

### Flash Method Derivation of Thermal Diffusivity

Begin the derivation starting with the equation of the temperature distribution within a thermally insulated solid of uniform thickness L:

$$T(x, t) = \frac{1}{L} \int_0^L T(x, 0) dx + \frac{2}{L} \sum_{n=1}^{\infty} \exp\left(\frac{-n^2 \pi^2 \alpha t}{L^2}\right) \cdot \cos \frac{n\pi x}{L} \int_0^L T(x, 0) \cdot \cos \frac{n\pi x}{L} dx$$

The initial conditions at time  $t = 0$  are made based on the assumption that a pulse of radiant energy  $Q$  is instantaneously and uniformly absorbed in the small depth  $g$  at the front surface  $x = 0$  thus making the temperature distribution at that instant:

$$\begin{aligned} \text{for } 0 < x < g \quad T(x, 0) &= \frac{Q}{\rho \cdot C \cdot g} \\ \text{for } g < x < L \quad T(x, 0) &= 0 \end{aligned}$$

Now split the interval from 0 to L for  $T(x, 0)$  to two intervals, 0 to  $g$  and  $g$  to L for  $T(x, 0)$  and then use substitution to substitute the initial conditions at  $t = 0$  into the equation of the temperature distribution within a thermally insulated solid of uniform thickness L:

$$\begin{aligned} T(x, t) &= \frac{1}{L} \left[ \int_0^g \frac{Q}{\rho \cdot C \cdot g} dx + \int_g^L 0 dx \right] + \frac{2}{L} \sum_{n=1}^{\infty} \exp\left(\frac{-n^2 \pi^2 \alpha t}{L^2}\right) \\ &\quad \cdot \cos \frac{n\pi x}{L} \left[ \int_0^g \frac{Q}{\rho \cdot C \cdot g} \cdot \cos \frac{n\pi x}{L} dx + \int_g^L 0 \cdot \cos \frac{n\pi x}{L} dx \right] \end{aligned}$$

The integral is simplified by removing the terms that are multiplied by 0 and then taking the integral of the function then simplify:

$$\begin{aligned} T(x, t) &= \frac{1}{L} \left( \left[ \frac{Q}{\rho \cdot C \cdot g} x \right]_0^g + 0 \right) + \frac{2}{L} \sum_{n=1}^{\infty} \exp\left(\frac{-n^2 \pi^2 \alpha t}{L^2}\right) \\ &\quad \cdot \cos \frac{n\pi x}{L} \left( \left[ \frac{Q}{\rho \cdot C \cdot g} \sin \frac{n\pi x}{L} \cdot \frac{L}{n\pi} \right]_0^g + 0 \right) \end{aligned}$$

$$T(x, t) = \frac{1}{L} \left( \frac{Q}{\rho \cdot C \cdot g} \cdot g - \frac{Q}{\rho \cdot C \cdot g} \cdot 0 \right) + \frac{2}{L} \sum_{n=1}^{\infty} \exp \left( \frac{-n^2 \pi^2 \alpha t}{L^2} \right) \cdot \cos \frac{n\pi x}{L} \left( \frac{QL}{\rho \cdot C \cdot g \cdot n\pi} \left( \sin \frac{n\pi g}{L} - \sin \frac{n\pi 0}{L} \right) \right)$$

$$T(x, t) = \frac{1}{L} \left( \frac{Q}{\rho \cdot C} \right) + \frac{2}{L} \sum_{n=1}^{\infty} \exp \left( \frac{-n^2 \pi^2 \alpha t}{L^2} \right) \cdot \cos \frac{n\pi x}{L} \left( \frac{QL}{\rho \cdot C \cdot g \cdot n\pi} \right) \sin \frac{n\pi g}{L}$$

Factor out common terms and then rewrite the equation in a simpler form:

$$T(x, t) = \frac{Q}{\rho \cdot C \cdot L} \left[ 1 + 2 \sum_{n=1}^{\infty} \exp \left( \frac{-n^2 \pi^2 \alpha t}{L^2} \right) \left( \cos \frac{n\pi x}{L} \right) \left( \sin \frac{n\pi g}{L} \right) \left( \frac{L}{g \cdot n\pi} \right) \right]$$

Since the distance  $g$  that is absorbing the instantaneous pulse of energy is a very small number for opaque materials it is can concluded that:

$$\sin \frac{n\pi g}{L} \approx \frac{n\pi g}{L}$$

Now substitute the estimated assumption into the equation and then simplify:

$$T(x, t) = \frac{Q}{\rho \cdot C \cdot L} \left[ 1 + 2 \sum_{n=1}^{\infty} \exp \left( \frac{-n^2 \pi^2 \alpha t}{L^2} \right) \left( \cos \frac{n\pi x}{L} \right) \left( \frac{n\pi g}{L} \right) \left( \frac{L}{n\pi g} \right) \right]$$

$$T(x, t) = \frac{Q}{\rho \cdot C \cdot L} \left[ 1 + 2 \sum_{n=1}^{\infty} \left( \cos \frac{n\pi x}{L} \right) \exp \left( \frac{-n^2 \pi^2 \alpha t}{L^2} \right) \right]$$

Now evaluate the expression at the rear surface  $T(L, t)$ , thus substituting  $L$  into  $x$

$$T(L, t) = \frac{Q}{\rho C L} \left[ 1 + 2 \sum_{n=1}^{\infty} \left( \cos \frac{n\pi L}{L} \right) \exp \left( \frac{-n^2 \pi^2 \alpha t}{L^2} \right) \right]$$

The expression is simplified by simplifying the summation expression from  $\cos(n\pi)$  to  $-1$  based on the properties of trigonometry functions:

$$T(L, t) = \frac{Q}{\rho C L} \left[ 1 + 2 \sum_{n=1}^{\infty} (-1)^n \exp \left( \frac{-n^2 \pi^2 \alpha t}{L^2} \right) \right]$$



Two dimensionless parameters,  $V$  and  $\omega$  can be defined where  $V$  is the percentage of temperature at the rear surface as it changes with time and  $\omega$  is simply a variable used to simplify the expression of  $V(L,t)$

$$V(L, t) = \frac{T(L, t)}{T_m}$$

$$\omega = \frac{\pi^2 \alpha t}{L^2}$$

$T_m$  represents the maximum temperature at the rear surface:

$$\text{where } T_m = \frac{Q}{\rho CL}$$

Then substitute the appropriate expressions into the  $V(L,t)$  equation and then simplify:

$$V(L, t) = \frac{\frac{Q}{\rho CL} [1 + 2 \sum_{n=1}^{\infty} (-1)^n \exp(-n^2 \omega)]}{\frac{Q}{\rho CL}}$$

$$V(L, t) = \left[ 1 + 2 \sum_{n=1}^{\infty} (-1)^n \exp(-n^2 \omega) \right]$$

The flash method used in testing evaluates  $V(L,t)$  at  $t_{1/2}$  which yields 50% of the maximum temperature:

$$V(L, t_{1/2}) = 0.5$$

Evaluate the expression to solve for  $\omega$ :

$$0.5 = \left[ 1 + 2 \sum_{n=1}^{\infty} (-1)^n \exp(-n^2 \omega) \right]$$

$$-0.5 = 2 \sum_{n=1}^{\infty} (-1)^n \exp(-n^2 \omega)$$

$$-0.25 = \sum_{n=1}^{\infty} (-1)^n \exp(-n^2 \omega)$$

$$-0.25 = (-1)^1 \exp(-1^2 \omega) + (-1)^2 \exp(-2^2 \omega) + (-1)^3 \exp(-3^2 \omega) \dots$$

$$-0.25 = (-e^{-\omega}) + (e^{-4\omega}) - (e^{-9\omega}) + (e^{-16\omega}) - (e^{-25\omega}) \dots$$

Because the values in the summation are growing smaller as the next terms are continuing to be added, the expression can be evaluated using the first three terms:

$$-0.25 = (-e^{-\omega}) + (e^{-4\omega}) - (e^{-9\omega})$$

This complex expression is solved using sufficient programs capable of solving complex functions:

$$\omega = 1.369756$$

The equation is rearranged in a way to solve for the thermal diffusivity,  $\alpha$ , and then simplified:

$$\omega = \frac{\pi^2 \alpha t_{1/2}}{L^2}$$

$$\alpha = \frac{\omega L^2}{\pi^2 t_{1/2}}$$

$$\alpha = \frac{1.369756 L^2}{\pi^2 t_{1/2}}$$

The final expression allows the thermal diffusivity,  $\alpha$ , of any material, theoretically, to be calculated if the thickness,  $L$ , and the half time are known:

$$\alpha = \frac{0.138785 L^2}{t_{1/2}}$$

## Appendix B

### *Complete Computational Procedure: Thermal Diffusivity*

The following is a step by step procedure for running thermal diffusivity measurements using the xenon flash method and the Anter Corporation FlashLine™ 2000 software. Step one is to open the software. The platform is displayed in Figure B.1.

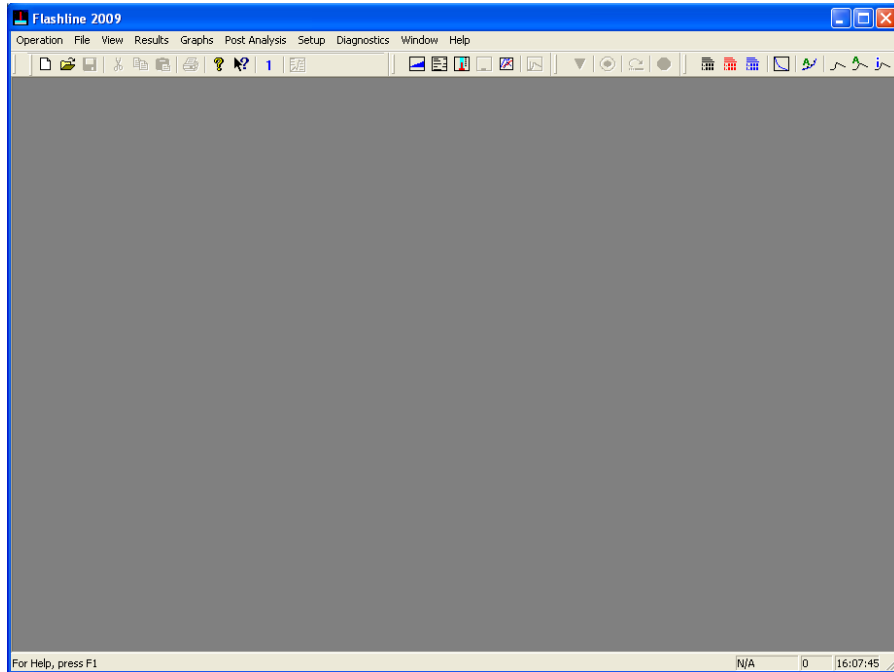


*Figure B.1.* Initial FlashLine™ 2000 Software Window

From here, click on “Operation” and then “Startup Information” as shown in Figure B.2. In Figure B.3, the next window to appear will be the furnace type selection. There should only be one furnace type which is the “2000” furnace. Select “OK.” Turn the FlashLine™ 2000 Thermal Properties Analyzer apparatus on in order to use the “Controller Parameter File” as shown in Figure B.4. Select “Yes.”

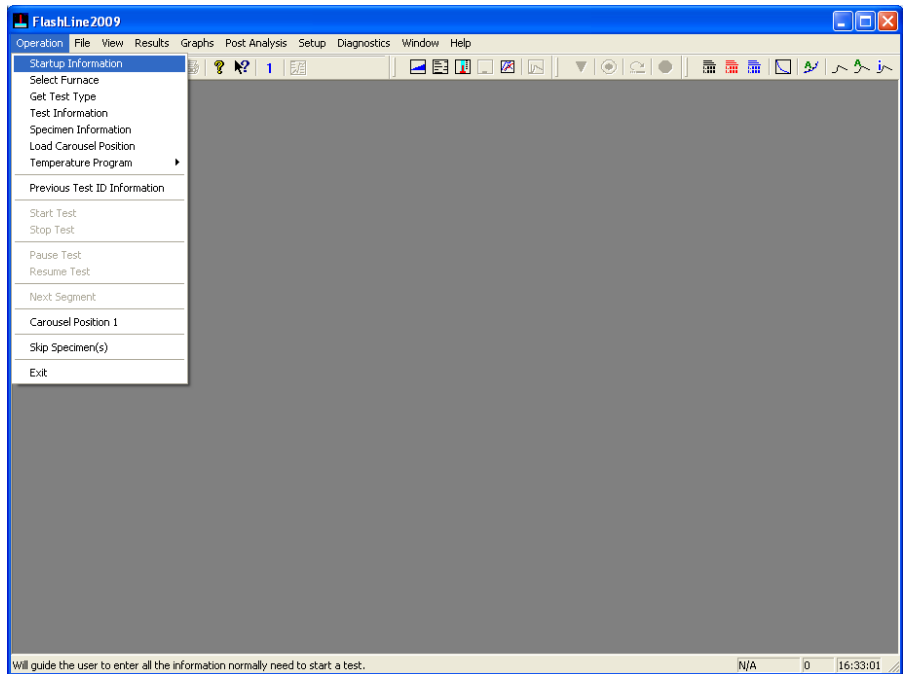


Figure B.2. Startup Information Operation

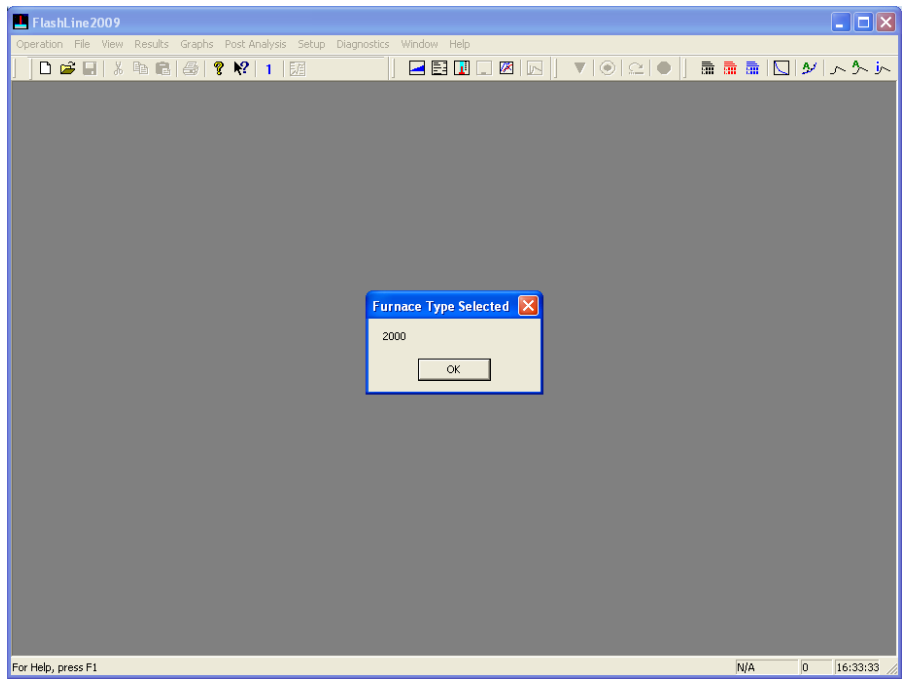
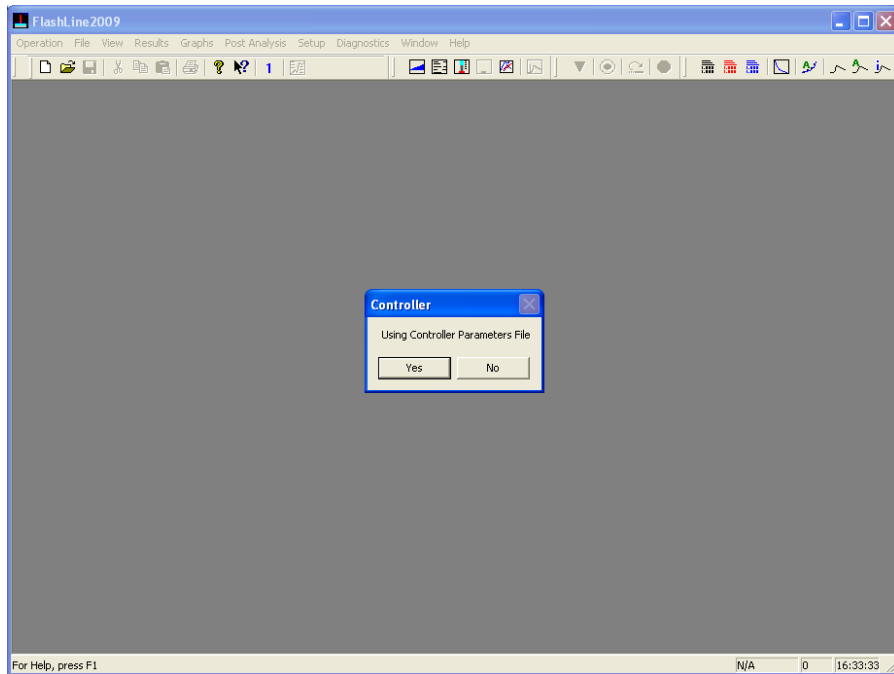
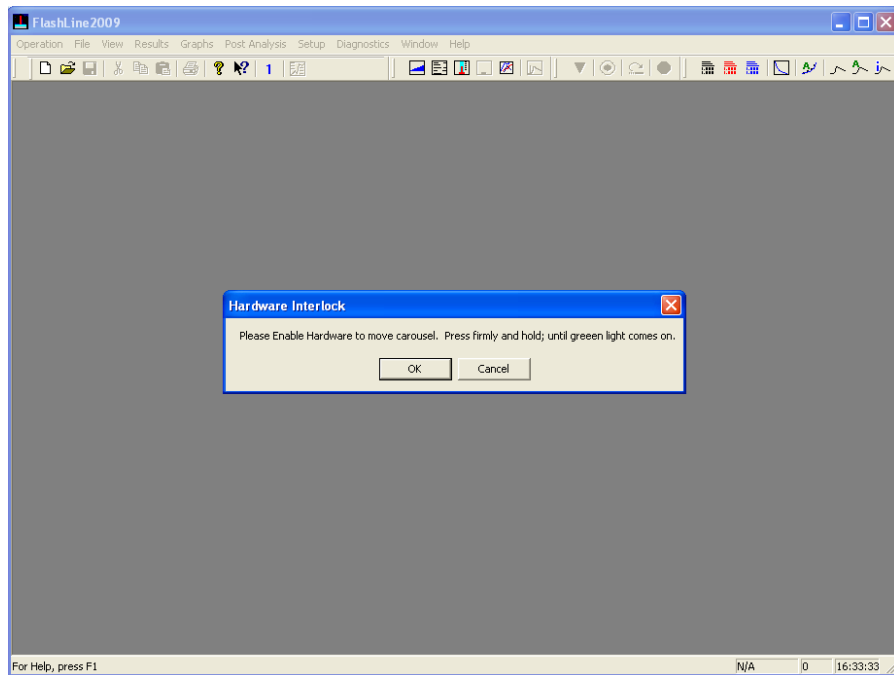


Figure B.3. Furnace Type Selection Window



*Figure B.4. Controller Window*



*Figure B.5. Hardware Interlock Window*



Figure B.6. Hardware Interlock Enable on the FlashLine™ Apparatus

Press the “Hardware Enable” button on the apparatus to enable carousel movement.  
Press firmly until the green light comes on as displayed in Figure B.6.

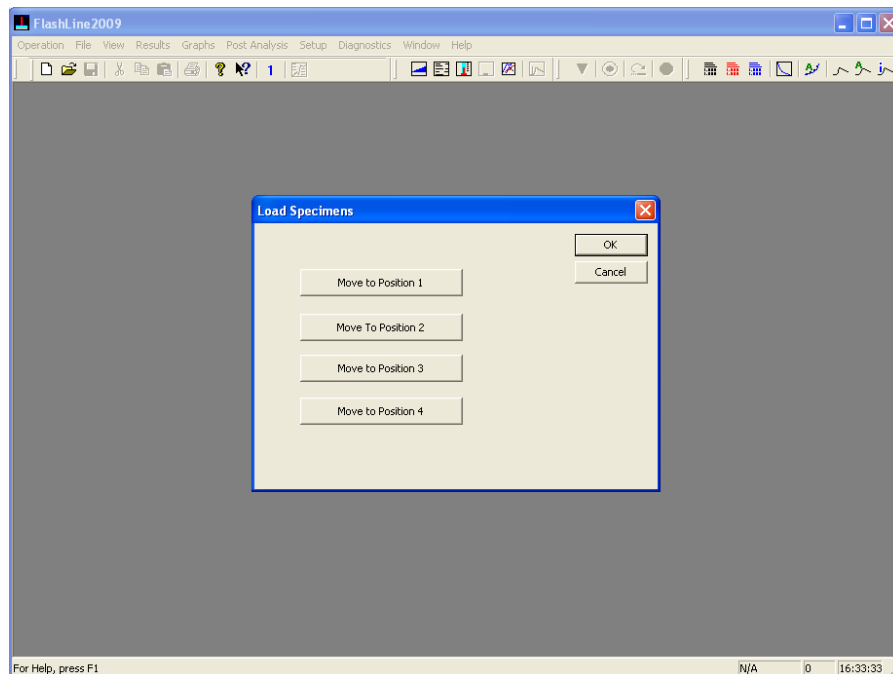


Figure B.7. Load Specimens Window



Figure B.8. Specimen Loading Position 1 in the Apparatus

Load the specimens desired for testing and note the position (one to four) in which each specimen is placed. Enter the test and specimen information as shown in Figure B.9.

FlashLine 2009

Operation

**Test Information**

Test Title: AISI 316 SS Use Information From Previous Test

Test ID: 422 Sequence Number:  Cancel

Operator: John Doel Date: Sep 02, 2013

Common Specimen ID: Common Specimen Title: Common Thickness (cm): Use Expansion:

	Specimen ID	Specimen Title	Thickness (cm)	Diameter (cm)	Weight (g)
1	AISI_316	Stainless Steel	0.1640	2.548	4.5150
2	Carbon_Foam_30_2	NG CFoam 30	0.2330	1.243	0.1400
3	Carbon_Foam_30_3	NG CFoam 30	0.2030	1.242	0.1220
4	Through_thickness_2	Through thickness CCC not sprayed	0.3116	1.245	0.6175

Test Segment	Temperature (°)	Ramp (C°/Min.)	Repeat Points	Power Level	Point 1 Level	Point 2 Level	Point 3 Level	Point 4 Level
1	25	5.0	3	500.0	500			
2	50	5.0	3	500.0	500			
3	75	5.0	3	500.0	500			

Uniform  
 Temperatures  
 Ramp Rate  
 Repeat Points  
 Power Level

Clear Program Add Segment Delete Segment Insert Segment List Programs Save Program Safety Temperature (C) 400

Start Test  Specific Heat/Conductivity  In Plane

For Help, press F1 N/A 0 16:33:33

Figure B.9. Test Information Window

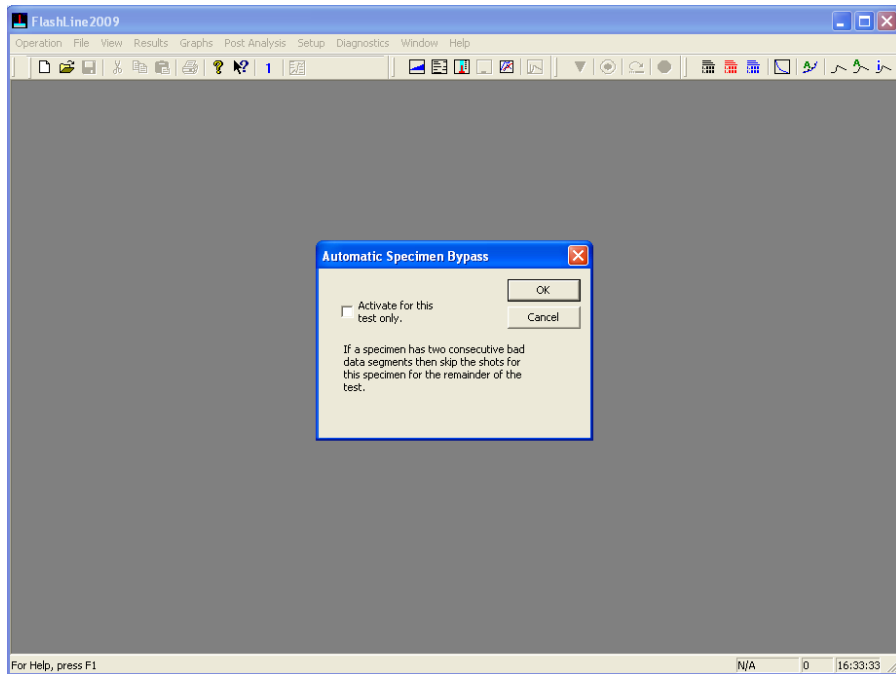


Figure B.10. Automatic Specimen Bypass Window

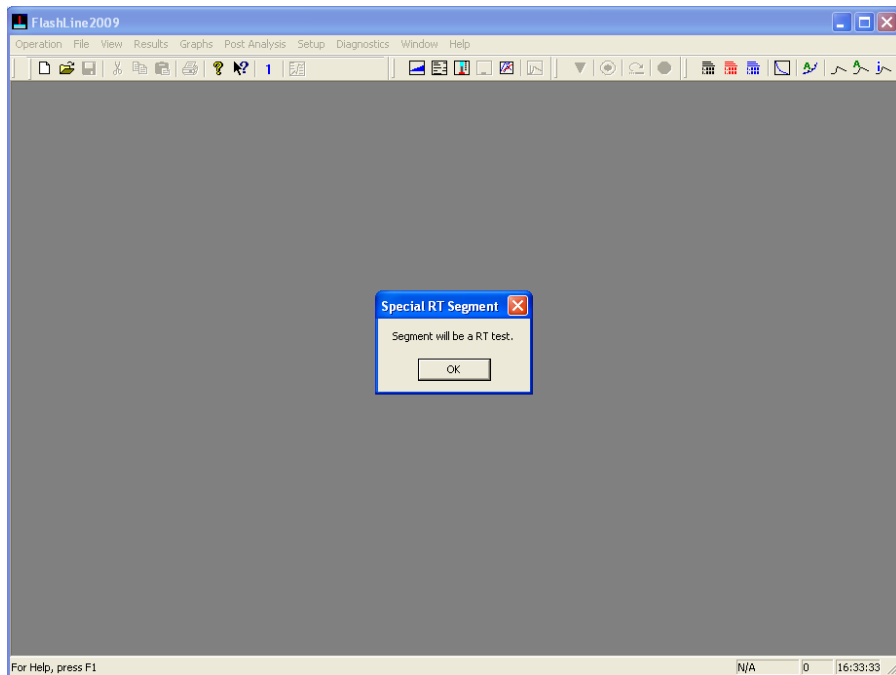


Figure B.11. Special RT Segment Window



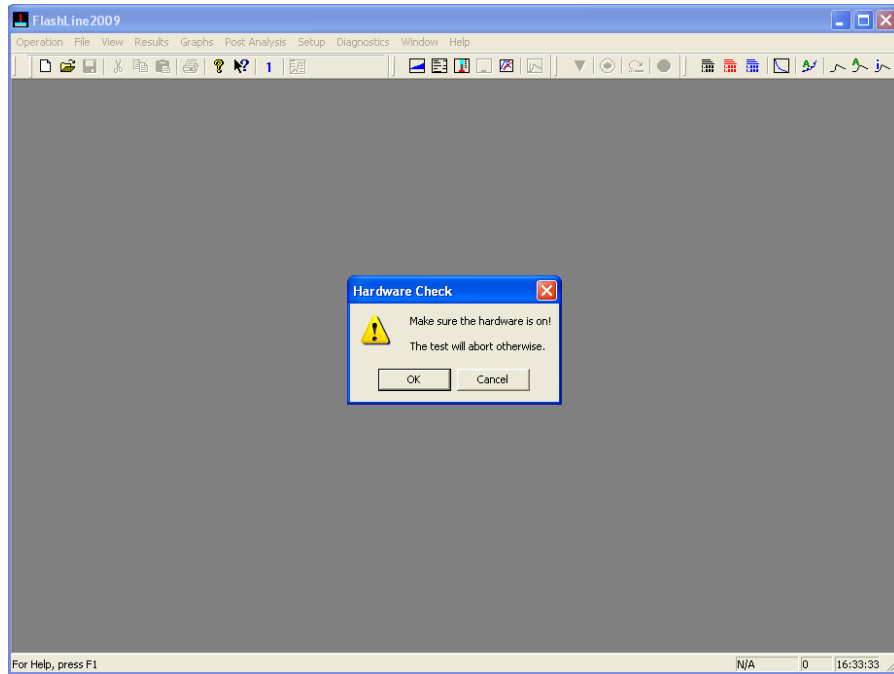


Figure B.12. Hardware Check Window

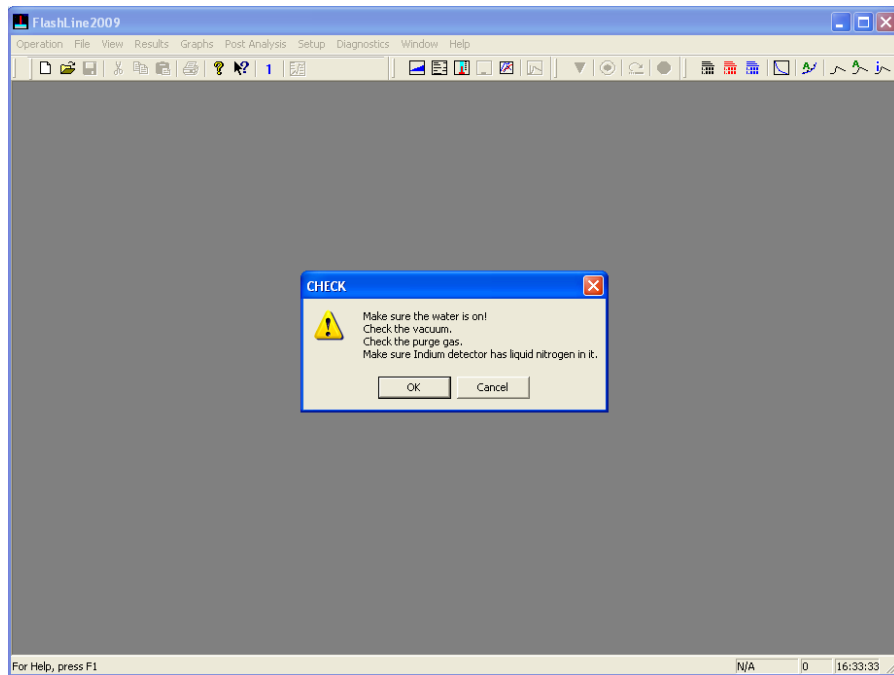


Figure B.13. Oil, Vacuum, Gas, and Detector Check Window

(Note: Allow for half an hour of periodic pouring of liquid nitrogen in order to fill the Indium detector. If the liquid nitrogen is continuously poured, it will continue to boil and cause

condensation to freeze inside the detector. The Indium detector needs to cool down dramatically for it to fill up with liquid nitrogen.)



Figure B.14. Compressed Nitrogen Gas and Liquid Nitrogen Indium Detector

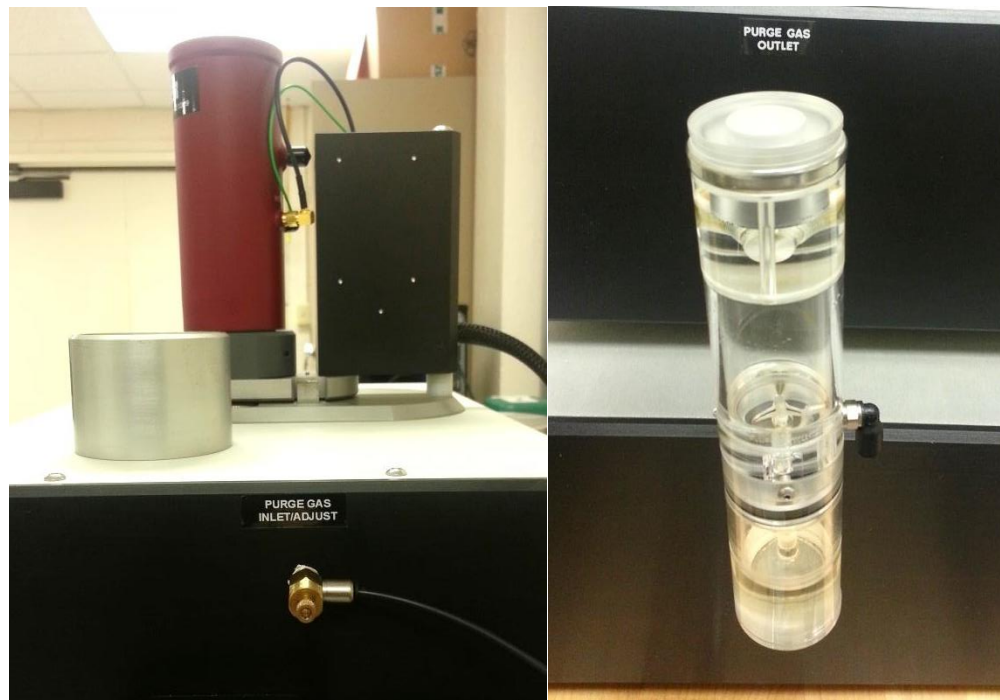


Figure B.15. Purge Gas Inlet Adjuster and the Purge Gas Outlet Oiler

After the compressed nitrogen gas (Figure B.14) is set to about 5 psi, adjust the gas inlet knob so that the bubbles in the purge gas outlet oiler appear approximately 3 times per second. The inlet is located on the right of the apparatus and the oiler on the left side of the apparatus.

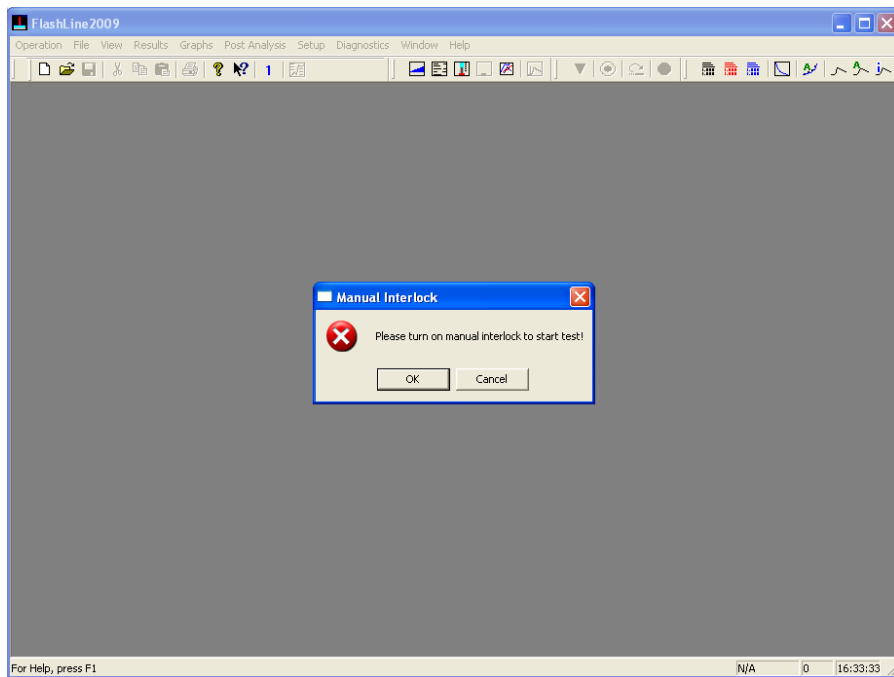


Figure B.16. Manual Interlock Window



Figure B.17. On and Off Interlock Switch on the Apparatus

Press the “ON” button to turn on the manual interlock as shown in Figure B.17, and then select “OK” in the “Manual Interlock” window shown in Figure B.16. The test will commence.

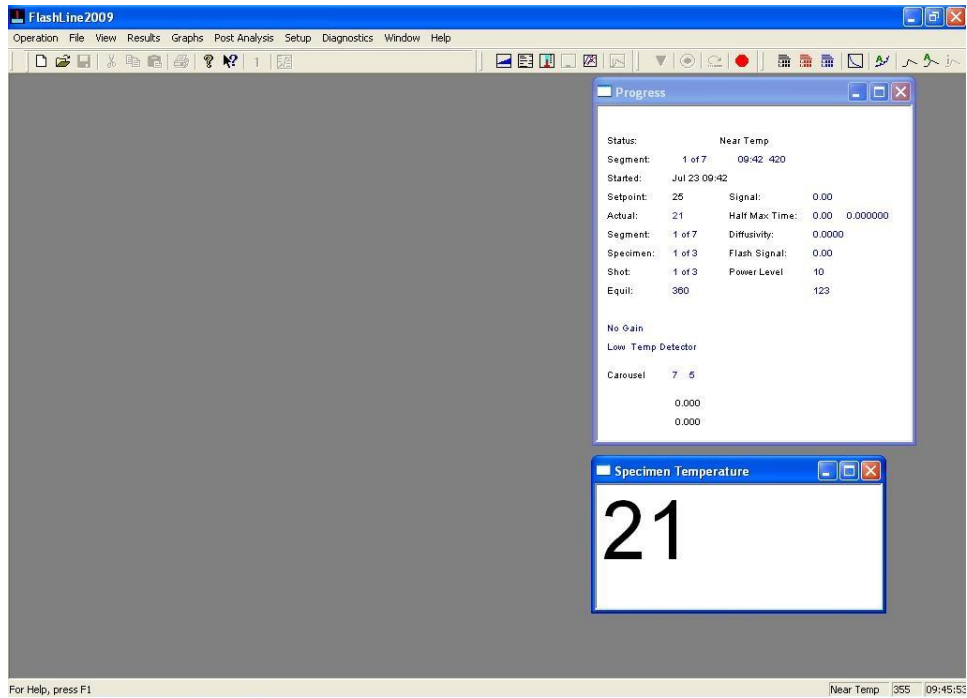


Figure B.18. Initial Screen after Started Test

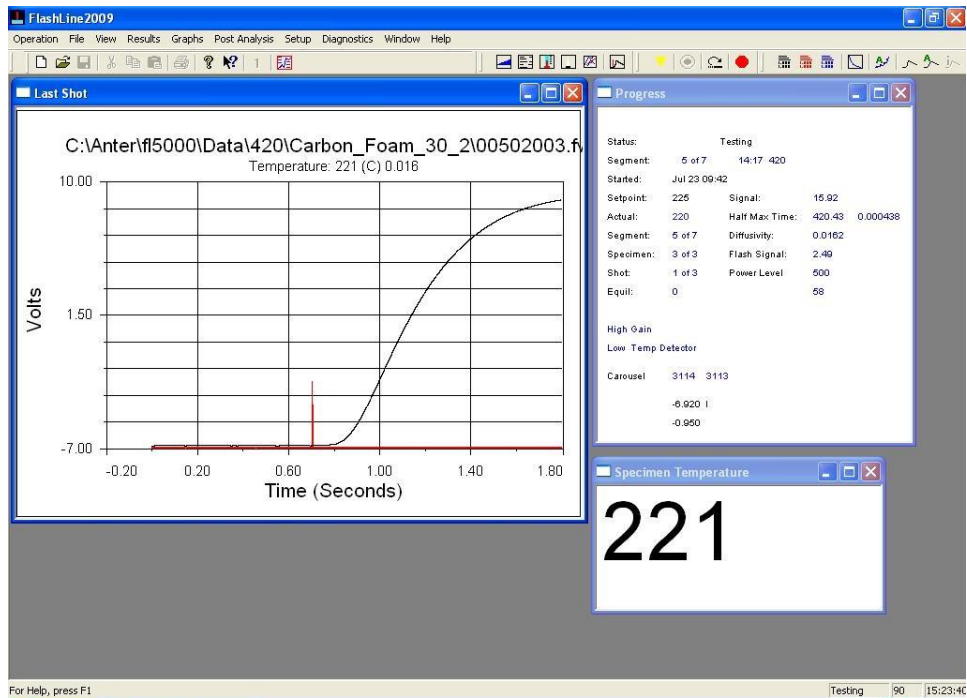


Figure B.19. Testing Window with the Last Shot

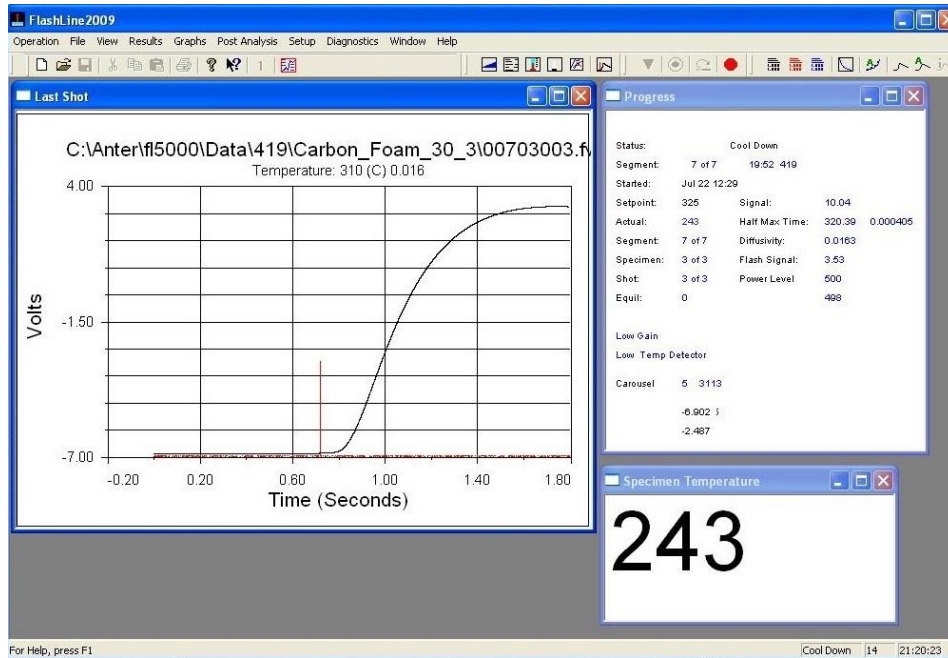


Figure B.20. Cool Down After Final Shot

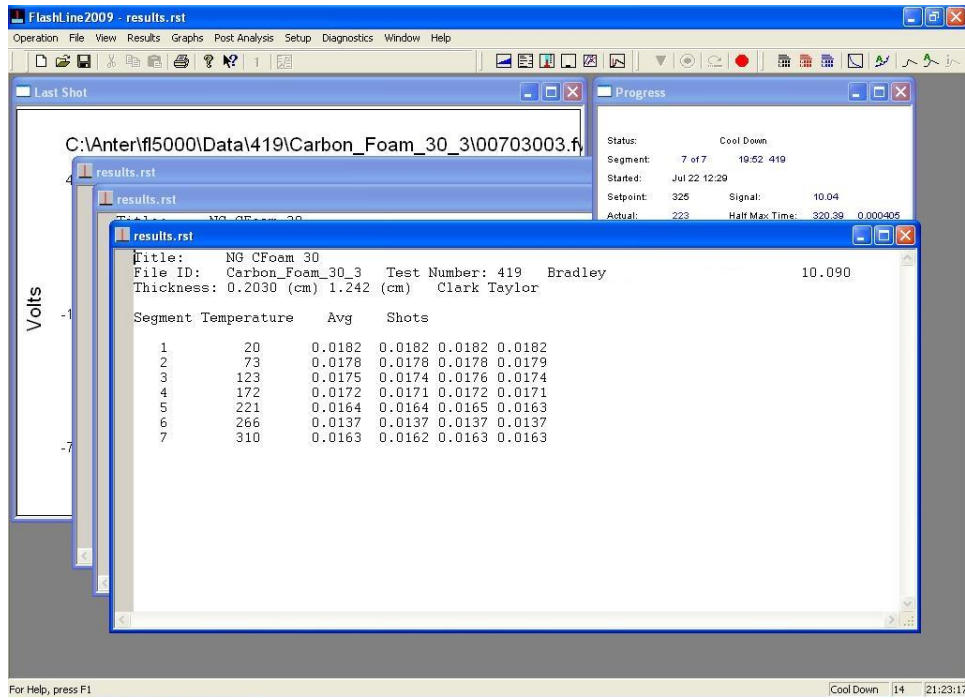


Figure B.21. Test Completion and Displayed Results

Figure B.21 shows the results of the completed test. The test duration can range from a few hours up to as much as 24 hours depending on the number of shots, temperature range, and

the time increment that is chosen. If running a longer test, it is important to refill the liquid nitrogen indium detector about halfway through the test in order to ensure that there is no noise in the graph (Figure B.20) and also that the results will be accurate. (Note: During testing, only fill the Indium detector with liquid nitrogen while the apparatus is heating and not while it is shooting. The data can be altered if the apparatus is not stable during the shots.) If there is anything else wrong with the test run (e.g., the gas is not thoroughly purged or the half-times are too high or too low), this will be indicated by noise in the “Last Shot” graph as shown in Figure B.20.

Once the test is completed, the data is now ready to be analyzed further in Excel. Note the folder in which the data was saved. After opening this folder, each sample folder will be displayed. Open a sample folder, and find the files named “results.all,” “results.clt,” and the files with the extension “.fw0.” The results files will provide the thermal diffusivity results, and the “.fw0” extension files will provide the thermogram data. The results files are easily imported into Excel for analyzing.

In order to convert the “.fw0” extension files into Excel compatibility, open the FlashLine™ 2000 software. Select the tab “Post Analysis” and click “Shot to Text File.” Select the file and sample folder that contains the “.fw0” extension. Change the “Files of Type” to “.fw0” to display the corresponding extension files, select a file, and click “OK.” (Note: Only one file can be converted to a text file at a time.) A “Copy Successful” should be displayed. Note the folder in which the text file was saved. Repeat these steps as necessary, and import the text files into excel for analyzing.

## Appendix C

### *Complete Computational Procedure: Specific Heat*

The following is a step by step procedure for running specific heat measurements using differential scanning calorimetry and the NETSZCH DSC Measurement software. Step one is to open the software.

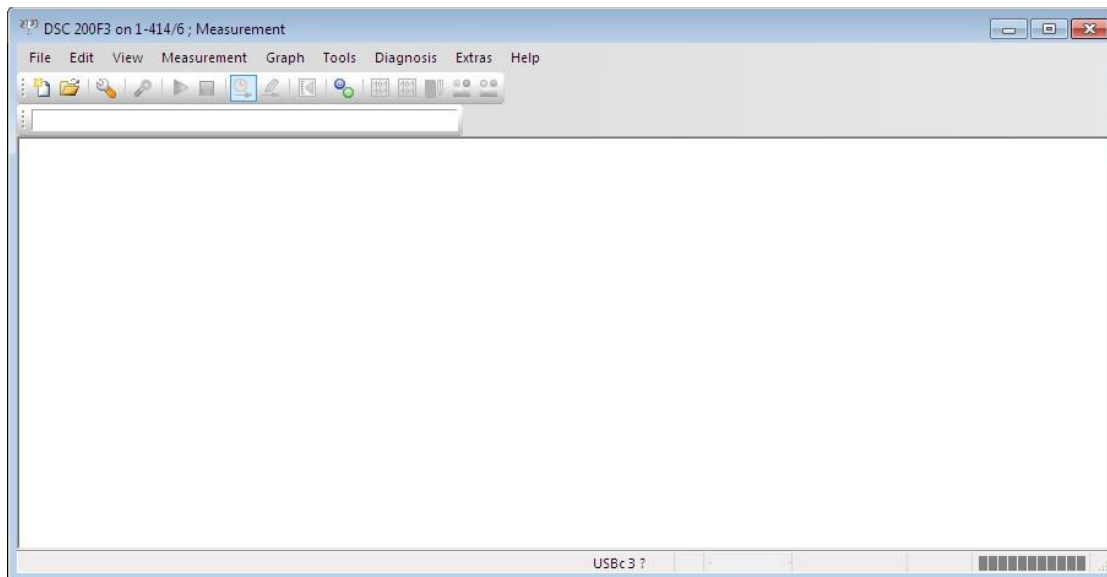


*Figure C.1.* Initial DSC Measurement Application Window

From here, click on “File” and “New” to open up the “Measurement Definition” screen and to begin a new specific heat experimental run. On this screen, the green circles indicate that the inputs are “OK.” If the inputs are not “OK;” however, the circles will light up red instead. The first tab is the “Fast Definition” tab. Select the desired measurement type, identity, sample name, sample mass, and crucible mass. Run a correction measurement type for a baseline run, a sample for just a sample run only, or a correction and sample run for both. Once all of the data is typed in, select “Forward.” It is important to note that throughout the measurement definition window, some of the circles will still be red after “Forward” is selected. Some circles might not change green until the “Last Items” tab and folder is selected in which to save the data.

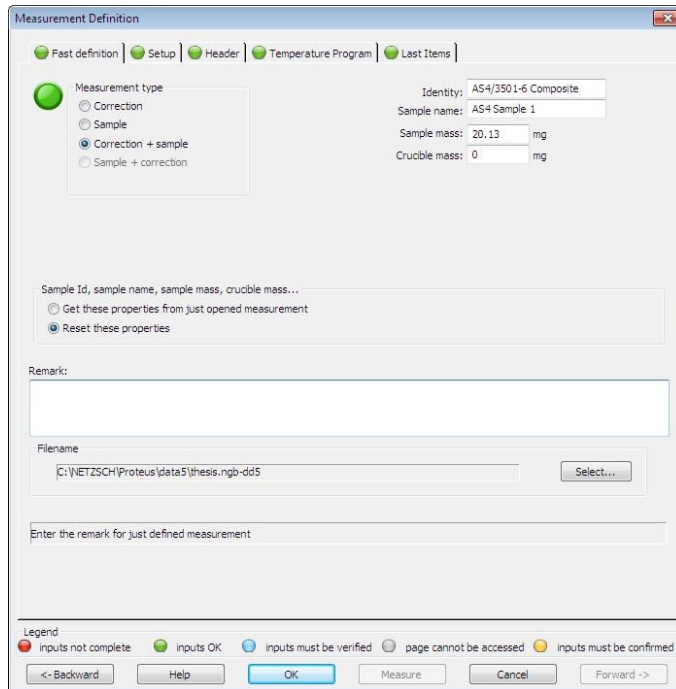


Figure C.2. Measurement Definition Window

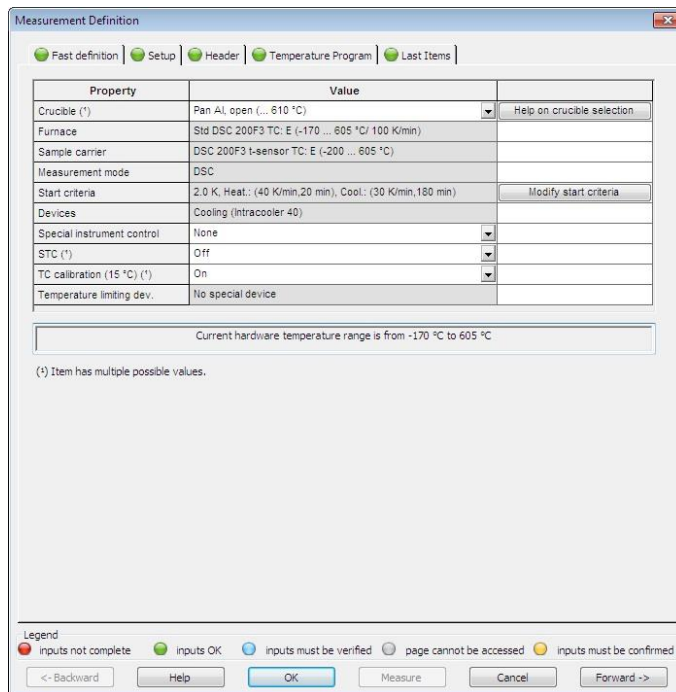


Figure C.3. Setup Tab in the Measurement Definition Window



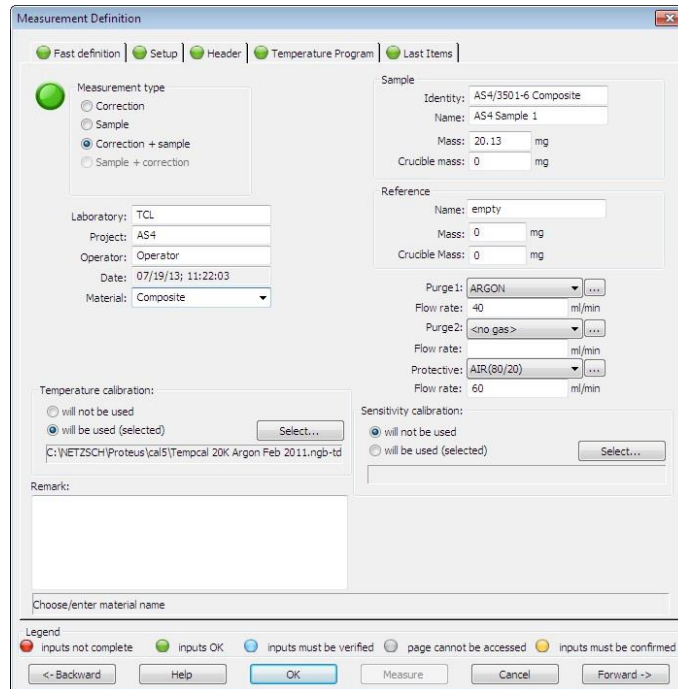


Figure C.4. First Measurement Application Window

The “Temperature Program” tab, as shown in Figure C.5, is an important window to pay close attention to because it determines the working temperatures during the experiment. Here, the temperatures for initial standby, dynamic, isothermal, and final categories are chosen in accordance with the limitations of the material being tested. The first temperature that is set is the initial temperature. This temperature is generally room temperature, and it will be the starting temperature of the material. During the test displayed, the specimen is cooled down to 5 degrees Celsius and is then held at an isotherm. Next, the apparatus dynamically heats until the desired temperature and holds at another isotherm. From there, set the emergency cut-off temperature at roughly 10 degrees higher than the isothermal temperature for safety. Finally, the chiller will cool the apparatus. Remember to select the rate in Kelvin per minute at which to cool and heat. Select a destination for the results, and save as shown in Figure C.6.

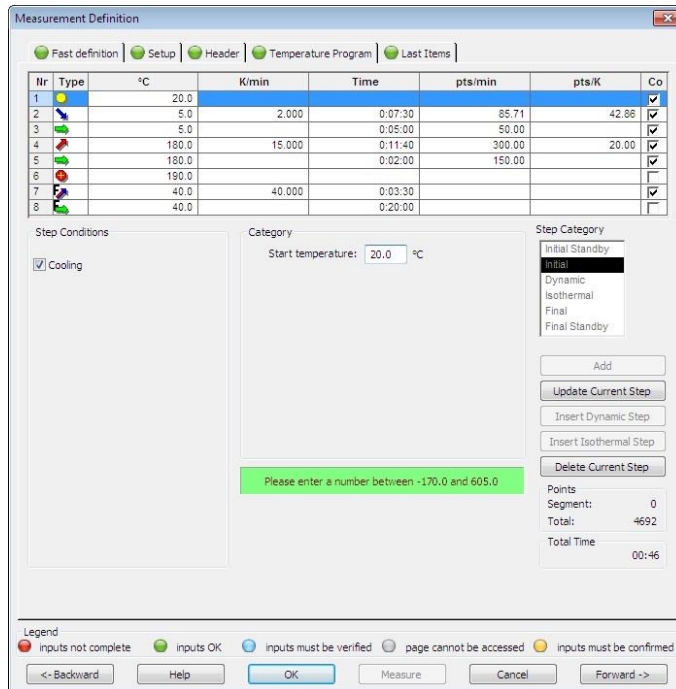


Figure C.5. Temperature Program Tab in the Measurement Definition Window

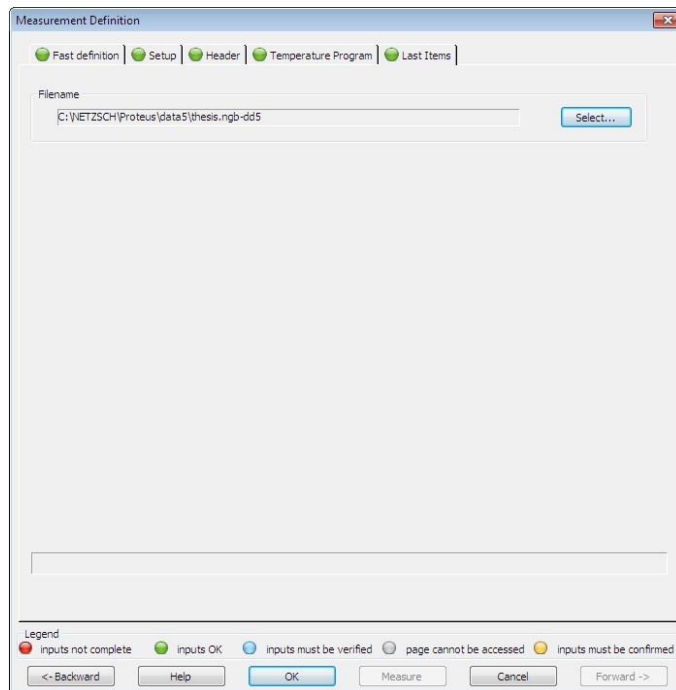
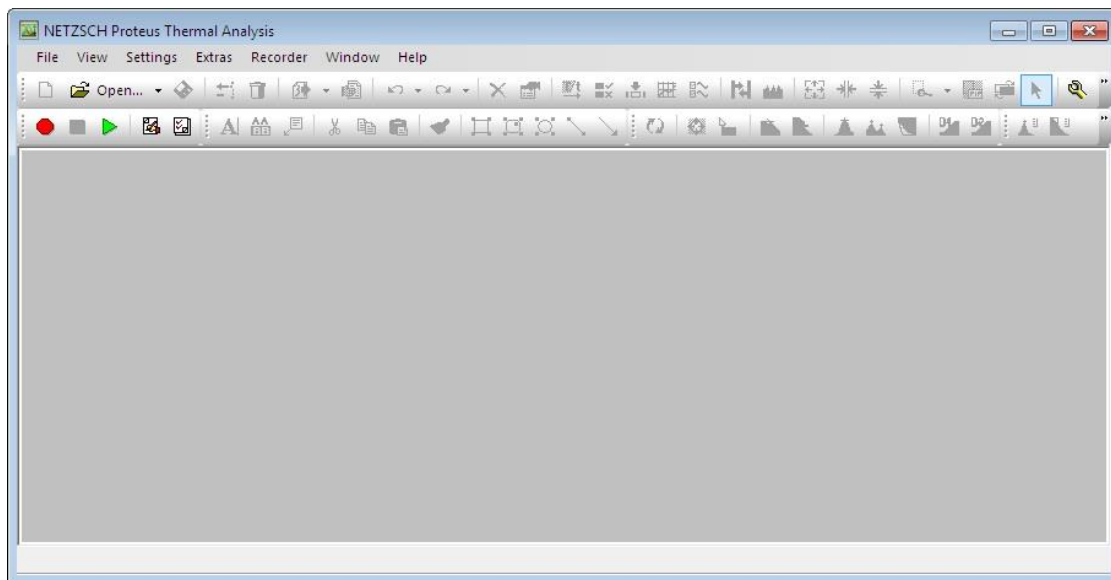


Figure C.6. Last Items Tab in the Measurement Definition Window

As shown in Figure C.7, set the compressed Argon gas tank to about 4-5 psi to purge the environment within the apparatus.



*Figure C.7. Compressed Argon Gas*



*Figure C.8. Initial NETZSCH Proteus Thermal Analysis Window*

After the test is completed, the data is now ready for analysis. Open the NETZSCH Proteus Thermal Analysis software. Go to “File” and “Open” and select the test runs that were saved along with the concurrent baseline. A graph of the data will open as shown in Figure C.10.

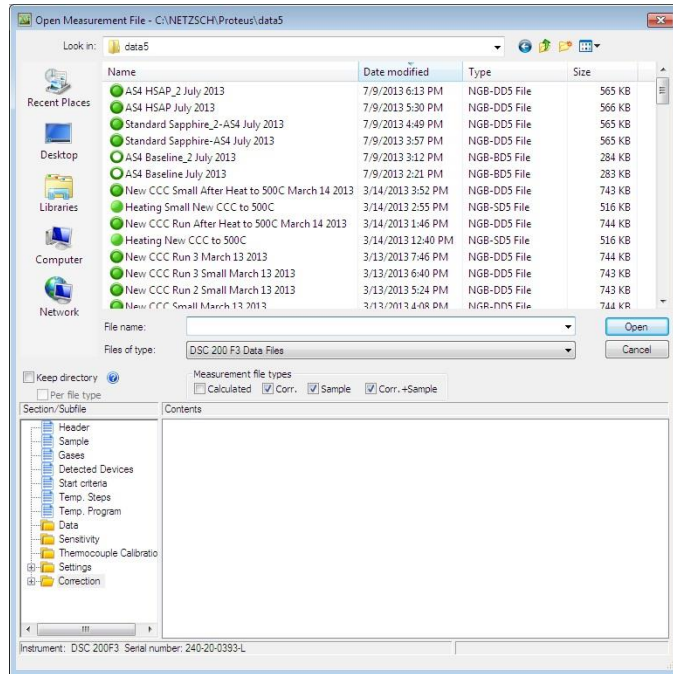


Figure C.9. Open Measurement File Window

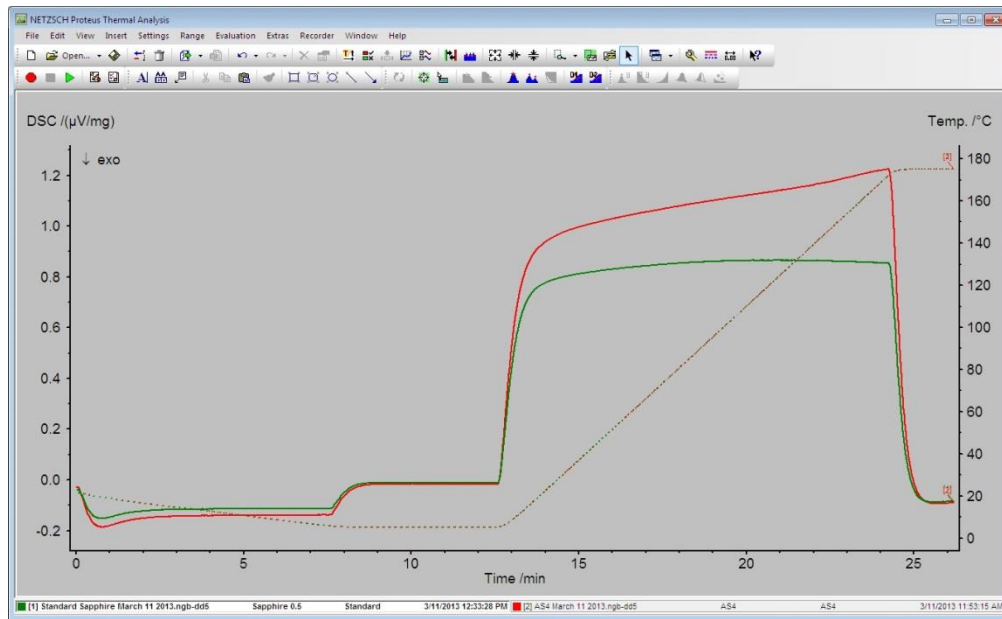


Figure C.10. Graph of the Specific Heat Runs

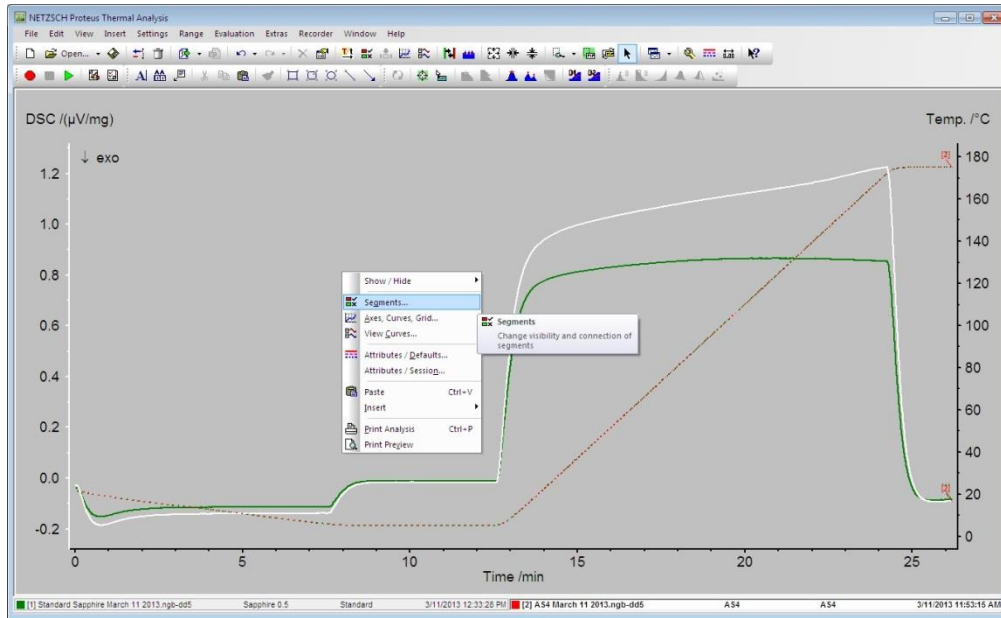


Figure C.11. Graph of the Specific Heat Runs and Right-click Options

Right-click anywhere on the graph, and select “Segments...” (Note: The “Segments...” option will not appear if a curve is right-clicked. The curve that is highlighted is also highlighted at the bottom of the screen for differentiation). The “Segments” window will pop up as shown in Figure C.12. Segments allow for the change of visibility and connection of segments.

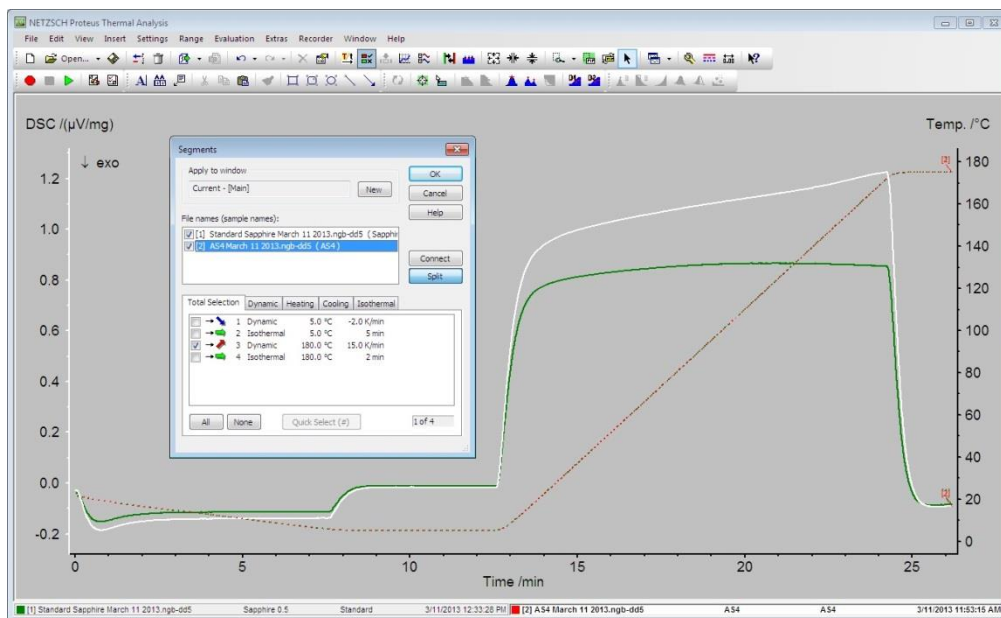


Figure C.12. Segments Window

Under the “File names (sample names):” box, click on the standard sample and tested sample one at a time, and only check the **dynamic** heating and/or cooling boxes to display the dynamic heating and/or cooling segments of the graph for both the standard and the sample. The result is shown in Figure C.13. For the sample shown, dynamic cooling was not applicable.

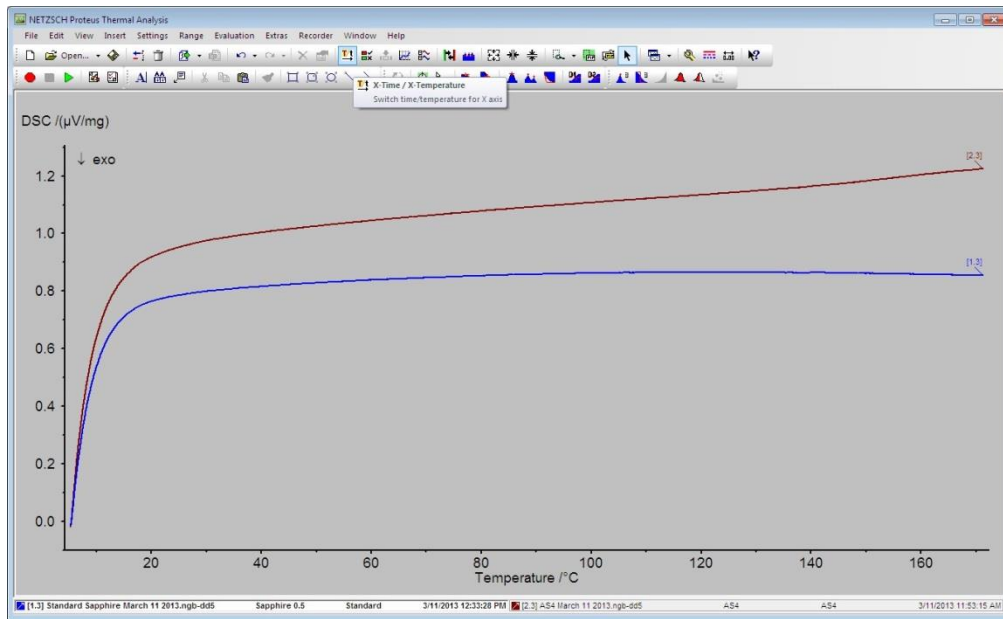


Figure C.13. Display of the Dynamic Heating Segments

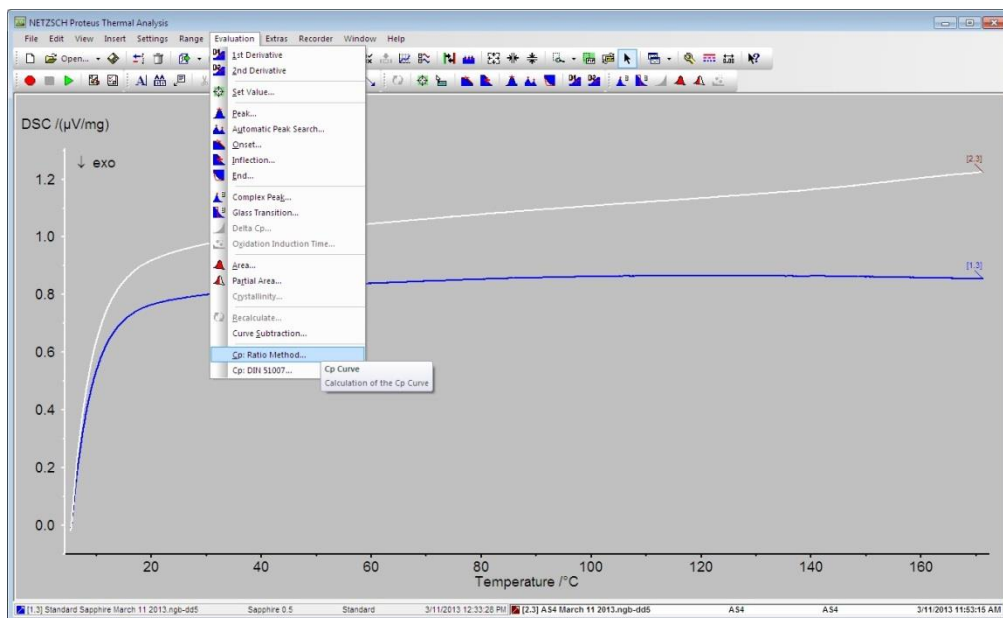


Figure C.14. Evaluating the Dynamic Heating Segments

In order to compute the specific heat, click on “Evaluation,” and select “Cp: Ratio Method...” This option will calculate the specific heat of the curve of the graph. The “Open Cp Standard File” window will appear as shown in Figure C.15. Select the corresponding standard, and click “Open.”

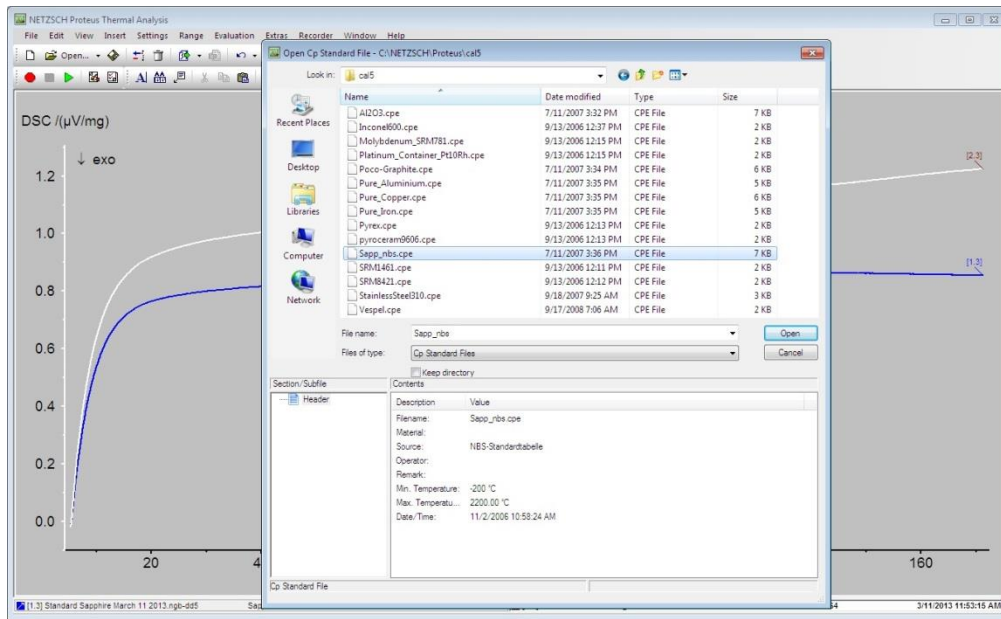


Figure C.15. Opening the Specific Heat Standard

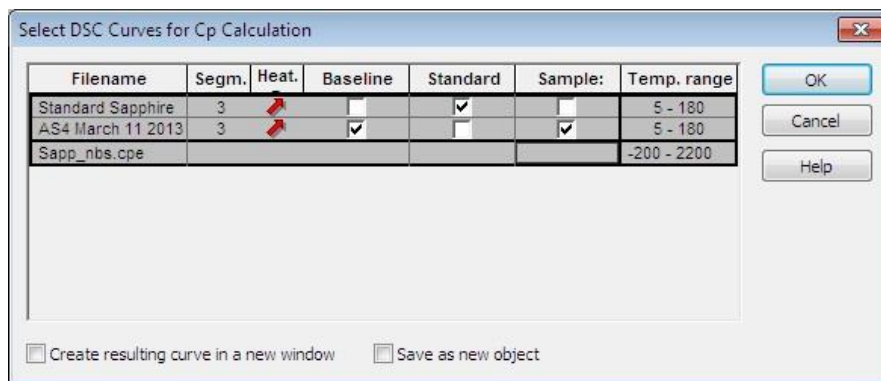


Figure C.16. Select DSC Curves for Cp Calculation Window

The “Select DSC Curves for Cp Calculation” window, as shown in Figure C.16, should appear next. It is important to check the standard as the standard and the sample as the sample.

The “Baseline” column does not necessarily matter. Select “OK.” The specific heat curve will now be shown on the graph as displayed in Figure C.17.

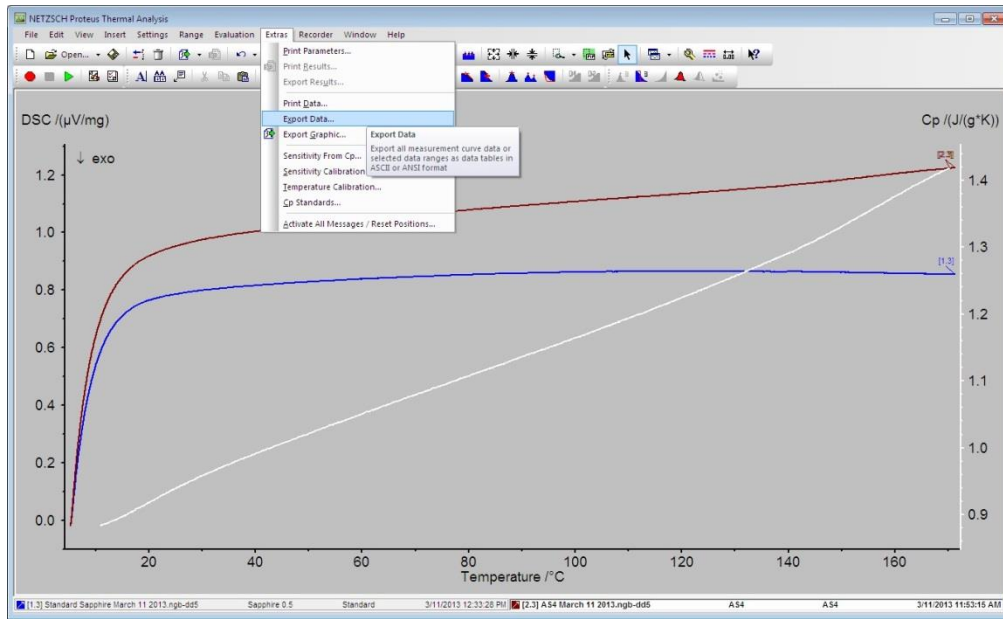


Figure C.17. Specific Heat Curve Shown on the Graph

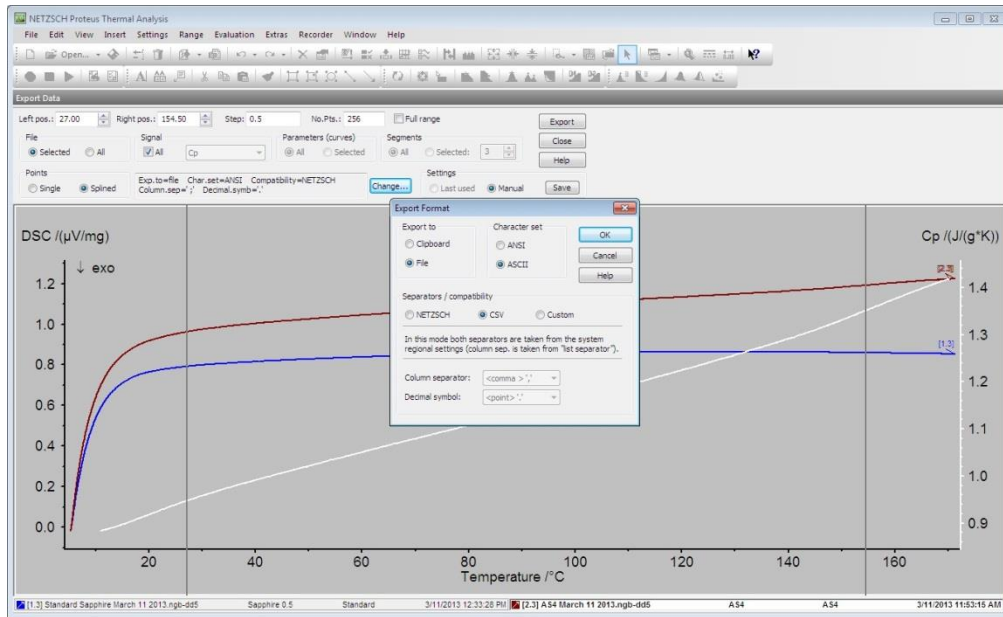


Figure C.18. Export Data and Export Format Window

Finally, the data is now ready to be exported and analyzed further in Excel. In order to do this, click on the “Extras” tab, and select “Export Data...” This will export all measurement data



ranges as data tables in ASCII or ANSI format. The first window displayed is the “Export Data” option set as displayed in Figure C.18. After the range for the specific heat values has been selected, click “Change...” to modify the format of the exported specific heat data. The ASCII character set and the CSV separator are the most practical for general purpose use in an Excel file. Select “OK,” and transfer the data using a flash drive to further analyze the specific heat data in Excel. Close the software.

## Appendix D

### *Future Research: Computational Procedure for Thermal Expansion*

The following is a step by step procedure for running thermal expansion measurements using the Dilatometer 1000 software by Anter Corporation. Step one is to open the software. The platform is displayed in Figure D.1.

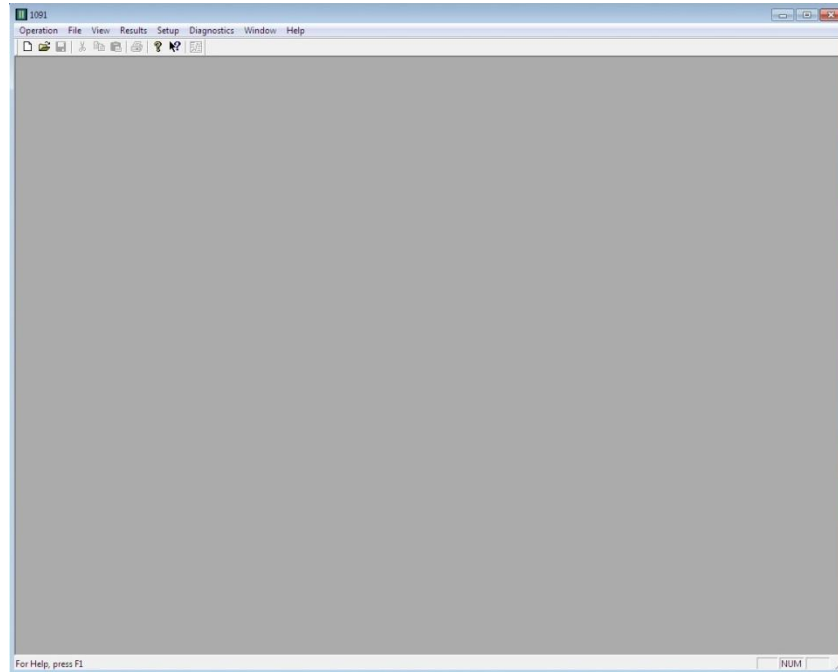


*Figure D.1.* Initial Dilatometer 1000 Software Screen

From here, click on ‘Operation’ and then ‘Startup Information’ as shown in Figure D.2. In Figure D.3, the next window to appear will be the furnace type selection. There should only be one furnace type which is the ‘1091’ furnace. Select ‘OK.’ Turn the Unitherm™ Dilatometer System Series 1000 apparatus on in order to use the ‘Controller Parameter File’ as shown in Figure D.4. Select ‘No’ unless major changes are being made for the test (e.g., calibration, etc.). (Note: Make sure all cables are properly connected including the orange Ethernet cable and that there is a network connection. See the ‘Dil Soft Manual 10-5.pdf’ file for the Software Manual Dilatometer System for additional help or information.)

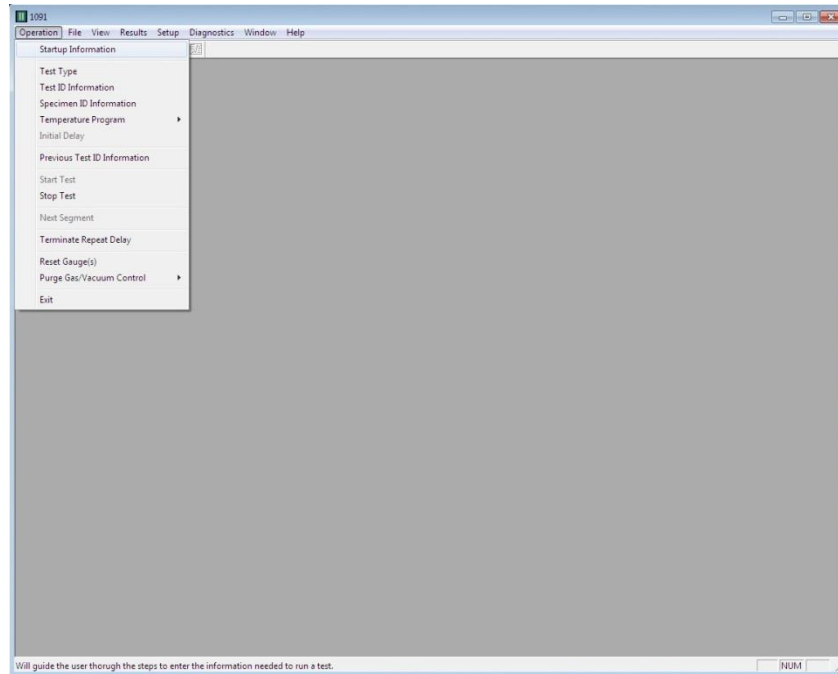


Figure D.2. Startup Information Operation

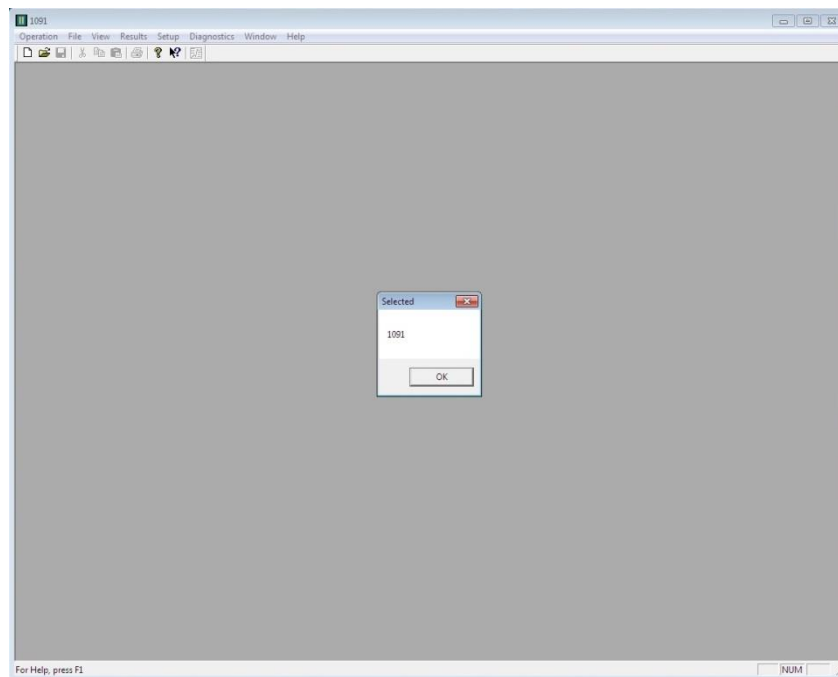
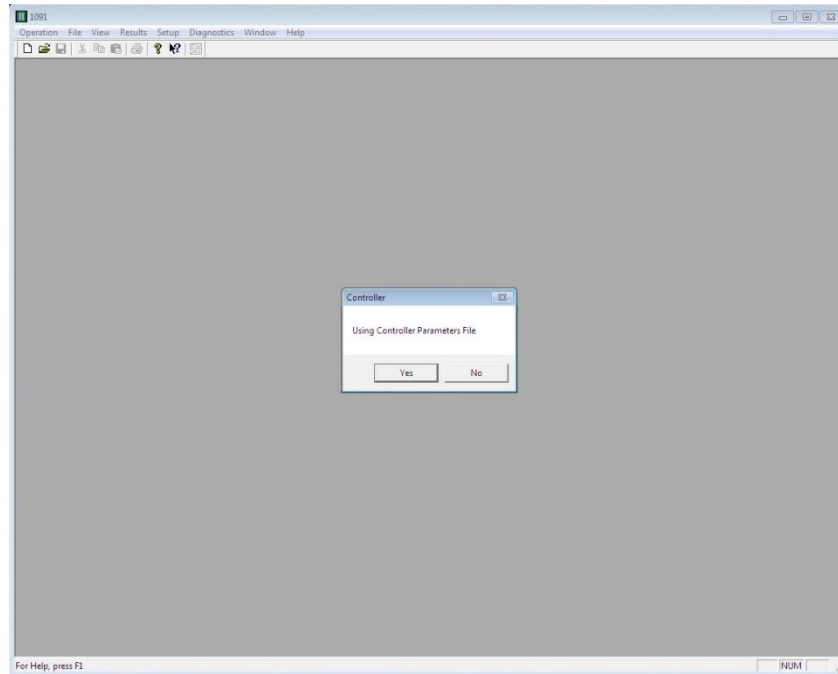
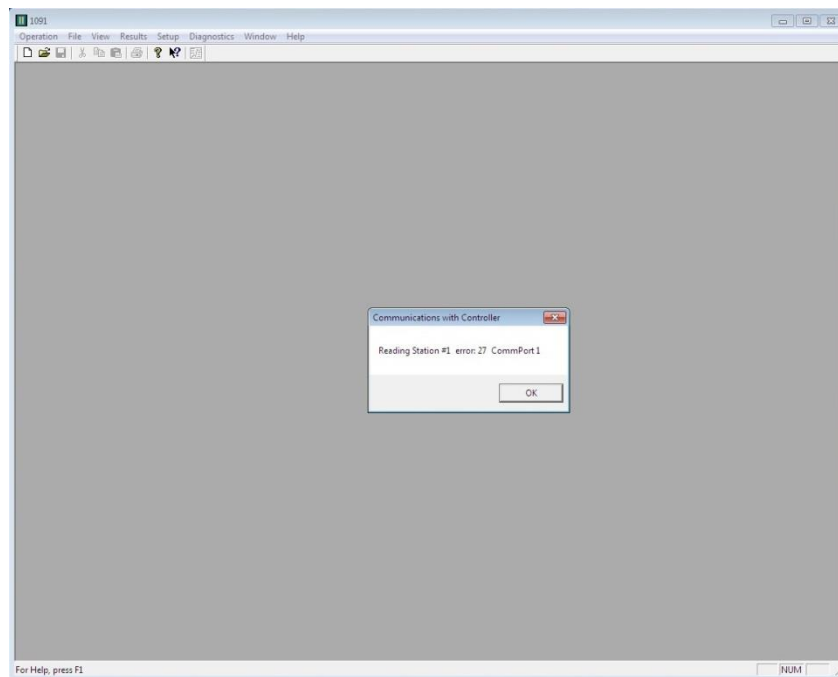


Figure D.3. Furnace Type Selection Window



*Figure D.4. Controller Window*



*Figure D.5. Communications with Controller Error Window*

If this error window is shown, as in Figure D.5, check all connections, and make sure the orange Ethernet cable is properly connected with the correct IP address. In Figure D.6, the first test ran should be a ‘Calibration Test.’

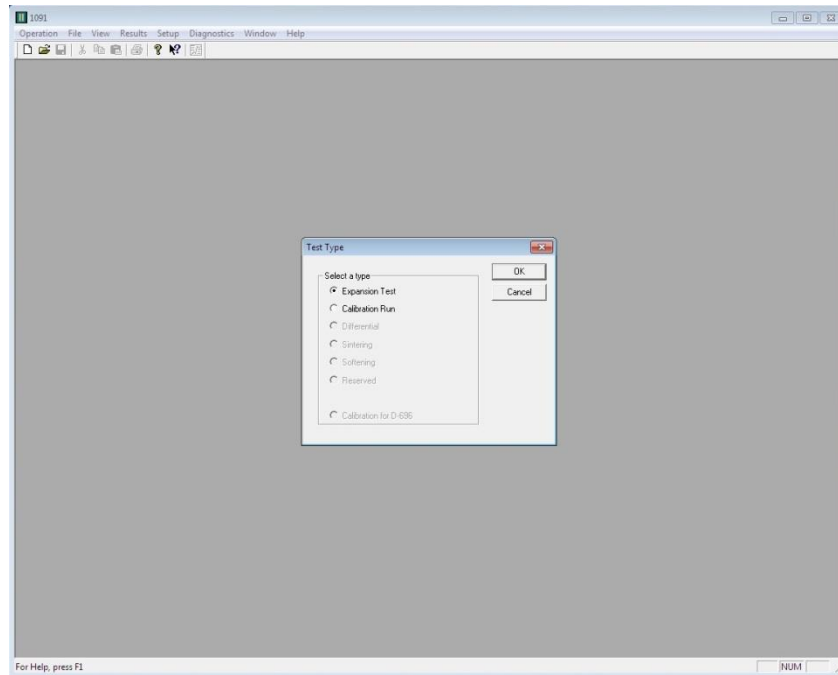


*Figure D.6.* Test Type Window

Select the test type desired for the test that is to be run as shown in Figure D.6, and then select the calibration information file to be used in correspondence with the test being run.

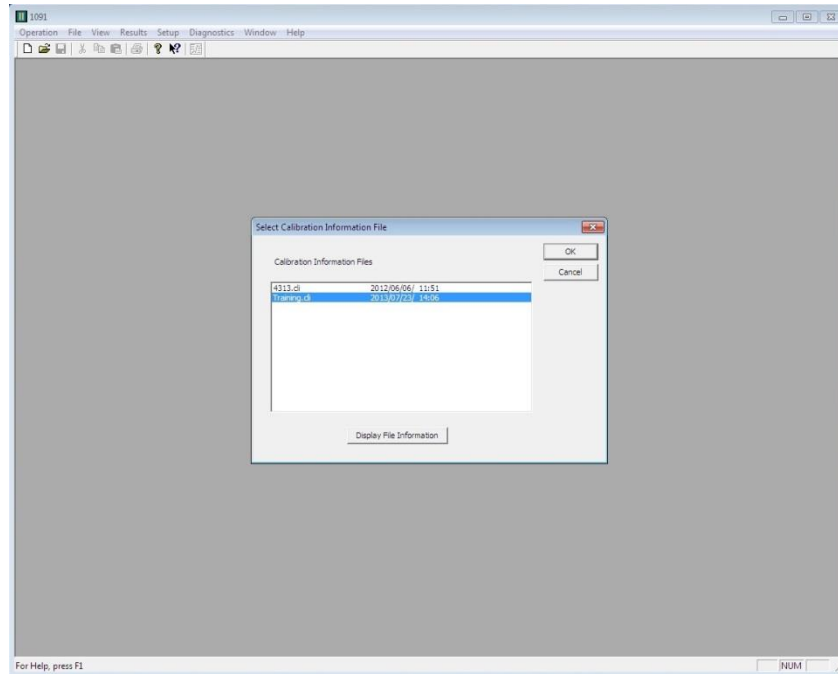


*Figure D.7.* Calibration Information File Window

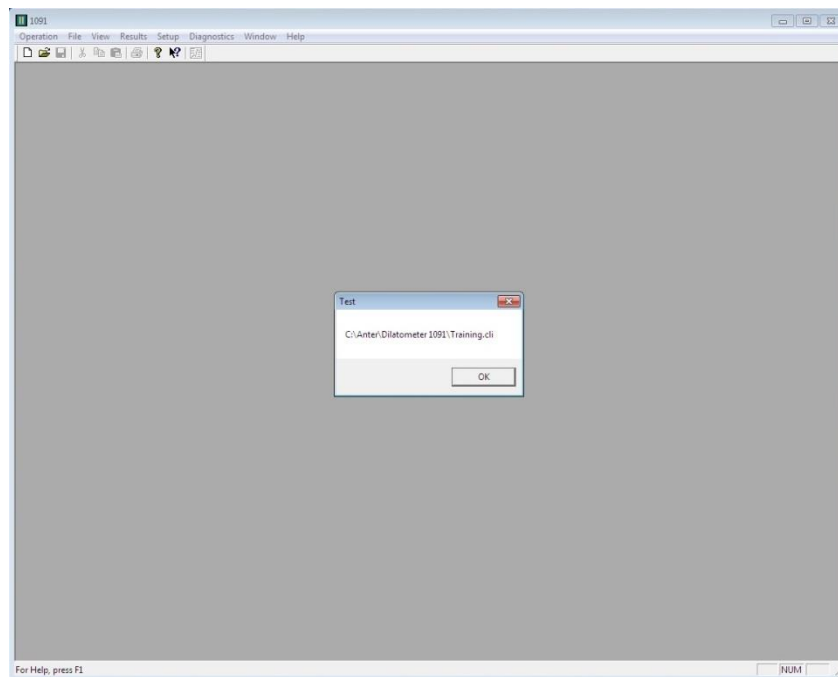


*Figure D.8.* Test Location Window

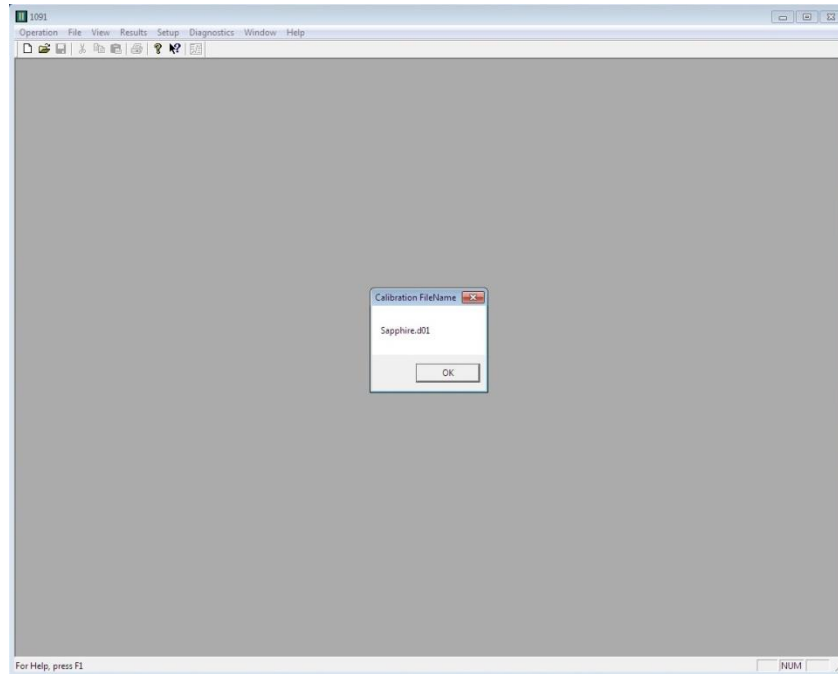


*Figure D.9. Calibration File Name Window*

Select 'OK' for the test location and calibration file name as shown in Figures D.8 and D.9 to confirm the information entered previously.

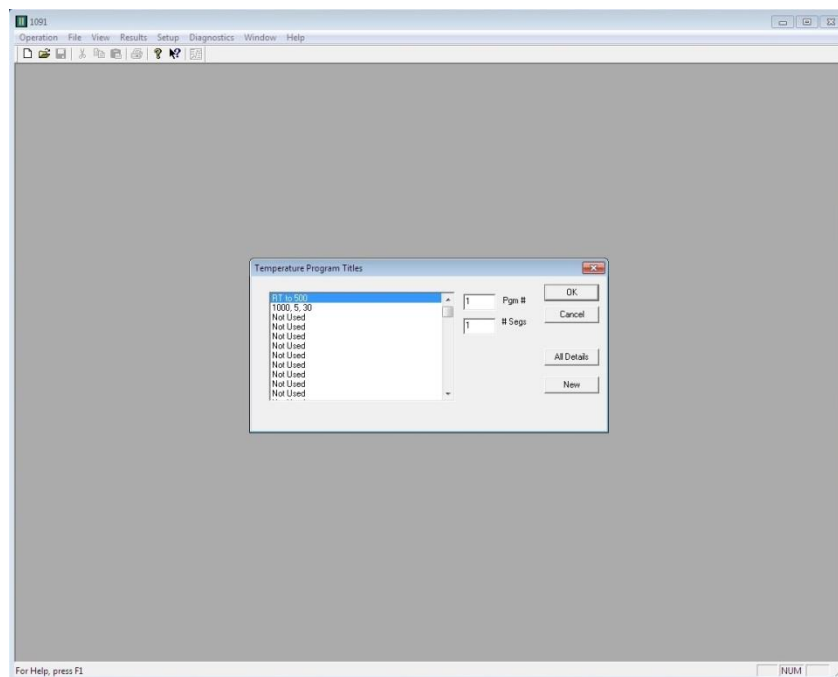


*Figure D.10. Temperature Program Titles Window*

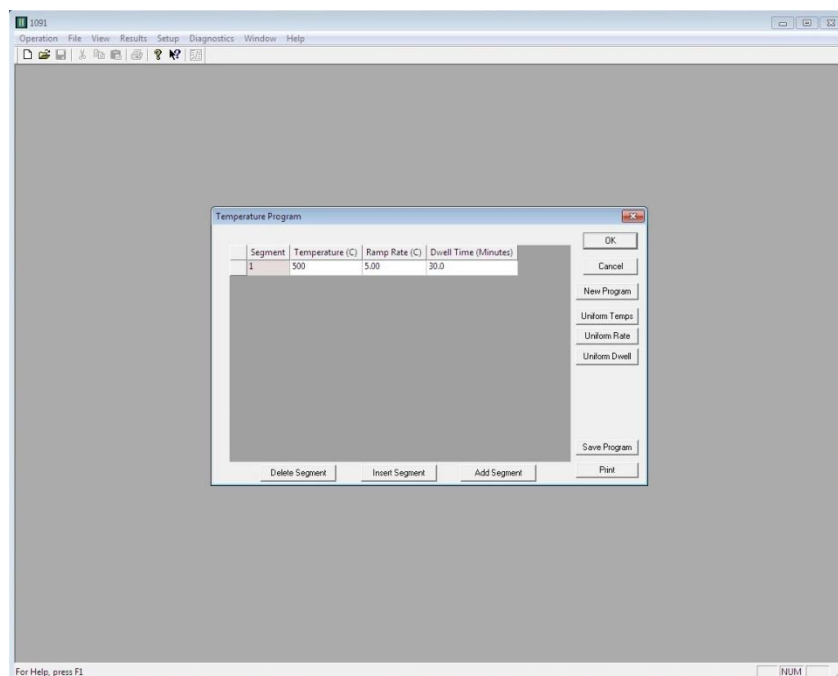


*Figure D.11.* Temperature Program Window

In Figure D.10, select 'RT (room temperature) to 500,' and select 'OK' to set the temperature program title or select 'New' to create a new temperature program title. In Figure D.11, enter the final temperature for the test in column two, the ramp rate in degrees Celsius per minute in column three, the dwell time in column four. (Note: The dwell time can be set to 0 because there is no need to hold, or 'dwell,' at the segment temperature unless there will be a suspected reaction to occur.)



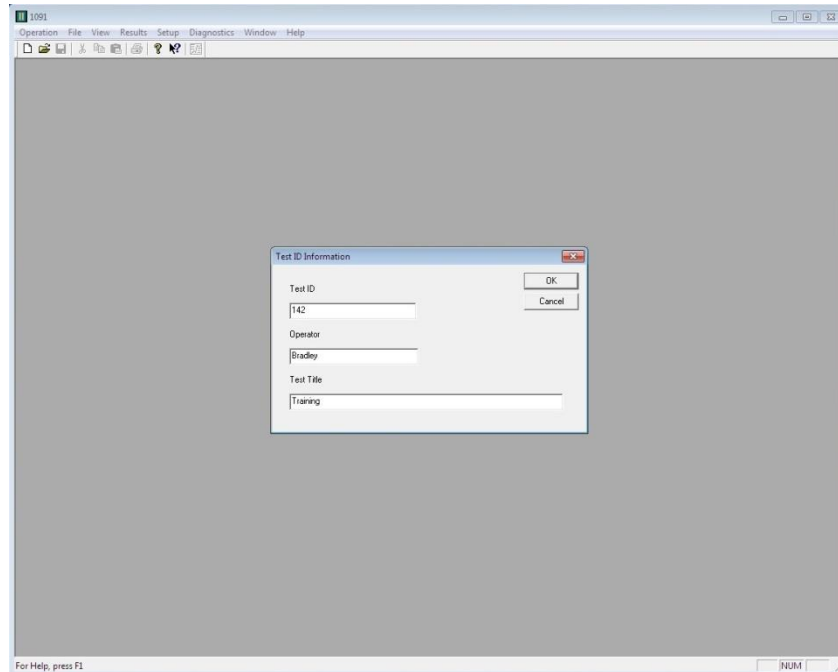


*Figure D.12.* Test ID Information Window

Enter the test ID information in the window shown in Figure D.12. After that, the next window will prompt for the specimen information. Enter the corresponding specimen information as shown in Figure D.13. Figure D.14 shows the initial delay settings. Under ‘Parameters,’ the time can be set to 0. The time can be set to 1.5 or 3 hours, if desired, in order to be certain that the system has achieved equilibrium. The gas purge will only take a few minutes, and the water purge does not need any time at all; therefore, the initial delay of anything else besides 0, is not necessary for the means of the experiments. Select ‘OK.’

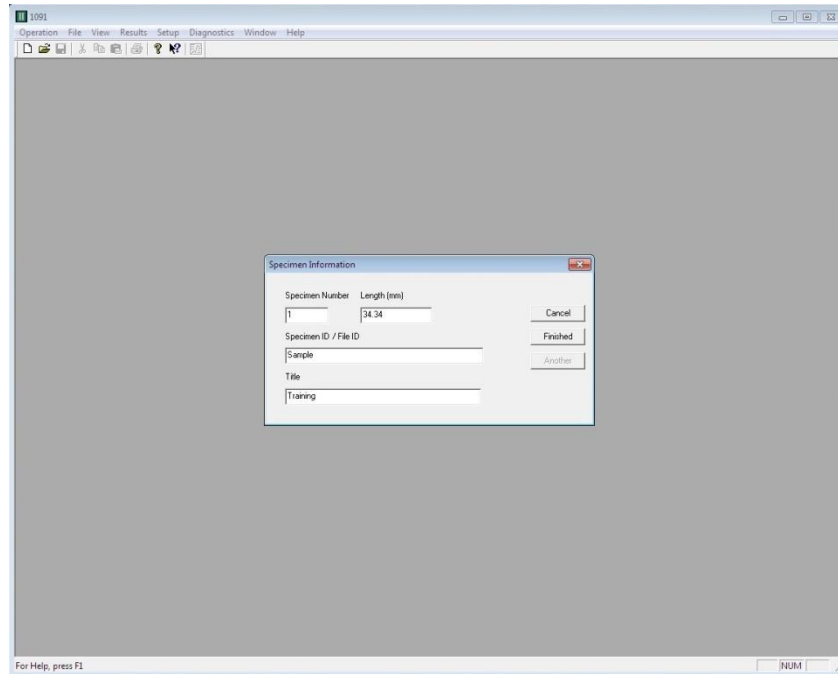


Figure D.13. Specimen Information Window

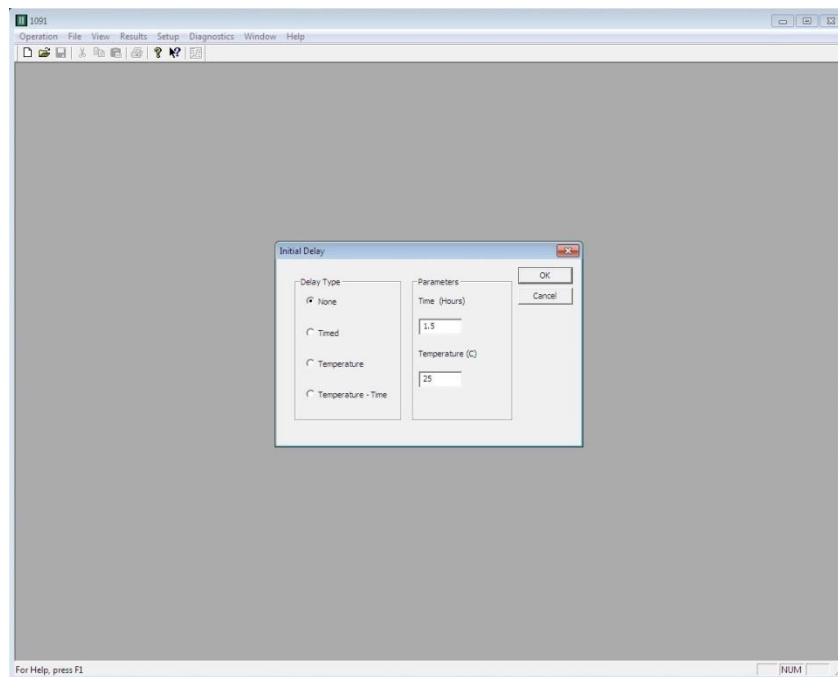
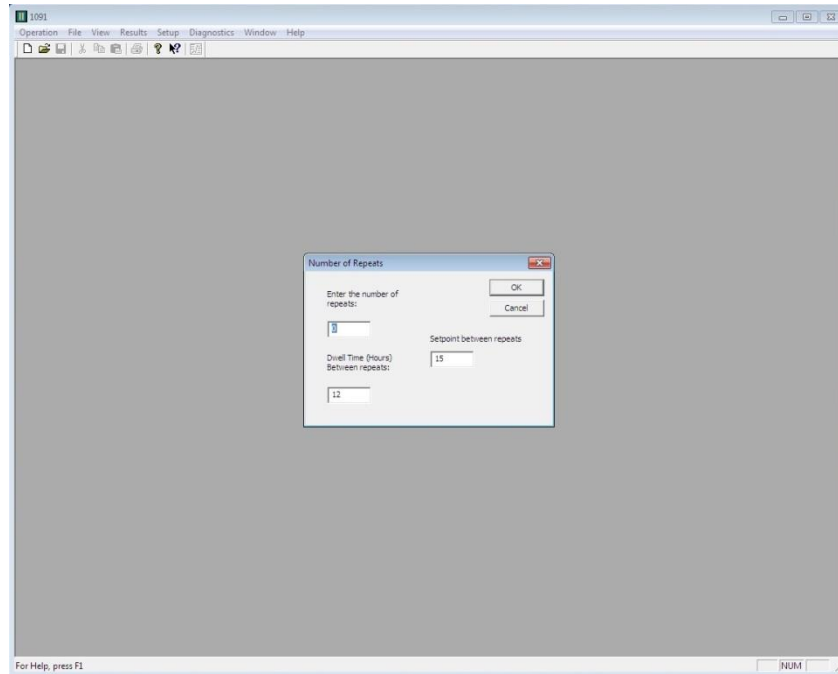
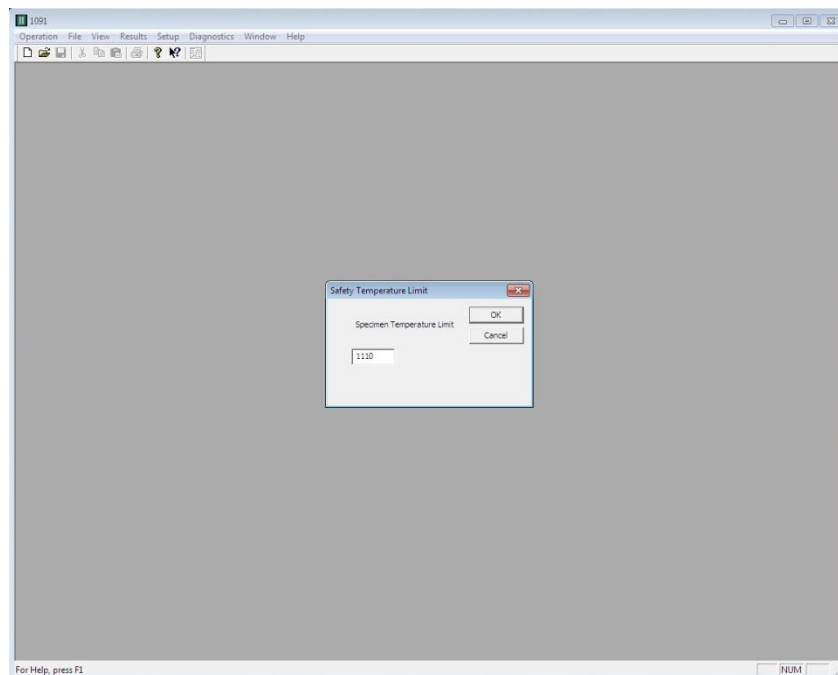


Figure D.14. Initial Delay Window



*Figure D.15.* Number of Repeats



*Figure D.16.* Safety Temperature Limit Window

The default safety temperature limit is 1110 °C which is appropriate for testing. Select 'OK' for Figures D.16 and D.17 if no repeat experiments are desired.

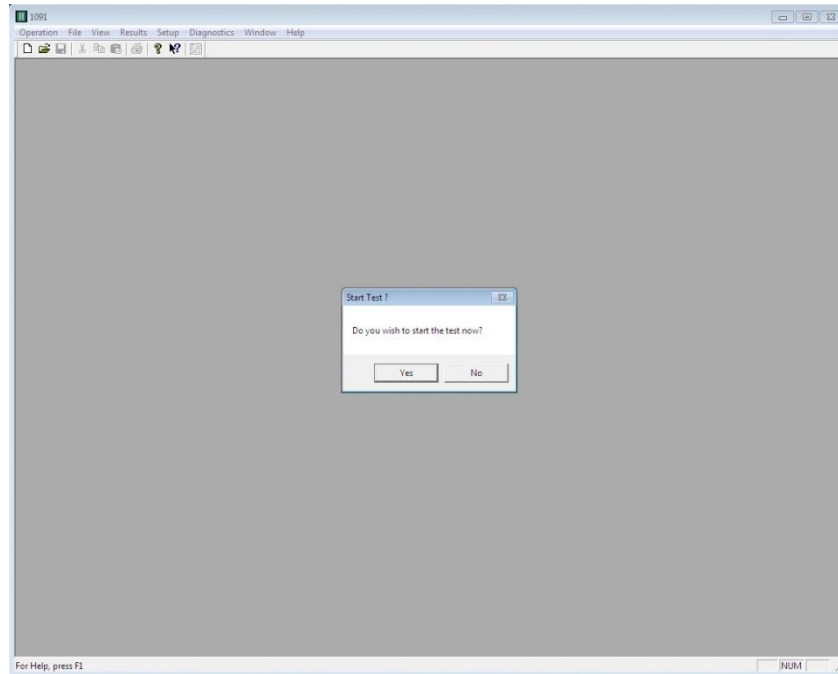


*Figure D.17. Start Test Window*

(Note: The test will not start after clicking 'Yes' in the window shown in Figure D.17.)

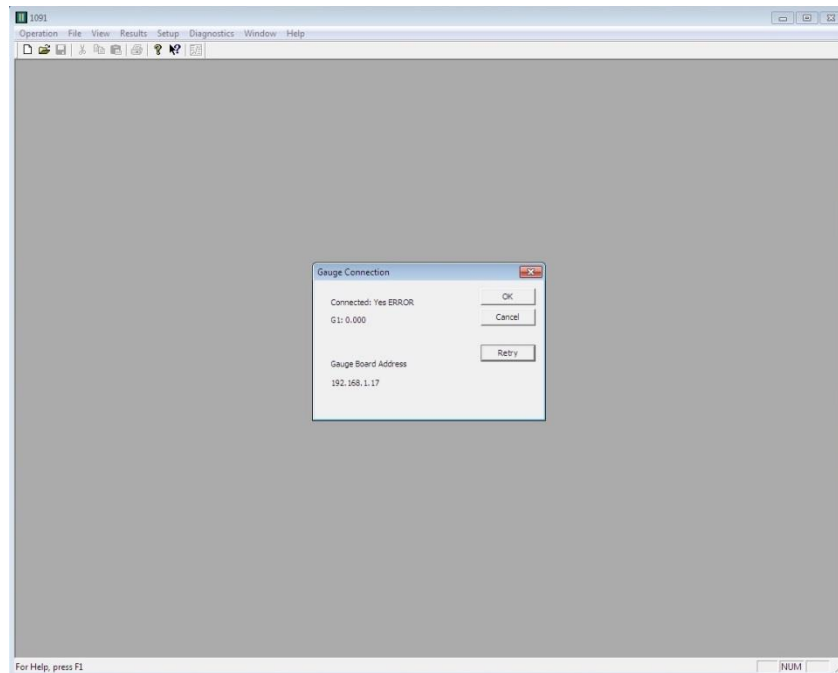


*Figure D.18. Gauge Connection Window*

The window in Figure D.18 checks for errors in the gauge connection and verifies that IP addresses are working properly. See the software manual for additional information.

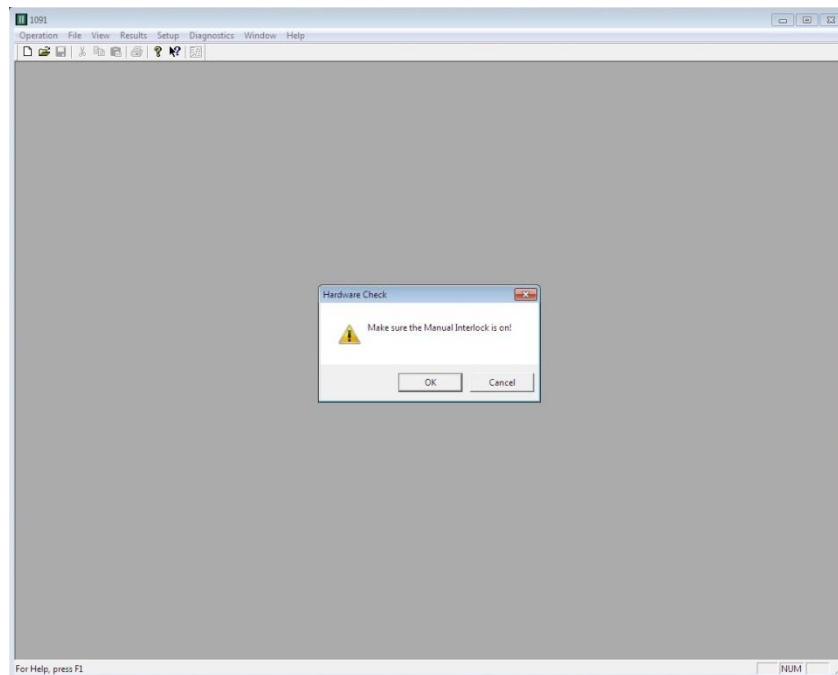


*Figure D.19.* Manual Interlock Check Window

Make sure the hardware is turned on as displayed in Figure D.20, and then select 'Ok' in Figure D.19 to proceed.



Figure D.20. Unitherm™ Dilatometer System Series 1000

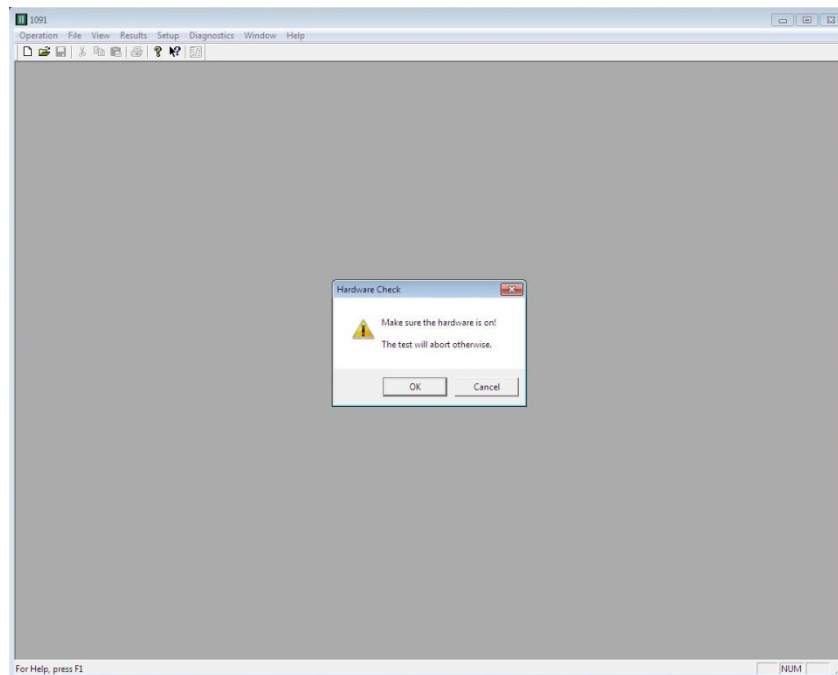


Figure D.21. Hardware Check Window

(Note: The hardware is automatically on. There is no need to check it. Click 'OK.')

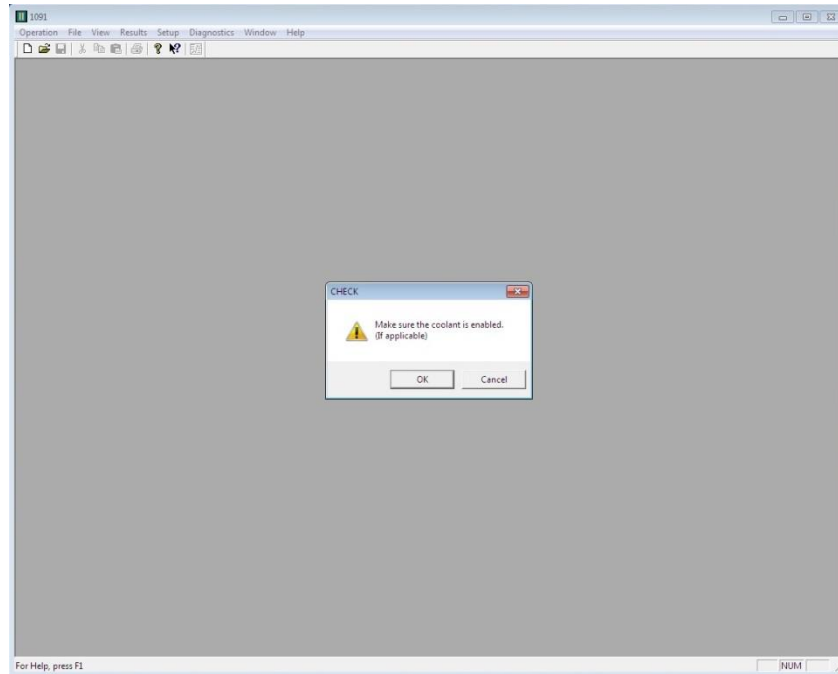


Figure D.22. Coolant Check Window

(Note: Make sure the cool water at the faucet is running. The test will proceed to initiate after this window.)

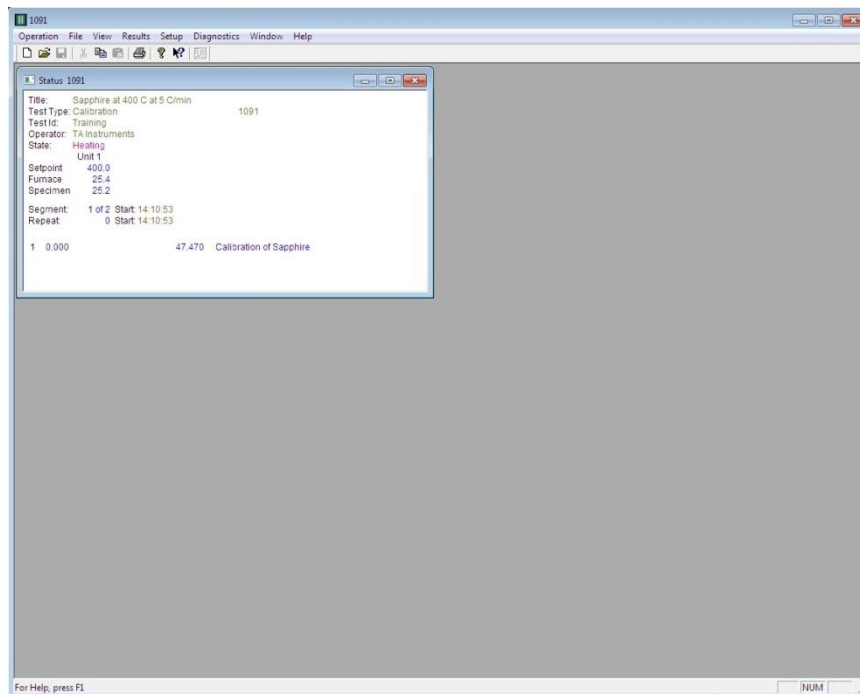
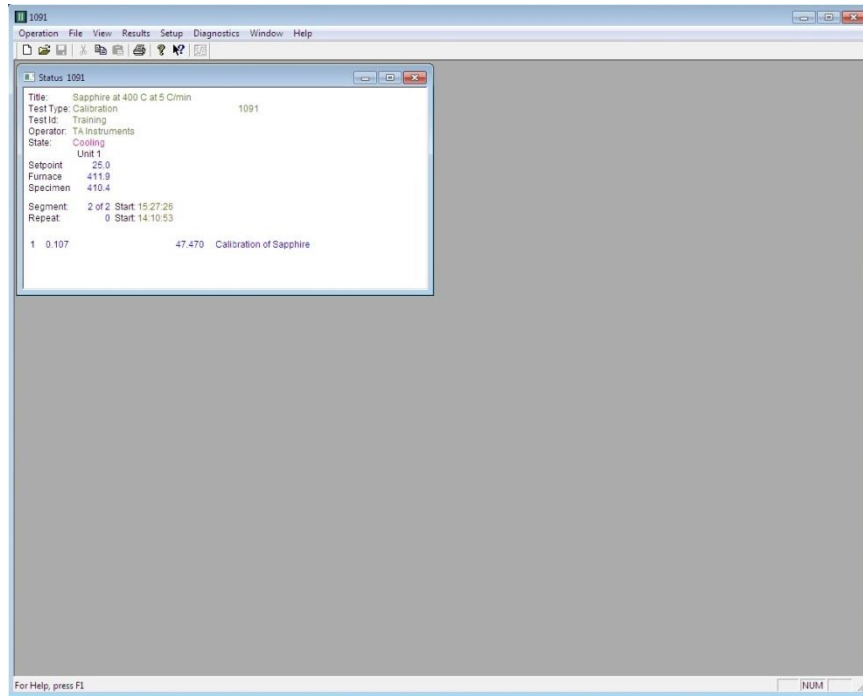


Figure D.23. Thermal Expansion Test on Heating Segment



*Figure D.24.* Thermal Expansion Test on Cooling Segment

After the test is completed, the data is now ready to be analyzed via Excel.